The Role of Concentrating Solar Power in a South African Large Scale Renewable Energy Scenario

A Dissertation submitted in partial fulfilment for the degree of

Master of Philosophy in Energy and Development Studies at the University of Cape Town

Haydn Liam May

Supervisors:

A. Stone

P. Gauché

July 2014

Abstract

This thesis investigates a hypothetical large scale renewable energy system for South Africa over the long term future using 2050 as a nominal year of analysis. Simulation modeling was used to assess the integration of three renewable energy technologies, which are currently being installed at utility scales in South Africa, at much higher penetrations. These technologies, namely wind, photovoltaic and concentrating solar power, are studied here within future scenarios (2050) over a period of one year at hourly intervals using real weather and solar irradiance data from 2010-11. The electricity demand profile for these scenario years was projected by scaling up the 2011 South African demand profile to the total annual energy demand projected for 2050 by the Draft South African Integrated Energy Plan reference case.

The dispatch of electrical energy from CSP plants with thermal energy storage has the potential to support other more intermittent renewable energy technologies. To evaluate this potential role, CSP production and available storage is assessed over one year relative to the production from wind and photovoltaics. Electrical energy is dispatched from thermal energy storage in a controlled fashion, thereby complementing the use and integration of more intermittent technologies. The effects of using thermal storage are monitored with regard to system cost and impact on overall system reliability. The results of the modelling exercise identified potential benefits gained when using thermal energy storage to backup intermittent renewables. These results were consistent with those reported in the literature. CSP plants which are equipped with thermal energy storage facilities are termed 'dispatchable' due to the amount of electricity that can be dispatched when needed with reasonably good reliability. The additional costs incurred to build CSP plants, relative to wind and photovoltaic plants, can be offset by better system reliability.

A more expensive dispatchable system using thermal energy storage displays better reliability. When utilising the more expensive fully dispatchable renewable energy system which is defined here by the use of thermal energy storage primarily being used to back-up other renewables, the fractional increase in cost can be argued on the grounds of increased fulfilment and decreased curtailment achieved by the renewable energy technologies installed on the grid. This allows for improvements to the economics of clean energy and lowers total carbon emissions produced by the supply of electricity.

Scenarios of high penetration of the three renewables in different ratios, with unfulfilled energy being met by a single representative fossil fuel alternative (natural gas fired combined cycle gas turbine), were compared to each other using a range of indicators with cost of generation being determined with the Levelised Cost of Electricity (LCOE) method. The cost of renewable energy technologies has declined in recent years and is envisioned to continue to become more cost-competitive with conventional generation technologies. To account for this expected reduction in renewable energy costs, technology learning has been applied to the LCOE calculation. Additionally, a sensitivity analysis of one of these scenarios assesses the LCOE of a system with increasing RE penetration, spanning from low RE with 95% of energy supplied by gas-fired CCGT to high RE with 26% of energy supplied by gas-fired CCGT. Technology learning rates, as estimated by the Integrated Resource Plan for 2030, are used in the interests of being conservative on estimating actual costs in 2050. When technology learning rates are assumed for 2030 and a fuel cost of R860.38 per MWh electricity generated for gas is used, the three RE technologies within the modeled system can

contribute 85% to total energy requirement over the year (TWh) and attain an LCOE of R0.75/kWh. In the event that the same system is moved towards a heavier CCGT reliance of 95%, the LCOE is raised to R0.96/kWh due to the impact of expensive variable operating and maintenance costs for CCGT. Capital costs for the different RE technologies assessed here are expected to be lowered by continued learning from 2030 to 2050.

PLAGIARISM DECLARATION

I know that plagiarism is wrong. Plagiarism is using another's work and to pretend that it is one's own.

2. I have used the Modern Language Association (MLA) convention for citation and referencing. Each significant contribution to, and quotation in, this essay/report/project/… from the work, or works of other people has been attributed and has been cited and referenced.
3. This thesis is my own work.
4. I have not allowed, and will not allow, anyone to copy my work with the intention of passing it off as his or her own work.
5. I acknowledge that copying someone else's assignment or essay, or part of it, is wrong, and declare that this is my own work

SIGNATURE: ___________________________

DATE: __________________

Dedication

This thesis is dedicated to my parents.

Acknowledgements

The author wishes to thank the following;

His supervisor, Adrian Stone for guidance and encouragement.

His co-supervisor, Paul Gauché for help in constructing this thesis.

The Andrew Mellon Foundation, for financial assistance.

Contents Table

List of Figures

Nomenclature

Abbreviations

BP – British Petroleum

CAES – Compressed Air Energy Storage

CC – Curtailment Coefficient

CCGT – Closed Cycle Gas Turbine

CCS – Carbon Capture and Storage

CDIAC – Carbon Dioxide Information Analysis Centre

CF – Capacity Factor

Co-Gen – Combined Generation

CO_2 – Carbon Dioxide

CR – Central Receiver

CSIR – Council for Scientific and Industrial Research

CSP – Concentrating Solar Power

DNI – Direct Normal Irradiance, (Watt/m^2)

DOE – Department of Energy, (South Africa)

EIA – Environmental Impact Assessment

ERC – Energy Research Centre, (University of Cape Town)

Eskom – Electricity Supply Commission

FBC – Fluidized Bed Combustion

FC – Fulfilment Coefficient

GDP – Gross Domestic Product

GHG – Green House Gases

GHI – Global Horizontal Irradiance, (Watt/m^2)

GIS – Geographic Information System

HWR – Heavy Water Reactor

IEP – Integrated Energy Plan

IPP – Independent Power Producer

RE – Renewable Energy

REIPPPP – Renewable Energy Independent Power Producer Procurement Programme

IRP – Integrated Resource Plan

LCOE – Levelised Cost of Electricity, (Rand/kWh)

LEC – Levelised Electricity Cost (Lifetime)

LWR – Light Water Reactor

NREL – National Renewable Energy Laboratory

OCGT – Open Cycle Gas Turbine

PCM – Phase Change Material

PHS – Pumped Hydro Storage

PJ – Petajoule

PT – Parabolic Trough

PV – Photovoltaic

QGIS – Quantum Geographic Information System

RE – Renewable Energy

REFlex – Renewable Energy Flexibility Model

Riso DTU – Technical University of Denmark

R/kWh – Rand per kilowatt

R/W – Rand per Watt

SANERI – South African National Energy Research Institute

SAWS – South Africa Weather Service

STERG – Solar Thermal Energy Research Group, (Stellenbosch University)

SU – Stellenbosch University

TES – Thermal Energy Storage

VG – Variable Generation

WASA – Wind Atlas for South Africa

WPF – Wind Power Factor

List of Symbols

A – Cross sectional area of air parcel

Ft – Fuel Cost in year t

fv – future value of capital costs

I_t – Costs in year t

Mt – Operation and Maintenance in year t

pmt – payment

pv – present value of capital costs

r – Discount rate

t – lifetime of plant (years)

type – time of year payment is made

V – Velocity of air

Greek Symbols

η – Round trip efficiency

ρ – Density of air

Chapter One – Introduction

The topic for this thesis was selected, firstly, because of a keen passion and belief in the benefits to be gained from using renewable energy (from now on (RE) technologies) to generate electricity. Current concerns around climate change being caused by anthropogenic influences, specifically our dominant methods of sourcing energy, strengthen the argument for low-emission technologies. An opportunity was created to study the use of RE at large scales within South Africa, as the topic formed part of a continuation of research already carried out at Stellenbosch University, (Gauché 2012). This made available several Excel-based simulation energy models dealing with Photovoltaics and Concentrating Solar Power. The latter technology has the ability to produce continuous electrical energy through the use of thermal energy storage. This makes this technology, at least in theory, competitive with conventional technologies based purely on capacity factors.

Without an engineering background, and with no previous energy modelling experience, the available Excel models were more accessible for use in this thesis. Using these models also meant that accurate solar and wind resource data for South Africa could be incorporated and analysed. Creating a model framework involved constructing a single large excel 'master' spreadsheet which incorporated the thermal energy storage (TES) spreadsheet from US and a levelised cost of electricity spreadsheet created by the author. The resulting energy outputs from the PV and CSP model spreadsheets (US) were incorporated with those from a wind model constructed specifically for this work. The spreadsheet layout allowed different input variables like technology shares and costs to be tested, with the outcomes of these changes being simulated in terms of performance indicators.

The results of this spreadsheet based analysis are intended to provide at least a partial assessment of potential future outcomes for the construction of RE plants on a large scale in South Africa. The energy modelling process adapted here aims to contribute towards current discourse in South Africa on the use of large-scale RE within a fossil-fuel dominant grid.

Solar power has experienced a resurgence of interest in regions of the world that have high levels of solar irradiance. In the early 1980s, significant investment took place in research and development of concentrating solar power in California, (IEA, 2010). This was partially caused by high oil prices, but the interest in this solar technology waned when oil prices began to drop. At the present time solar power, both the concentrating and photovoltaic varieties, is again experiencing rapidly growing levels of interest and investment. A large volume of energy irradiates the surface of the earth daily, which could be used actively to generate electricity. World electricity demand in 2011 was 149,627 TWh (IEA, 2014), while annual solar irradiance was calculated here as being approximately 5,100 times greater over the surface of half the globe. Certain regions of the planet experience comparatively higher solar irradiance levels in relation to global averages. South Africa is one such place, with excellent solar resources, particularly in the Northern Cape. As part of climate change commitments and to lower the cost of renewables, South Africa has begun to develop an RE build programme. At the present time, about 85% of electrical energy in South Africa is supplied from coal, with generation dominated by one public company, Eskom. Given the large solar resources of the country and the current dependence on fossil fuels, it would appear beneficial to adequately study the enormous potential of solar resources in South Africa. Newer generations of solar technologies, such as thermal energy storage of concentrating solar power, are increasingly able to respond to changes in consumer demand. The economic feasibility of CSP technology is strengthened by increasing the availability of electrical energy delivered from the plant over time. This flexibility in providing electricity when needed, has led to the investigation of thermal storage potentially acting as backup to more intermittent RE technologies like wind and photovoltaics, (Denholm, et al., 2010; Brinkman, et al., 2011; Denholm & Hand, 2011; Denholm & Mehos, 2011). The primary outcomes of this thesis are intended to assess the potential benefits and drawbacks of using high penetrations of CSP in conjunction with thermal energy storage to complement other types of RE, when any demand deficit or shortfall in production from RE is backed up by gas turbines.

1.2 Problem Statement

In a scenario where wind and photovoltaic technologies, (PV), have substantially higher capacity allocations within an electrical system, problems relating to the intrinsically higher intermittency of these technologies may arise. Thermal energy storage, (TES), provides the option of dispatching electricity when needed. This dissertation investigates the dispatchability of electrical energy from concentrating solar power, (CSP), during periods when production from Wind and PV drop, with the aim of adequately matching demand. The supporting role for CSP is studied here within hypothetical future high RE share scenarios for South Africa.

1.3 Research Objectives

1) This thesis intends to use various indicators to assess the positive and negative implications of a large penetration of three renewable technologies, namely, wind, solar photovoltaic and centralised solar thermal plants, in a future hypothetical electrical energy system nominally set in the year 2050. To accomplish this, scenarios are investigated with varying shares of renewable technologies, considered within a hypothetical future electricity generation system.
2) This thesis seeks to investigate the potential dispatchability role of TES facilities at CSP plants, in supporting the demand deficit from more intermittent Wind and PV technologies.
3) This thesis aims to carry out a basic levelised cost comparison between RE and advanced combined cycle gas turbines (CCGTs), incorporating learning rate assumptions and a fuel price sensitivity analysis. This economic analysis is intended to evaluate both a current (2012) and a hypothetical future (2050) energy system with high capacity shares of the three renewable technologies considered.

1.4 Delineations & Limitations

The modelling process used here is limited to spreadsheet based analysis. In addition to the reasons stated above in the introduction, the use of the available models and platform meant that the TES component of CSP, developed by the Solar Thermal Energy Research Group, (Gauché 2012a), could be directly integrated and investigated against production from Wind and PV. In this manner, the role of TES in specifically supporting Wind and PV could be assessed. A rigorous engineering model was not the objective in this research process. The broader objective was to gain insight into future possible scenarios with large scale penetrations of RE using a straightforward approach. This type of approach incorporates detailed resource data and can generate useful and communicable insights from the scenarios.

This thesis primarily investigates a hypothetical large scale RE system in South Africa that could theoretically provide a large share of the total national demand for electricity in 2050. For the purposes of this thesis, this is assumed to be the forecast of the reference case of the Integrated Energy Plan of the Department of Energy (DOE, 2012). The modelling tools used in this thesis do not factor in the existing or planned electricity system in South Africa, some of which will be operating in 2050. However, these technologies and their installed capacities within the original South African Integrated Resource Plan of 2010, (IRP), document are briefly described in the Literature Review below in sections 2.4 - 2.6, (DOE, 2011).

CCGT technology has been incorporated into the modelling process, where proportions of the required electrical energy for the modeled 2050 system are provided by advanced CCGT. This technology was chosen because the nature of the demand shortfall required quick responding technology. The technology cost assumptions for advanced combined cycle gas turbines are taken from the IRP 2010, (IRP, 2010). Different fuel types for CCGT are not assessed with the availability of natural gas being assumed. The fuel price sensitivity analysis looks at the impacts of whether this fuel is either indigenous shale or imported liquefied natural gas (LNG).

Planned and unplanned outages of generation capacity caused by maintenance requirements, failures or unexpected conditions are not factored into the analysis. The energy and cost calculations for the plants only consider the availability of wind and solar resources.

1.5 Underlying assumptions

In several countries, covered in section 2.10.3 below, CSP is demonstrating successful electricity production, meeting the needs of dispatch or baseload generation, (Dinter & Gonzalez, 2013). The high solar resource of the Northern Cape region of South Africa would indicate that large volumes of competitively priced electricity could be generated, (Fluri, 2009). CSP technology is currently expensive, as would be expected when new technologies are introduced, (Delucchi & Jacobson, 2011). It is assumed here that given a sufficient period of time for the technology to mature, the cost of the three renewables is likely to decline based on further economies of scale, (Mcdonald & Schrattenholzer, 2001). These cost reductions will bring renewables closer to being financially competitive with conventionals. To account for this expected decrease in price, learning rates from the IRP 2013 update have been applied to the cost assumptions of the technologies, (DOE, 2013a). These learning rates display expected decreases in cost over time, up until 2030, the time horizon of the most recent IRP update. It is assumed that technology investment costs are constant between 2030 and 2050 in the interests of being more conservative and not overstating the case for RE system costs in 2050.

1.6 Significance

South Africa is already constructing RE generators as part of the Independent Power Producers Procurement Program (IPPPP) as planned by the IRP, (DOE, 2011). The IRP broadly aims to ensure that electrical energy supply meets both the development demands of the economy and the needs of a growing population, while complementing a globally increasing environmental concern relating to the burning of fossil fuels. This thesis aims to contribute to current energy research in South Africa by focusing on a possible future where RE plays a larger role in the country’s power sector.

1.7 Brief Chapter Overviews

In the second chapter literature is presented on electricity planning and procurement of RE generation capacity in South Africa, with research conducted within the IRP provided to give context to the potential for future RE builds within the country. To accurately understand the RE systems assessed in the modelling process here, some basic technical information is considered for each technology. Since renewable technologies are reliant on the availability of sufficient wind and solar resources, these parameters are covered within the land boundaries of South Africa. In order to better understand the developmental goals of the IRP, the energy history of South Africa is discussed. Here, the high emission score of the country, based on per capita carbon emissions, is highlighted according to international comparisons. Among various benefits, RE technologies produce fewer (or zero) carbon emissions relative to conventional technologies. Additionally, certain REs are able to provide continuous and reliable power, depending on the resource, through the use of storage, which makes these technologies comparable to conventionals. This ability, namely the dispatchability of electrical energy using thermal storage is covered in this first chapter, and is of primary interest to this thesis. In the closing portions of this chapter, the use of optimisation and simulation modelling is covered, with the latter being chosen for the purposes of this research exercise.

Chapter 3 provides a description of the overall thesis research design, and details the use of each of the sub-models incorporated into the scenario analysis. This method chapter provides information on the criteria used to assess the scenarios. Of specific interest here is the description of the curtailment and fulfilment coefficients, which are used as indicators of overall system efficiency and performance. Further indicators of performance include calculating the system LCOE, and assessing the effect of changing fuel prices for advanced CCGT technology. This allows a sensitivity analysis to be conducted into how system costs are impacted by potential fuel price volatility. Chapter 3 also provides a comprehensive description of the development of the modelling scenarios used here, with the accompanying scenario matrix being displayed.

Chapter 4 comprises multiple modelling results for the different scenarios, specified in Figure 50.

Chapter 5 involves a discussion of the findings presented in Chapter 4.

Chapter 6 provides conclusions attained through the modelling process.

Chapter Two – Literature Review

2.1 Introduction

This chapter reviews some of the available literature applicable to renewable energy technologies and how these technologies can be modeled within a future South African energy sector. The history of RE in South Africa is discussed, with particular mention of the Integrated Resources Plan (DOE, 2011), and how this document formalised the RE build plans of the country. Other sources of electrical energy in the IRP are discussed, namely nuclear and coal energy, as well as the current breakdown of both committed and new build options as designated by the IRP. An assessesment of the carbon dioxide (CO_2) emissions of South Africa is provided within a global context, as well as recent research conducted on the remaining coal resources of Southern Africa.

The focus of this thesis is RE, so descriptions of the RE technologies are provided. The three main technologies focused upon are Wind, Photovoltaic and Concentrating Solar Power. Three different CSP technologies are investigated, namely parabolic trough, linear fresnel and central receivers. The central receiver model used in this research is based on the Gemasolar 20MW plant, (Gauché, 2012b). Characteristics of this facility are examined. The potential cost reductions likely to occur within the CSP industry through research and development, in addition to increases in cumulative global installed capacity, are analysed. Storage technologies that offer utility scale (MWh), volumes of energy storage are examined. The concept of dispatchability is discussed, as the dispatch of electrical energy from thermal energy storage is critical in the large scale RE scenarios investigated here.

2.2 Energy History Overview of South Africa

The structure of the economy has influenced the energy history of South Africa. South Africa has a large heavy industry sector, with the minerals beneficiation industry playing an important role in total energy use. These industries are reliant on relatively low cost electricity, (Marquard, 2006). Within these industries mined raw materials are synthesised into more marketable products, such as steel and aluminium. These processes are energy intensive and would not be economically profitable without an abundance of cheap electricity. In sourcing this energy, heavy industries have traditionally relied on the mining industry to provide coal for electricity generation. The coal used locally within the Eskom fleet is of relatively poor quality, with the higher grade mineral being exported. The majority of South Africa's electricity generation is fuelled by coal feedstock, contributing some 92% to national generation, (Marquard, 2006). By the time of writing the contribution supplied by coal had decreased to 85% (Figure 1).

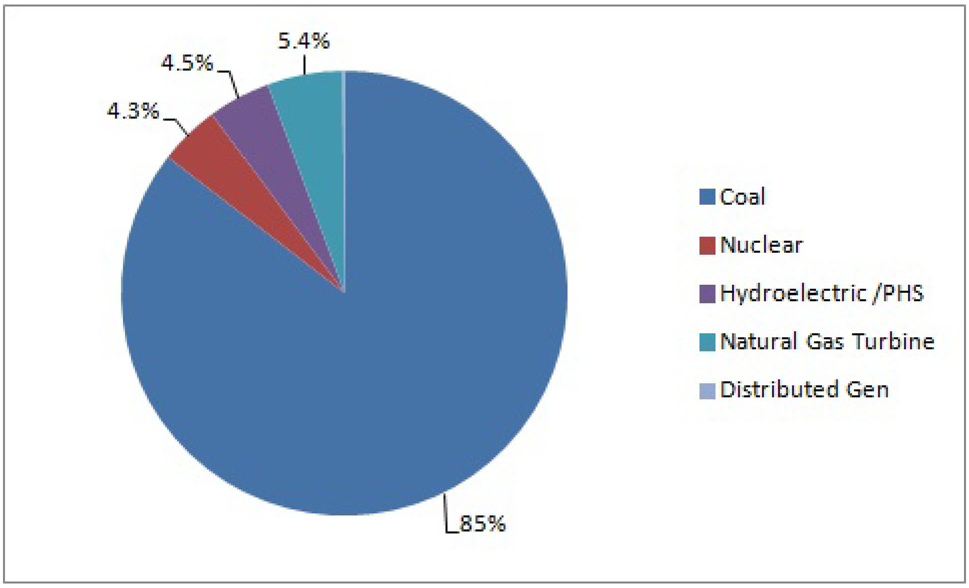

Figure 1: Delimited Eskom capacity 2013.

Source: (EIA, 2013)

2.3 Renewable Energy Overview of South Africa

The previous generation of electricity generating plants in South Africa is fossil fuel based. However, the South African government, through the Department of Energy, has begun work on implementing newer RE technologies. This process began in 2003 when the White Paper on Renewable Energy was published (Department of Minerals and Energy, 2003). A primary discussion point in this document was the targeted achievement of 10,000GWh or (0.8Mtoe) of electricity generated from RE sources by 2013. More recent work by the Department of Energy has seen the publication of the IRP in 2011. The IRP forms a robust strategy towards building local RE technologies and also provides guidance toward demand side management options such as energy efficiency. These local industries will be partially stimulated by the involvement of international corporations with experience in renewable energies. The low-carbon technologies included in the policy adjusted scenario in the IRP are divided into hydro, wind, solar photovoltaic (PV), concentrating solar power (CSP) and nuclear options. The policy adjusted IRP scenario was adopted by the Department of Energy after extensive public comment and recommendations. The allocations within this scenario are 8,400MW Wind, 8,400MW PV, 1,000MW CSP and 9,600MW Nuclear, (DOE, 2011), with construction taking place between 2010 and 2030. The IRP describes how the construction of these facilities will be coordinated through the Independent Power Producer Procurement Programme (IPPPP). The tendering procedure that guides the IPPPP has been divided into different stages, with the first two having already been concluded in 2013. The known capacities of RE generation finalised within the first two bidding stages are 787MW onshore wind, 450 PV, 200MW CSP, 16.5MW biomass and 18MW landfill gas, (DOE, 2013). The third bidding round of the IRP was conducted in the early part of 2014.

The cumulative MW allocations of the policy adjusted scenario are displayed below in Figure 2. This figure shows three primary groups of generators, namely those in existence, those committed to and the proposed new build options. The present breakdown of both options committed to and new build options proposed by the latest policy adjusted IRP is shown in Figure 3, with the existing fleet also shown. This graph consists of information from the same source as Figure 2, but the MW allocations have been delimited into separate technologies. In Figure 1 the majority of South Africa's currently installed baseload capacity is fuelled by coal, with small proportions of gas, nuclear and pumped hydro. During periods when system demand is at its highest, gas turbines and pumped storage facilities might be used to fulfill this raised load requirement, depending on the configuration of the power grid. These periods of higher demand occur over short lengths of time across the year, meaning plants are needed that can match this fluctuating demand profile. This is in contrast to baseload plants which aim to operate at higher CFs.

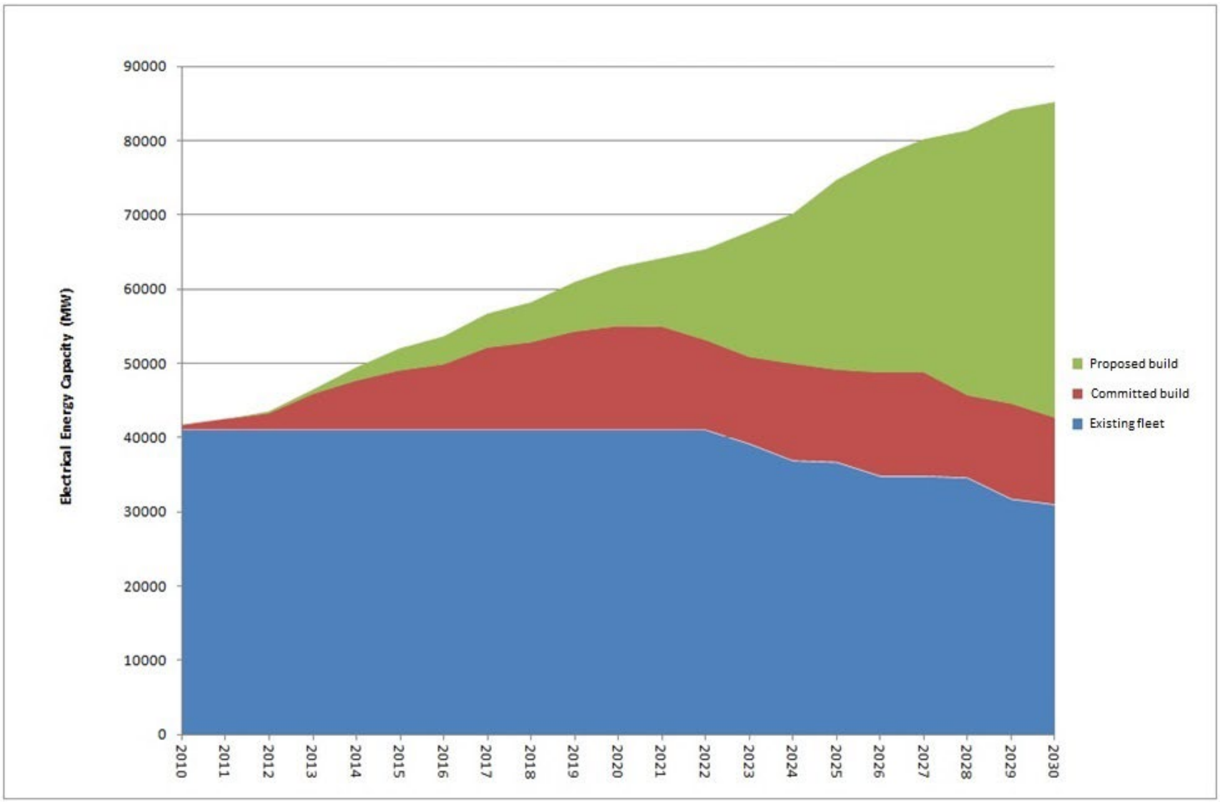

Figure 2: Proposed, Committed and Existing Capacities within the IRP Policy Adjusted scenario

Source: (DOE, 2011)

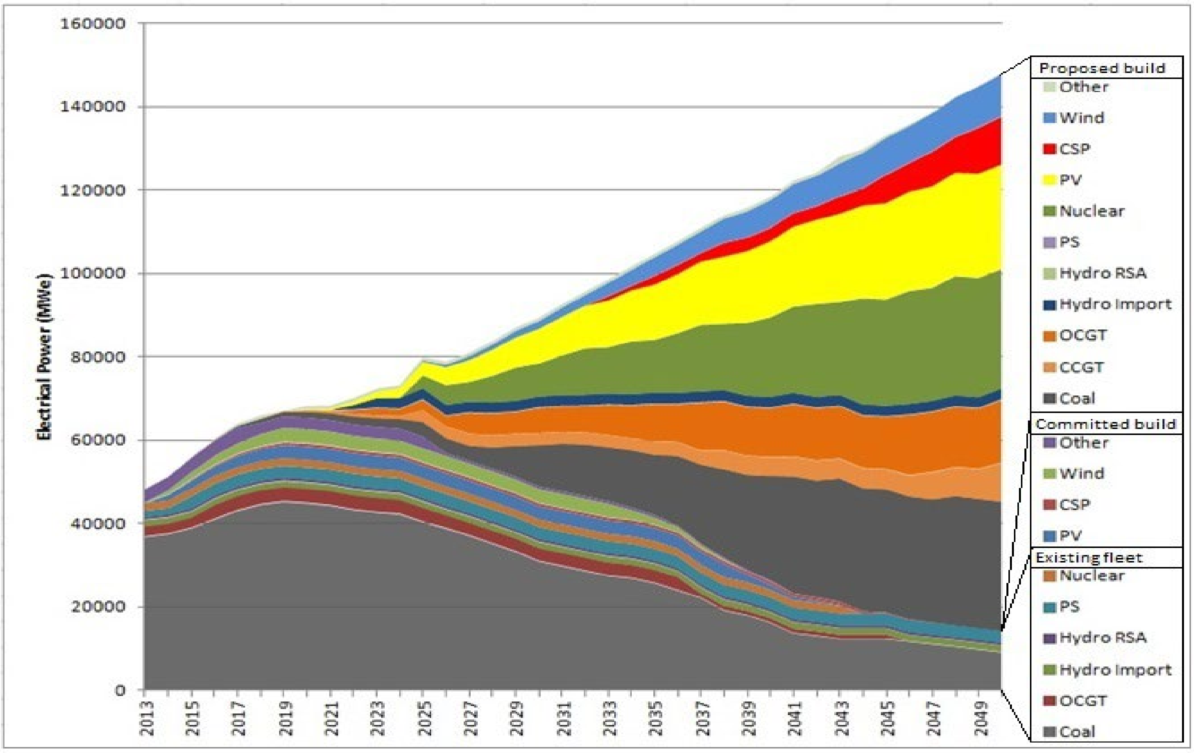

Figure 3: Capacities for Committed and New Build Options within the IRP Policy Adjusted scenario

Source: (DOE, 2011)

In the graph above, the GW allocations for committed build technologies which are phased out by 2050 are: Return to Service 1.46GW, Medupi 4.3GW, Kusile 4.3GW, Ingula 1.3GW, OCGT 1.0GW, Co-Gen 390MW, Wind 700MW, CSP 200MW, Landfill/Hydro 125MW, and the Sere wind farm 100MW. Those for proposed new build options are: coal 6.2GW, CCGT 2.3GW, OCGT 3.9GW, import hydro 2.6GW, Wind 8.4GW, PV 8.4GW, CSP 1.0GW and Nuclear 9.6GW, (IRP, 2011). These allocation values represent a high weighting towards nuclear, wind and PV as well as the intention to install large volumes of gas generation to fulfil the peaking role.

The updated IRP document has taken into account several changes over the earlier publication in 2011. These changes have involved "a revised economic and electricity sector outlook," (DOE, 2013) which led to a different demand prediction, where some 6,600MW of capacity are no longer needed. Some of this reduced demand relates to "a shift in economic development away from energy-intensive industries," (DOE, 2013). Another updated consideration is the uncertainty around fuel price volatility for coal, gas and nuclear. The main objective of the 2013 IRP update has been recalculation of the base case scenario up to 2050. These changes are displayed in Figure 4 below.

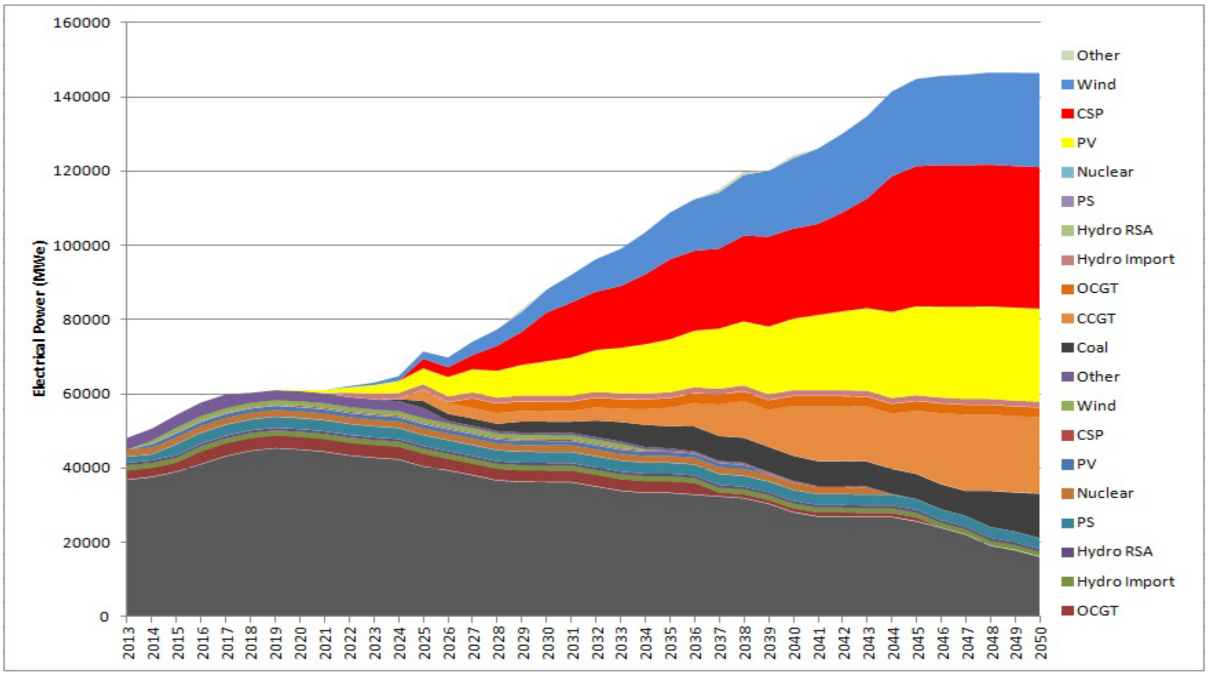

Figure 4: Capacities for the High Nuclear Cost Scenario within the IRP update 2013

Source: (DOE, 2013b)

2.4 Community Benefits from the Integrated Resource Plan

The broad aim of the IRP 2011 is to strengthen South Africa's energy security and begin shifting the balance of energy production away from coal towards other sources of electricity and heat, to reduce GHG and increase energy security. The influx of investment generated by the IRP 2011 will help local economies and create employment opportunities during multiple construction phases. Several clauses within the REIPPPP stipulate that the construction of RE facilities must benefit local communities and people, under the wider governmental mandate of Black Economic Empowerment, (Tait, Wlokas & Garside, 2013). Within the IPPPP bidding process, the local community benefit requirements are broadly "local job creation, local ownership, economic development and socio-economic development," (Tait, Wlokas & Garside, 2013). Due to these clauses, permanent employment positions will result from the everyday running of the plants as well as the operation and maintenance procedures. Overall, the IRP and the IPPPP process should be positive for the economy and people of South Africa, in that it includes a broad mandate of developmental benefits. The private investment nature of the competitive tendering procedure has been shown to push the cost of RE downwards.

2.5 Nuclear energy (IRP 2011)

The large allocation of nuclear energy is proposed on the grounds of stability of supply, with the capacity factor of this technology being high. The IRP 2011 states under "option 4.3a [it commits] to a full nuclear fleet of 9.6GW [to] provide acceptable assurance of security of supply in the event of a peak oil-type increase in fuel prices," (IRP, 2011). Questions have been raised with regard to the large nuclear build proposal, as there are concerns and uncertainty about the cost of nuclear energy and the current reduction in the cost of renewables, (Eberhard, 2013). The current IRP proposes the first operation of the nuclear build to begin by 2023, allowing for the fact that nuclear plants have construction times of 10-12 years (Majavu, 2007). This would indicate that construction should begin shortly.

One of the changes within the IRP update is the reduction in size of the nuclear commitment. The new potential allocation of nuclear energy within the updated IRP, in the base case scenario is 4.8GW, (DOE, 2013a). The update states that the decision on nuclear options could possibly be delayed, in light of regional hydro options and the potential for shale gas exploration in the Karoo.

2.6 Coal Energy (IRP 2011)

In the interests of increasing the production of electricity from South Africa's remaining coal deposits and to strengthen the reserve margin to accommodate a growing economy, the construction of two large coal plants is underway, namely Medupi and Kusile. Technology options to improve carbon emissions from coal plants are discussed by the IRP 2010, such as carbon capture and storage (CCS). However, these technologies are expensive and implementation will add to the cost of the new coal fleet. The coal allocation within the new build options of the IRP (6.2GW) is substantial and will add to the CO_2 emissions of the country.

2.7 Carbon Emissions

A primary emission source of CO_2 is the generation of electricity from gas and coal. Coal accounts for the majority share of these emissions as the amount of CO_2 released is roughly double that for gas, (Figure 5). In assessing the annual consumption of coal in South Africa, statistics from the year 2011 show coal consumption per GDP and industrial coal use (Figure 5 and 6). In the context of global CO_2 emissions, South Africa was ranked 10th highest emitter, with 511,410,000 tonnes, (CDIAC, 2013). Assuming the population of the country is 50,13 million people in 2013, South Africa's CO_2 emissions per capita were 10.2 metric tonnes (CDIAC, 2013).

Technology	Kg/MWh	Emission type
Coal	1020.12	Carbon Dioxide
	5.89	Sulphur Dioxide
	2.72	Nitrogen Oxides
Gas	514.82	Carbon Dioxide
	0.05	Sulphur Dioxide
Nuclear	10-130	Carbon Dioxide
Wind/Hydro	15-25	Carbon Dioxide
PV/Solar Thermal	90	Carbon Dioxide

Figure 5: GHG Emissions from different electricity generation technologies

Source: Environmental Protection Agency, United States, 2013, Lenzen, 2008

South Africa was ranked 73rd globally on a GDP per capita basis, (GDP per capita, 2013), while it had the 24th largest population worldwide, (Gapminder.org, 2013). A comparison of coal consumption and GDP data across countries, illustrated in Figure 6 and Figure 7, shows that emissions per unit added value of GDP are high for South Africa. The primary source of these emissions is the generation of electricity from coal. South Africa's electricity use per person places us 42nd in the world, (World Development Indicators, 2013). Simply stated, our country has a high energy use per GDP per capita, (Figure 6). The minerals beneficiation industry requires large volumes of energy either derived from electricity (from coal), or heat/electricity produced from coal on site. The industrial sector accounts for roughly 30% of coal consumption, shown in Figure 7 below.

The data above indicates that South Africa contributes a large amount of CO_2 annually, relative to population size and value added to GDP per tonne of coal consumed. Eskom emitted 225Mt of CO_2 in 2011 from energy production alone, (Eberhard, 2011). South Africa is conscious of its CO_2 emissions, relative to its GDP and population size and displayed by the work done towards building low-carbon technologies in the IRP 2011, however, it is not an Annex 1 country under the Kyoto Protocol (1997), meaning that it has no binding commitments to reduce its CO_2 emissions.

CO_2 emissions data from different energy generation technologies indicates that the most commonly used nuclear reactors (LWR and HWR) need to consume a proportion of the energy they generate to operate themselves, (Lenzen, 2008). This is known as parasitic energy consumption. This fraction of energy consumed by running the reactor can be translated into equivalent CO_2 emissions. These are additive to those emissions released during the enrichment and mining processes to create nuclear fuel. This value and corresponding values for other technologies are summarised in Figure 5 above. Although nuclear energy may be considered low carbon relative to traditional fossil energy sources, it is not without its own measurable emissions. The majority of these emissions occur in the "processing stages upstream and downstream from the plant," (Lenzen, 2008). CO_2 emissions from nuclear plants and solar thermal plants are only similar when gas backup is necessary in the solar thermal plant.

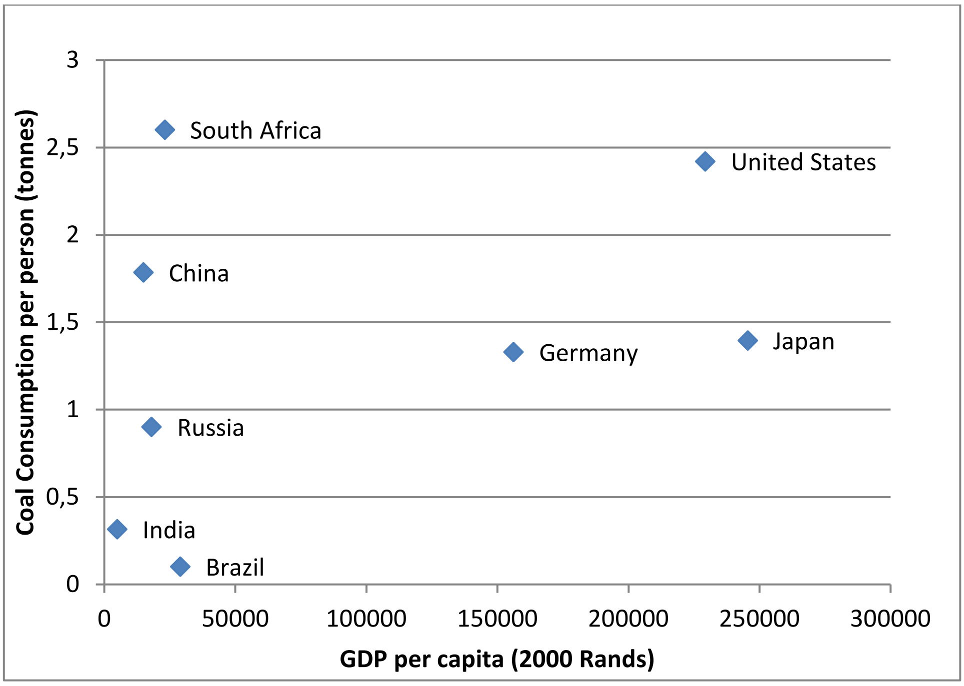

Figure 6: Coal consumption per country GDP per capita, 2011

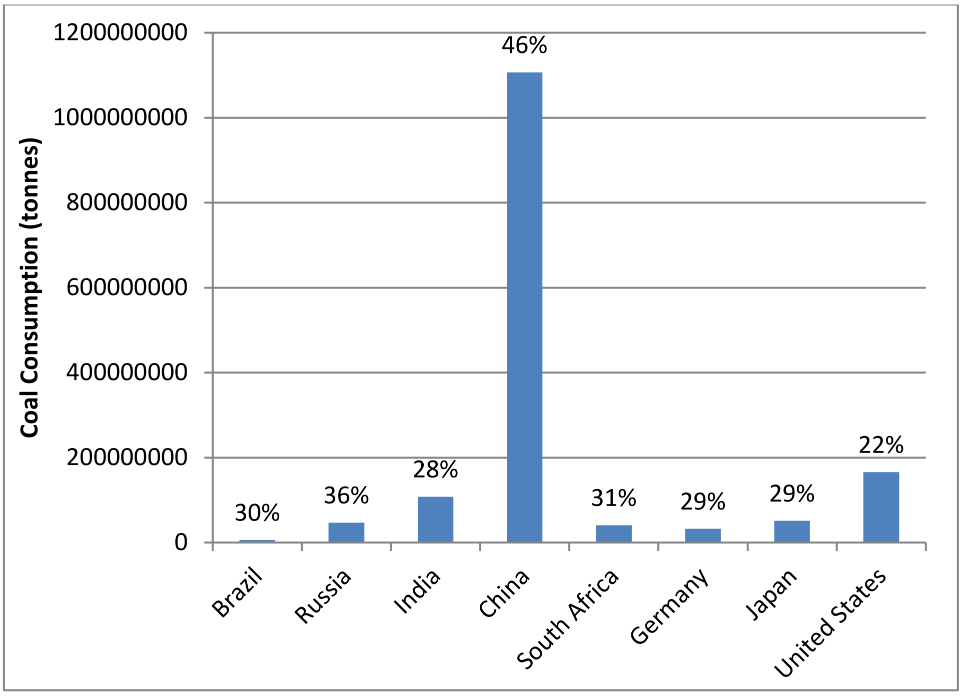

Figure 7: Coal consumption per industrial sector, 2010

Data sources : (World Energy, 2012), (World Development Indicators, 2013), (Historic Exchange Rates, 2013), (Energy Conversions, 2013), (World Energy 2012, 2012), (Industry (GDP), 2012)

2.8 Remaining Coal Reserves

Recent evaluations of the available coal reserves in South Africa, using techniques originally developed by Hubbert (Hubbert, 1982), suggest that previous estimates of remaining coal resources worldwide have possibly been overestimated. Rutledge (2011) estimates that African reserves, (essentially situated in South Africa, Botswana and Zimbabwe), may have reached 90% depletion by 2048, (Rutledge, 2011). Similarly, Hartnady (2010) discusses how the authoritative publications on coal reserves, such as the BP Statistical Review of World Energy and the South African Yearbook have reduced coal estimates for South Africa from around 52Gt prior to 2004 to 30Gt by 2008, (Hartnady, 2010). This shows a drop of some 22Gt in a reasonably short space of time. Another estimate from the same research suggests that "only 23Gt [are available] for the full recoverable cumulative coal resource in the African continent; of which about 8Gt was already consumed by production to end-2007," (Hartnady, 2010). This research on coal reserves concluded that approximately 15Gt of coal remain to be mined in the three coal producing countries of the Southern African subcontinent. To provide some context to this amount of coal, South Africa consumed approximately 0.13Gt of coal in 2011, (BP, 2012).

2.9 Review of South African Wind and Solar Resources

The availability of adequate wind and solar resources is important to the RE technologies examined here. Investigating these resources is needed to consider the feasibility of adopting large-scale RE technologies in South Africa. An estimation of the potential wind resource for the country comes from a study conducted by Hagemann (2008). This research reached a final wind energy potential of 80.5 TWh, with an assumed CF of the wind power system of 35.1%. This power output was achieved using 2MW wind turbines, "assuming a wind turbine density of unity for each 1km^2 grid cell," (Hagemann, 2008).

South Africa experiences good solar resources globally, with some portions of the Northern Cape region having DNI values between 8.0 and 8.5kWh/m^2 per day and ~3,000kWh annually, (Figure 8). The solar resource hotspots for the globe are shown below, with Western Australia, the central west coast of South America, and parts of North America, experiencing very good solar irradiance values.

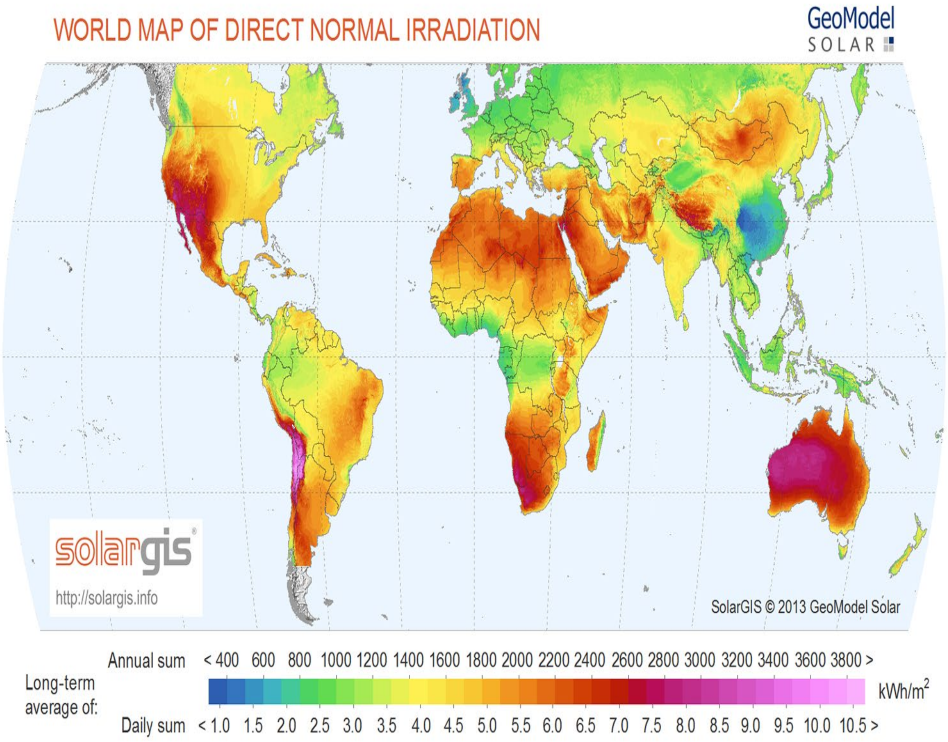

Figure 8: Daily and Annual Global DNI values, (kWh/m^2)

Source: (GeoModel Solar, 2014)

A study by Fluri (2009) investigated how much CSP capacity could be used realistically in South Africa, given the good average daily irradiance values for the country. Sensitive vegetation, suitable elevation and proximity to power lines were incorporated into this analysis. This study concluded that by factoring in the suitability criteria, 547.6GW of power could potentially be generated by CSP in South Africa in the short term (Fluri, 2009). The Northern Cape makes up the majority of this amount, with 510.3GW. In the Fluri (2009) study a reference parabolic trough plant with 6 hours of storage and a CF of 38.8% was used. Given the 547.6GW of potential capacity and the reference plant type, this translates to 1861 TWh of potential electrical energy generated per year. As reference, 273 TWh of electricity were generated in South Africa in 2008, (BP, 2009). Figure 9 below shows average daily irradiance values for South Africa.

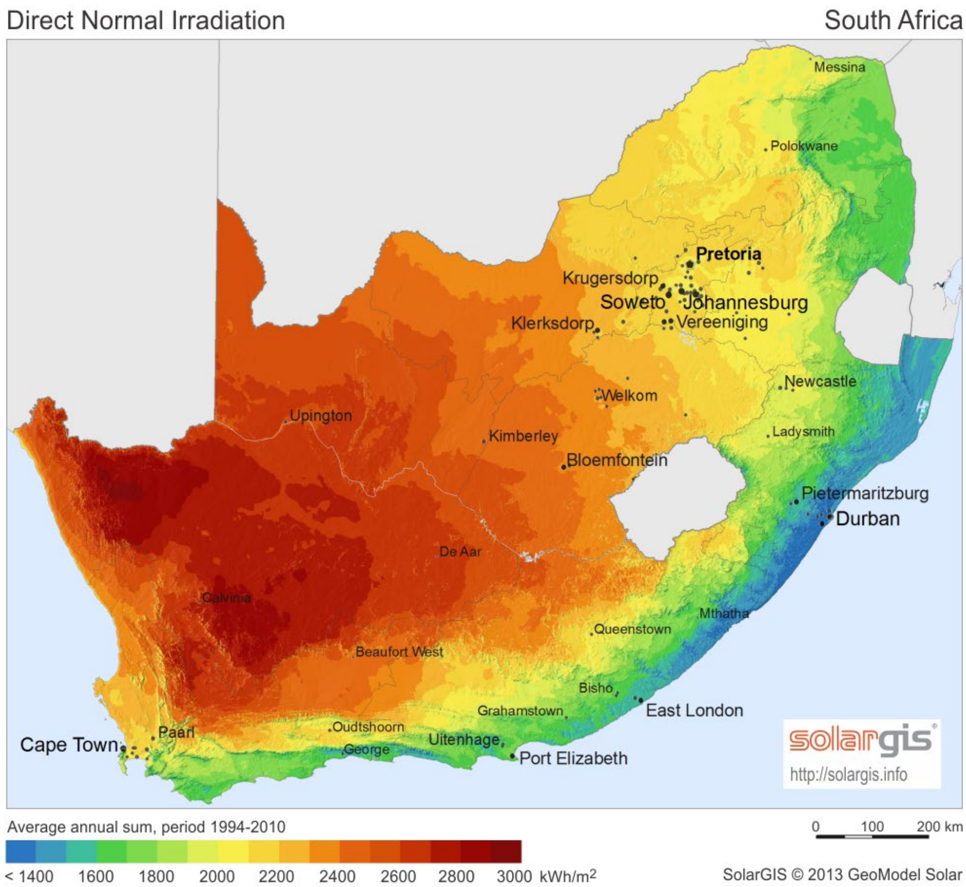

Figure 9: Average Annual DNI values for South Africa

Source: (GeoModel Solar, 2014)

2.10 Renewable Energy Technology Descriptions

2.10.1 Wind Power

To identify good wind resource locations, the Wind Atlas of South Africa (WASA) has been useful. This wind atlas was completed through collaboration between CSIR, SANERI, SAWS, UCT, and Riso DTU. The project was created to provide incentives to the local market in the form of wind data. The availability of reliable wind speed measurements, as well as numerous other atmospheric variables, is essential to an independent power producer (IPP) that needs accurate wind data to predict the potential power outputs of a wind facility. It is crucial that this data is available for an IPP to secure finance from banking institutions. This higher level of accuracy in forecasting power output, and thus financial payback periods, strengthens the economic viability of wind projects and facilitates the securing of financial backing.

The integration of wind facilities into electricity grids has been studied by NREL. This work investigated the adaptations needed for an energy utility to allow a higher penetration of variable RE sources, (Denholm, et al., 2010). Three factors need to be considered. Firstly, there is likely to be a higher need for frequency regulation due to the short term variability of wind power. Secondly, the ramping rate/response time of load following generators will increase. Finally, an increased level of uncertainty due to the wind resource will affect the predicted net load, (Denholm, et al., 2010). The culmination of these factors would require additional management by utilities in that, "the increased variability of the net load requires a greater amount of flexibility and operating reserves in the system, with more ramping capability to meet both the predicted and unpredicted variability," (Denholm, et al., 2010). Overall, additional costs will be incurred in fuel and maintenance in the rest of the system to accommodate variability and uncertainty in wind generation.

Date	Study	Wind Capacity Penetration (%)	Regulation Cost ($/MWh)	Load-Following Cost ($/MWh)	Unit Commitment Cost ($/MWh)	Other ($/MWh)	**Tot Oper. Cost Impact ($/MWh)**
2003	Xcel-UWIG	3.5	0	0.41	1.44	Na	**1.85**
2003	WE Energies	29	1.02	0.15	1.75	Na	**2.92**
2004	Xcel-MNDOC	15	0.23	na	4.37	Na	**4.6**
2005	PacifiCorp-2004	11	0	1.48	3.16	Na	**4.64**
2006	Calif. (multi-year)[a]	4	0.45	trace	trace	Na	**0.45**
2006	Xcel-PSCo[b]	15	0.2	na	3.32	1.45	**4.97**
2006	MN-MISO[c]	36	na	na	na	na	**4.41**
2007	Puget Sound Energy	12	na	na	na	na	**6.94**
2007	Arizona Pub. Service	15	0.37	2.65	1.06	na	**4.08**
2007	Avista Utilities[d]	30	1.43	4.4	3	na	**8.84**
2007	Idaho Power	20	na	na	na	na	**7.92**
2007	PacifiCorp-2007	18	na	1.1	4	na	**5.1**
2008	Xcel-PSCo[e]	20	na	na	na	na	**8.56**

Figure 10: The integration costs of wind power

Source: (Denholm, et al., 2010)

Many studies have been conducted which examined wind integration costs. These integration costs are typically a result of frequency regulation, load following, and wind forecast uncertainty, (Denholm, et al., 2010). According to the cost table above (Figure 10), most of the increases are lower than $5/MWh, which adds, "less than 10% to the cost of wind energy," (Denholm, et al., 2010). The same authors state that this relatively low additional cost of wind integration is due to the fact that utilities already deal with uncertainty in demand forecasts and therefore have in place significant load following capabilities and reserve margins. Also, spatial variation in the location of wind farms across a state (or country) would flatten out some of the variability in energy production by wind, as the wind may be blowing in one location and not another, (Denholm, et al., 2010). In studies which factor up to 30% penetration of wind energy into the grid no, "additional energy storage [is needed] to accommodate wind's variability and maintain reliable service," (Denholm, et al., 2010).

The wind energy to land area calculations were similarly adapted from the Denholm, et al, 2010 research involving the land-use evaluation of 178 wind farms in the United States. The total installed capacity of both operating and proposed wind farms in this analysis was 26GW. The type of changes to land-use caused by wind farms is divided into two categories, namely direct impact and total area. Direct impact is caused by the permanent infrastructural requirements of the plant such as roads, turbine bases, transmission lines and substations. Total area implies the extent of the wind power project and is much larger than the actual footprint (direct impact) of the plant. The total area results of the study ranged between 3+/-1.7MW/km^2, with the distribution of total project areas shown in Figure 12 below. A table explaining the uncertainty is provided in Figure 13. In the current thesis a value of 3 MW/km^2 was used in calculating total land area used by wind power.

The image below visually illustrates the difference between direct and total area land impacts.

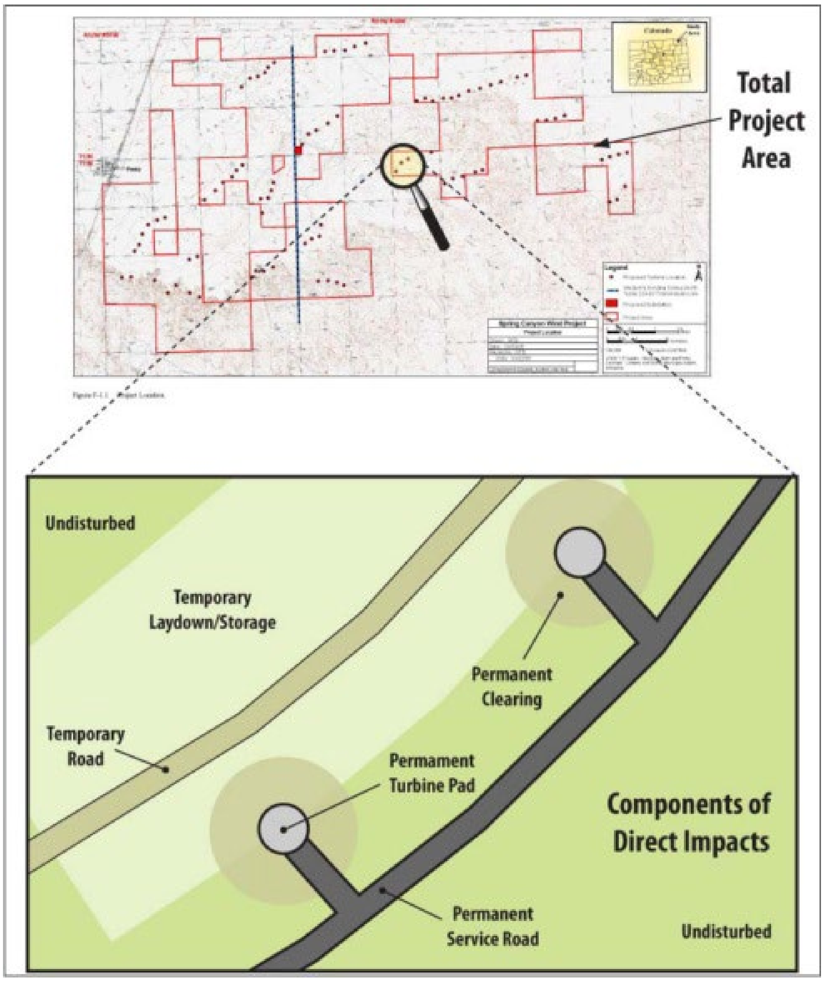

Figure 11: Total Project Area and Direct Impact of Wind Farms

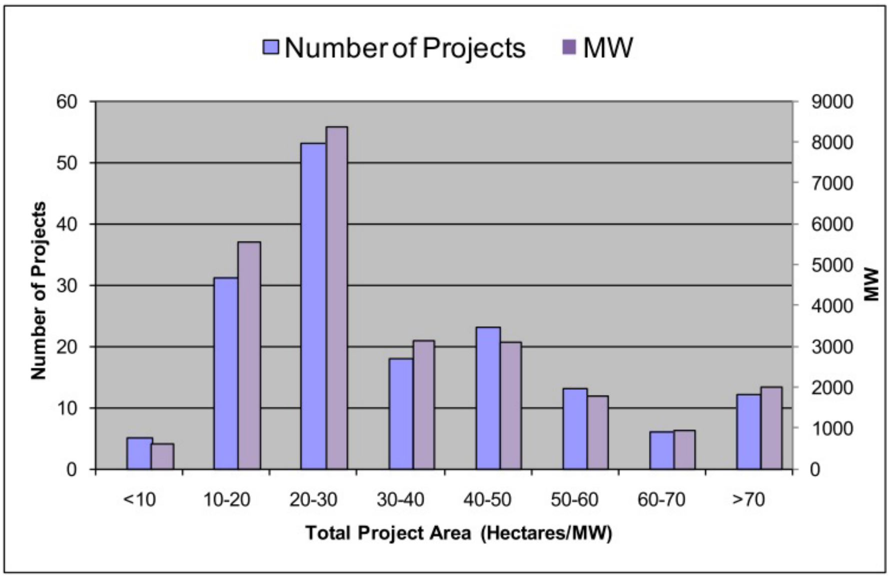

Figure 12: Distribution of wind power plant total project areas

Configuration	Average Area (hectares/MW)		
	Direct Impact Area (Permanent)	Direct Impact Area (Temp)	Total Area
Parallel Strings	0.33 ± 0.32	0.80 ± 0.55	34.7 ± 17.0
Multiple Strings	0.21 ± 0.15	0.38 ± 0.33	27.7 ± 24.0
Single String	0.34 ± 0.28	1.00 ± 1.13	30.3 ± 18.3
Cluster	0.24 ± 0.24	0.78 ± 0.63	39.8 ± 22.0

Figure 13: Table showing wind farm total area uncertainty

Environmental Impacts of Wind Farms:

The study above found that wind farms in general were unlikely to negatively impact the migratory routes of terrestrial animals or to separate breeding groups from each other. The spread-out nature of wind farm infrastructure in general means animals are generally free to move, except in the case of perimeter fencing. The surface areas within wind farms can find additional uses, such as farming or recreation. Impacts to bird species are likely more concerning.

2.10.2 Photovoltaics

The conversion of sunlight into electrical energy, through the use of semiconductors, is a globally expanding industry. Low complexity adds to its popularity and has helped establish this technology as a recognised process of generating RE. The costs of PV have steadily dropped as the industry has expanded. Government subsidies, both in research and development and power purchasing agreements, have helped increase the feasibility of this technology. Figure 11 shows the cross section of a solar cell with the two types of silicon being layered.

A detailed technology description of PV is provided in the Appendices, (Section 2).

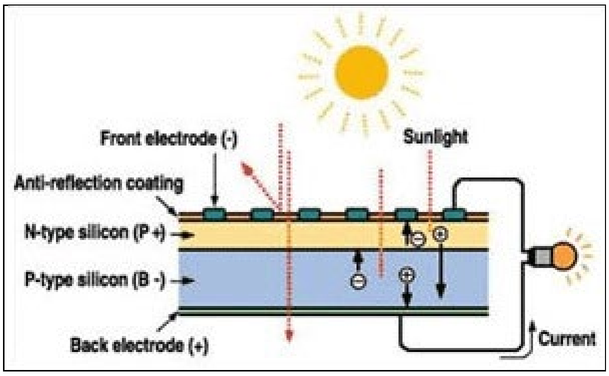

Figure 14: Photovoltaic Cell cross section

Source: ("Photovoltaics," 2013)

2.10.3 Concentrating Solar Power

Harnessing sunlight to produce heat and electricity has a long history. One of the earliest known usages of the parabolic trough design occurred in Egypt in 1914, where solar power was harnessed to create steam driving a 73kW pump moving 2,000m^3 of irrigation water per hour, (Stinnesbeck, 1914, originally referenced in Müller-steinhagen, 2004). Although obtaining diffuse energy from the sun is conceptually simple, the actual implementation of the technology is more complex. These complexities are progressively being surmounted, as the application of solar power technology shows itself as an attractive option for power generation and processing heat for a number of reasons. The solar irradiance fuel source is abundant and technically infinitely renewable on human timescales. The solar resource also is not subject to any fluctuations in pricing. This is attractive to plant developers who factor this into the levelised cost of electricity (LCOE) calculations of the plant, bringing the overall operation and maintenance costs down. Investors or utilities looking at building conventional generators need to include the uncertainty created by volatile fuel prices dependent on global markets. The technology emits low or zero greenhouse gases, depending on whether the CSP plant is hybridised with gas backup or not, an ever more pressing concern in the age of global warming.

CSP was first demonstrated on a viable commercial scale in the solar energy generating systems, (SEGS) plants in California in the eighties. A total of 354MW of capacity is generated using parabolic troughs with thermal oil as the heat-transfer-fluid (HTF). These plants are still in operation today and are more efficient than when they were built. A newer version of CSP technology was demonstrated by the Solar One plant, built in 1981, which had a capacity of 10MW, (Müller-steinhagen, 2010). This solar energy generation facility used a central tower design surrounded by dual axis tracking heliostats focusing the radiation of the sun onto the focal point of the central tower. Moving many years forward, 'power tower' technology has been improved through iterations of the central receiver concept. Today there are power tower facilities that produce base load electricity. An example of such a system is the Gemasolar 20MW plant in Seville, Spain. This plant was the first to produce 24 hours of continuous electricity via the innovative use of molten salt storage. Gemasolar has a capacity factor of 75%, (NREL, 2013), which makes it comparable to conventional power plants. Several much larger central receiver towers with TES are under construction, for example, the 392MW Ivanpah CSP plant in San Bernardino, California (NREL, 2013).

The International Energy Agency (IEA) envisions that in areas of the world that experience high solar resources, “CSP can be expected to become a competitive source of bulk power in peak and intermediate loads by 2020, and of base-load power by 2025-2030,” (IEA, 2010). CSP technology will become progressively more advanced and efficient with further research and development. With the addition of thermal storage capabilities into CSP plant design, and capacity factors dependent on the size of the thermal storage tanks and available solar resource, CSP with TES is beginning to offer a competitive alternative to conventional thermal plants using natural gas/diesel/coal. This is already considering that older technologies have undergone progressive reductions in cost over time through learning rates. Richter, et al. (2009) state that, “the cost of CSP electricity is coming down and many developers say it will soon be cost-competitive with thermal generation from mid-sized gas plants,” (Richter, Teske, & Short, 2009).

As with any new technology, start-up costs are initially high. However, TES offers CSP plants higher financial security by ensuring that capacity factors are increasing, (75% for Gemasolar). This makes the return on investment period shorter as the plant can sell electricity at a more significant rate during peak demand and price times by using TES. Richter, et al. (2009) discuss the life cycle assessment of existing CSP plants and show that the period of time needed to recoup the energy utilised in the manufacture and installation of the plant can be as short as five months, depending on the available solar resource. The same research paper discusses how the costs of CSP can be expected to drop with “technology improvements, mass production, economies of scale and improved operation,” (Richter, et al., 2009).

Further benefits of including thermal storage into CSP plant design are that it increases, “availability and dispatchability, decreases its cost, (by making more effective use of power generation equipment), and reducing technology risk by allowing conventional fuel use when needed,” (Geyer & Stine, 2001). Richter, et al. (2009), make the same point stating that, “with storage or in hybrid operation with fossil fuels [CSP can offer] firm capacity and dispatchable power on demand,” (Richter, et al., 2009). The section on energy storage, (2.10.11), will further describe this energy storage technology and highlight some additional advantages of using thermal storage.

There are three main CSP technologies currently being researched and utilised, namely parabolic trough, Linear Fresnel, and central receiver towers, (Müller-steinhagen, 2004:45). A fourth technology, dish-stirling, will not be discussed in this thesis. Two of the mentioned technologies, parabolic trough and central receiver towers, have demonstrated the ability to produce multi-megawatt capacities as shown in California, Spain and Germany since the 1980s. The following sections deal with these three solar technologies.

2.10.4 Parabolic Trough

The parabolic trough falls into the ‘line-focusing system’ group as sunlight is directed from every point within a parabolic shaped reflector to a receiver tube at the focal point running the length of the trough. The tube is specifically designed to absorb the maximum available solar irradiance (high absorptivity), and to emit minimal radiation (low emissivity). Although the parabolic trough is the most mature of the CSP technologies, there are complexities involved in the design of the flexible HTF joints which need to rotate as the trough tracks the position of the sun throughout the day.

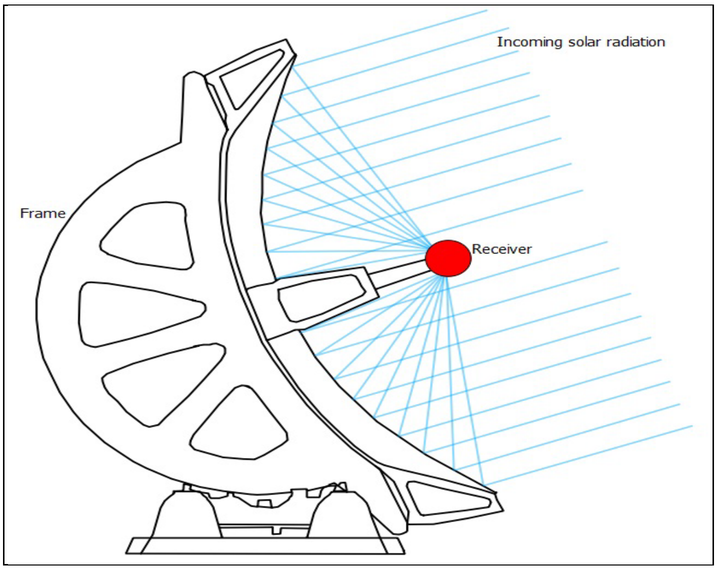

Figure 15: Conceptual side profile of a parabolic trough

Reproduced with QGIS after: ("Parabolic Trough Design," 2013)

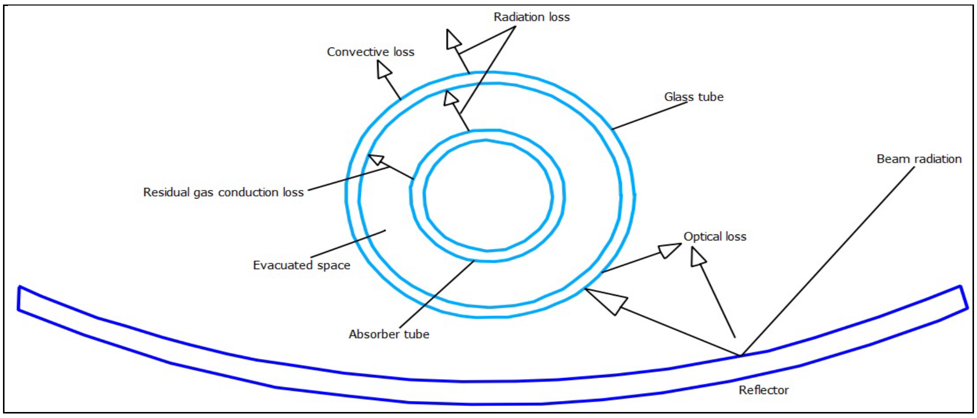

Figure 16: Cross section of a parabolic trough receiver tube

Reproduced with QGIS after: (Odeh, Morrison, & Behnia, 1998)

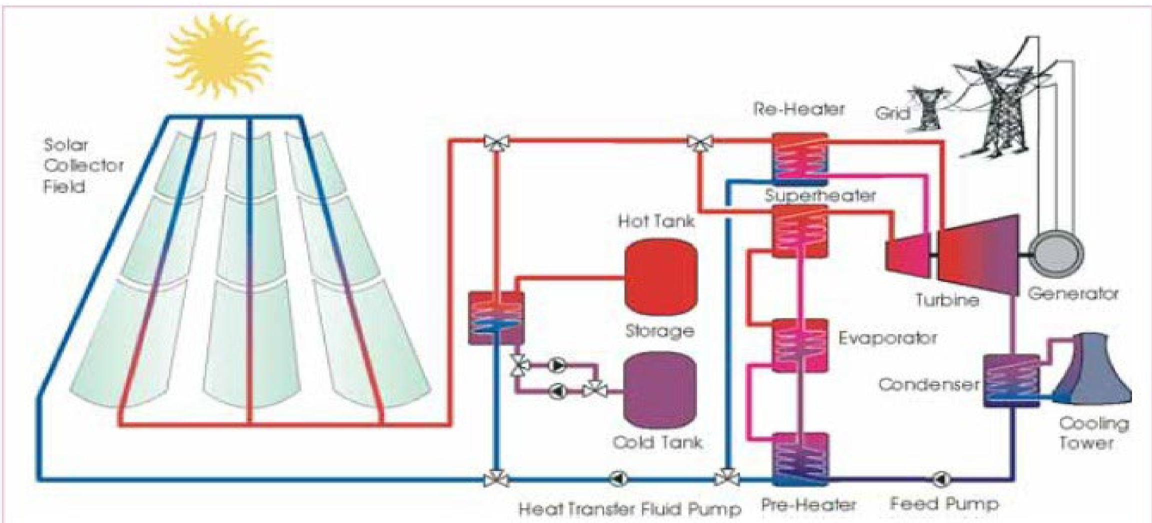

Figure 17: Layout of a typical parabolic trough plant

Source: (Müller-steinhagen, 2004)

Shown above is a conceptual diagram of how a parabolic trough plant works. In this example the receiver tubes can produce steam directly at 350-550°C at 80-120bar, (Müller-steinhagen, 2004). The plant schematic above shows how the solar collector field can run the power block directly while also heating the hot storage tank. Alternatively, thermal storage can provide heat to power the generator when the solar resource drops.

Thermal energy is used either to vaporise water directly within the receiver tubes generating steam, or a HTF such as thermal oil is used to absorb heat energy and then transfer it to the power block. This is the case in the parabolic troughs of the SEGS plants in California. This state has an installed capacity of 354MW of parabolic trough solar power plants which employ thermal oil as the HTF, (Müller-steinhagen, 2004). Within these SEGS plants the synthetic thermal oil is heated to temperatures of ±400°C, (Müller-steinhagen, 2004). This temperature is used to produce steam at 5-10Mpa in order to drive a steam turbine to generate electricity. The 354MW of installed solar thermal capacity in California is accounted for by nine separate plants which have fed an equivalent of 11 billion kWh into the grid and have generated 1.4 billion USD in revenue since their construction (Müller-steinhagen, 2010).

The nine SEGS plants were constructed between 1984 and 1991 by an American/Israeli developer and range in size from 14 MWe initially to 80MWe in the final two instances, (Richter, et al., 2009). These plants are hybrid systems which can use gas backup in the event that the solar resource drops. Gas backup is limited to a maximum of 25% of overall heat input per annum to the turbines, (Richter, et al., 2009).

2.10.5 Linear Fresnel

The linear Fresnel design consists of long flat mirrors placed parallel to each other on a single plane. Each mirror is able to rotate on one axis so that the tilt angle allows solar irradiation to be reflected throughout the day to a stationary collector tube above the mirrors. Because this design is relatively simple, overall costs are reduced. The efficiency of solar energy to electricity is equally lowered by the reduction in temperatures achieved. The stationary receiver tube is an asset to the linear Fresnel design when compared to the moving receiver tubes of the parabolic trough system.

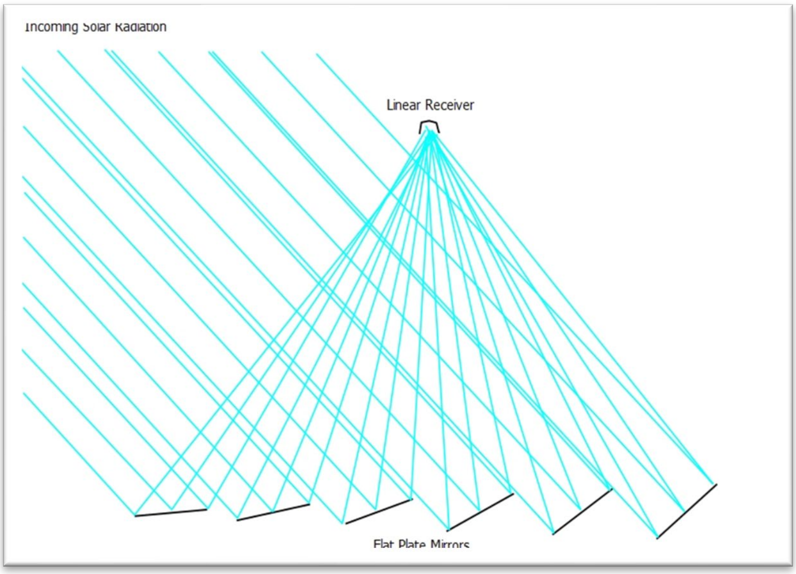

Figure 18: Cross section of the Linear Fresnel design

Reproduced with QGIS after: ("Soltigua Concentrating Solutions," 2013)

2.10.6 Central Receiver Tower

The central receiver system consists of a tall tower positioned centrally, surrounded by a field of multiple independently tracking heliostats. A large number of heliostats have the combined ability to intensify the sun's energy to higher concentrations. Direct beam radiation from the sun is reflected by each heliostat to the central receiver, (Duffie & Beckman, 2006). Each heliostat tracks the sun about two axes to maximise the amount of solar radiation captured and reflected to the collector over the course of a day. The equations used to determine the position of the heliostats are described in the Appendices, (Section 1).

The high concentration of solar energy at the receiver is transferred to a HTF by thermal conduction and convection, (Sebitosi & Meyer, 2010) and this is then pumped down the tower to produce steam. Different HTFs are used in both operational and demonstration plants. Some of these examples are "water/steam, liquid sodium or molten salt, (sodium nitrate/potassium nitrate)," (Sebitosi & Meyer, 2010). Different designs of the receiver/tower system use variations of the Carnot cycle but the overall process is similar to all central receivers (Cengel & Boles, 2011). These alternative designs are covered in subsequent sections of this thesis.

The main focus of this thesis has been CSP via central receiver technology. Continued interest in this technology has arisen due to the very high temperatures achieved at the collector surface. Temperatures range from 800°C to well above 1,000°C. Temperatures as high as 1,500°C are reported by Sebitosi and Meyer (2010), who state that central receivers, "could achieve concentrations between 300 and 1,500°C," (Sebitosi & Meyer, 2010). This high temperature allows for greater efficiencies of conversion between the collector surface and the outlet from the turbine. This relates to the Second Law of Thermodynamics, which deals with the entropy of a system continuously increasing. The system will always move to a state of higher disorder, as the energy concentration within the system diminishes.

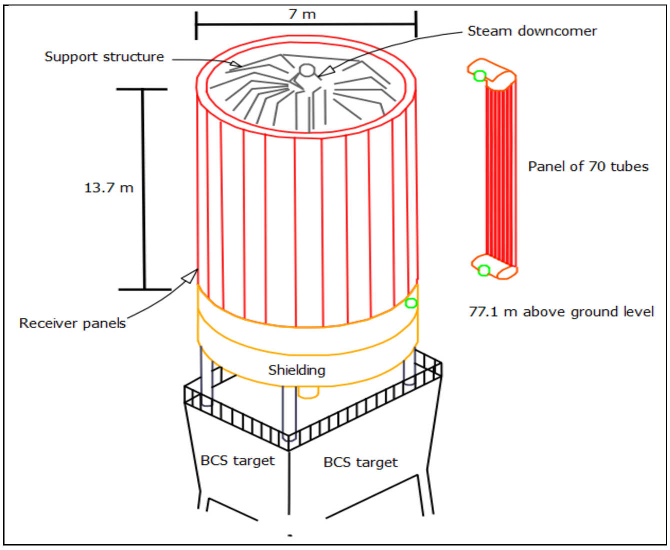

Figure 19: Central receiver design utilising steam as the HTF

Reproduced with QGIS after: (Geyer & Stine, 2001)

The higher temperatures attained by central receiver plants due to the higher concentration ratios result in higher thermodynamic efficiencies and higher thermal energy storage densities, (Gauché, 2012c). This is the reason for the Gemasolar plant being able to sustain production for twenty-four hours per day, in comparison to the storage abilities of parabolic trough plants, (Gauché, 2012c). Another crucial factor of the high temperatures reached by central receiver plants is that dry cooling becomes more viable. This is particularly attractive in the water scarce regions of South Africa within which the high solar resource zones are also located. Due to the high temperature differential between the central receiver and the ambient air, adequate cooling is still attainable despite a loss in efficiency.

A central receiver plant has fewer moving parts for the HTF to travel through compared to the multiple rotating pipes/joins connecting the numerous parabolic trough segments connected in series. This reduces the maintenance costs over the year as the likelihood of a leak occurring is reduced. If leakage occurs, it would bring plant production to a standstill, reducing its capacity factor and increasing the cost of its electricity. In some systems the heat transfer fluid used is molten salt, which is then transferred to a heat exchange surface within a boiler generating steam used to drive a conventional turbine (Richter, et al., 2009). Even without the added advantages gained by incorporating thermal energy storage capability, central receiver plants are able to produce electricity for up to thirty minutes in the event of intermittent cloud cover due to the thermal inertia of the system, (Gauche, 2012c).

2.10.6.1 Central Receiver Design Variations

The basic central receiver plant design consists of a central tower housing the receiver at the top surrounded by a field of heliostats at ground level which reflect solar radiation towards the receiver. There are several receiver designs. Three variations are discussed here, namely the cavity, external and volumetric receiver types.

2.10.6.2 Cavity Receiver

Convection and radiation losses from any thermal receiver need to be reduced in order to maximise overall system efficiencies. In an effort to accomplish this, engineers have designed the cavity receiver which places “the flux absorbing surface inside an insulated cavity,” (Geyer & Stine, 2001). Radiation from the heliostat field is reflected through the aperture of the cavity receiver onto the internal absorption surface behind/inside of which a HTF is transported. The size of the aperture is typically “one-third to one-half of the internal absorbing surface,” (Geyer & Stine, 2001). The main design consideration of a cavity receiver is the flux absorption capability. The radiation flux reaching the aperture plane of the cavity receiver must be balanced to not exceed the heat absorption capabilities of the cavity receiver and the HTF used. Both the heliostat field and the cavity receiver design must be matched according to the performance abilities of both. An example of an operational cavity receiver is the 5MW plant designed and built by eSolar in the Mojave desert in California.

2.10.6.3 External Receiver

An example of an external receiver is that built by RocketDyne and used in the Solar One and Two demonstration plants in California which used steam as the HTF in a direct steam loop. Solar One was later upgraded to allow molten salt to flow through the receiver as the HTF and was renamed Solar Two, (Kolb, Ho, Mancini, & Gary, 2011). In the past, external receivers have typically been cylindrical in shape and consist of vertical tubes that are welded together; these tubes are normally 20-56mm in diameter. Heated fluid is removed from the top of these tubes via a header while ‘cool’ HTF is pumped through the bottom of each tube, (Geyer & Stine, 2001). The external receiver for Solar One consists of, “24 panels, each 13,7m, (45ft), high, consisting of 70 – 12,7mm (1/2inch) diameter tubes,” (Geyer & Stine, 2001). 18 of the 24 panels produce steam directly, while the remaining tubes are used for preheating.

2.10.6.4 Volumetric Receiver

The volumetric CSP system does not use a liquid in the receiver. A gas, normally air, although hydrogen and helium variations exist, is pumped through the focal point of the reflected solar radiation. The Brayton Cycle refers to the gas power cycle normally used in gas turbine power plants and aircraft engines. An example of a volumetric design based on the Brayton Cycle is that investigated by a researcher at SU. This design is referred to as the Stellenbosch University Solar Power Thermodynamic cycle, (SUNSPOT), and it incorporates several state-of-the-art components to harness solar power, (Kröger, 2011). The SUNSPOT cycle is considered in more detail below.

The use of expanding hot air heated in the volumetric receiver produces steam which powers the turbine attached to the generator, (Kröger, 2011). The turbine inlet air temperature reaches 800°C. Hot exhaust gases from the turbine are then pumped through hot rock storage beds. This stored thermal energy can then be used at night, or dispatched when needed, by running the typical Rankine cycle steam turbine at lower temperatures, (Kröger, 2011). The SUNSPOT cycle is also hybridised with natural gas, (or bio fuel), so that “changes in electrical output due to fluctuations in solar radiation during cloudy or rainy periods lasting hours or even days may be eliminated,” (Kröger, 2011). Note that due to the aridity of areas in SA which contain the best solar resource, (as is generally applicable worldwide), the dry cooling system in the SUNSPOT cycle is suited to the large variation in diurnal maximum and minimum temperatures experienced in these areas. Desert environments typically have very cool night-time temperatures. At night the ambient temperature can be 20°C lower compared to the day time averages, (Kröger, 2011). These lower average temperatures at night allow for higher efficiencies in the operation of dry cooling units. Even considering the lower relative humidity of the air in these locations, the loss in cooling effect of the dry cooled unit is offset by improvements gained from the drop in temperature at night.

2.10.7 Gemasolar 20MW CSP Plant

The Gemasolar plant has recently been constructed in Spain (end of 2011) and has a total output of $20MW_e$. It is also the first plant of its kind to have demonstrated twenty-four hour base load electricity production during its first year of operation. The cost of the plant was in the region of 390 million Euros to construct and was part of a partnership between Torresol and the Spanish government, (Burgaleta, Arias, & Ramirez, 2011). This high cost is associated with the plant being a pilot, with costs for such plants normally being 2-3 times the cost of the mature technology, (Gauché, 2013a).

Gemasolar is equipped with molten salt storage capable of holding enough thermal energy to run the power block of the plant for fifteen hours. Temperatures in the storage tanks reach a maximum of 565°C, (Burgaleta, et al., 2011). The length of the storage capability is dependent on the availability of sufficient solar radiation. In the event that the available solar resource is insufficient to allow continuous production, the option of using a maximum of 15% gas backup annually is allowed at Gemasolar. Due to improvements in availability of electrical energy offered by TES the Gemasolar plant demonstrates a 75% capacity factor annually, (NREL, 2013). The heliostat field of the plant comprises of 2,650 mirrors and is oversized, ($120MW_{th}$), to provide additional thermal energy to the storage tanks when available. Gemasolar is one of the first commercially sized CSP plants that employed molten salt as the heat transfer fluid as well as the storage medium.

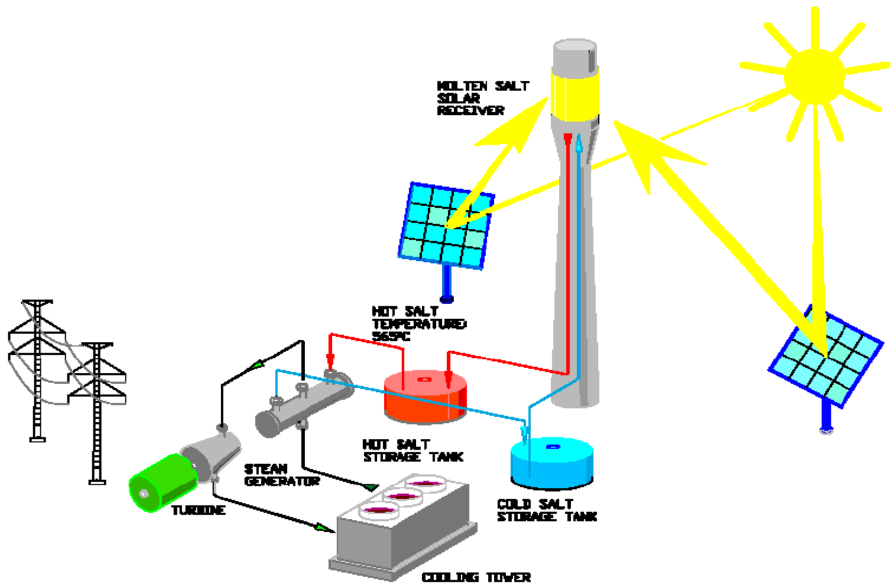

Figure 20: Basic Gemasolar plant schematic

Source: (Burgaleta et al., 2011)

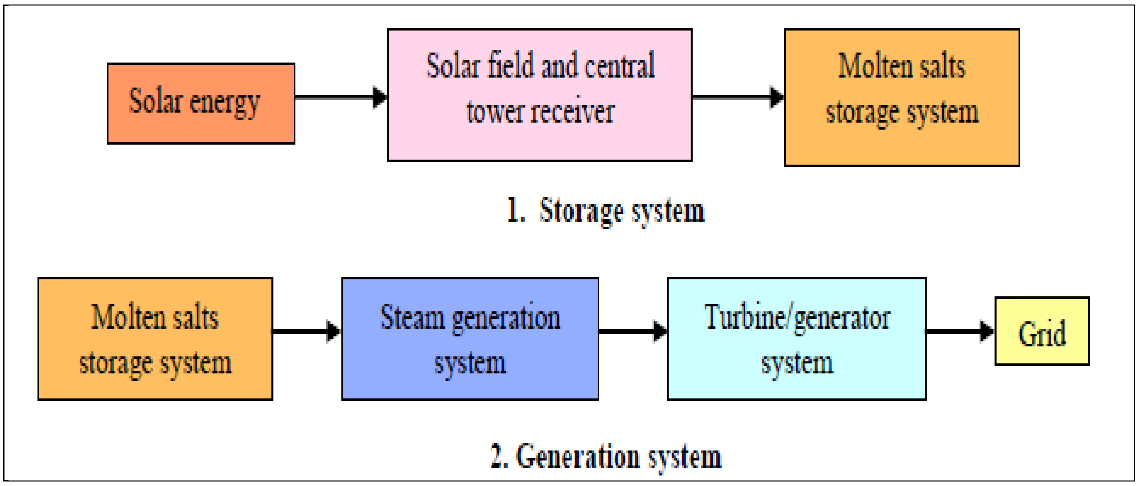

Figure 21: Gemasolar energy flow diagram

Source: (Burgaleta, et al., 2011)

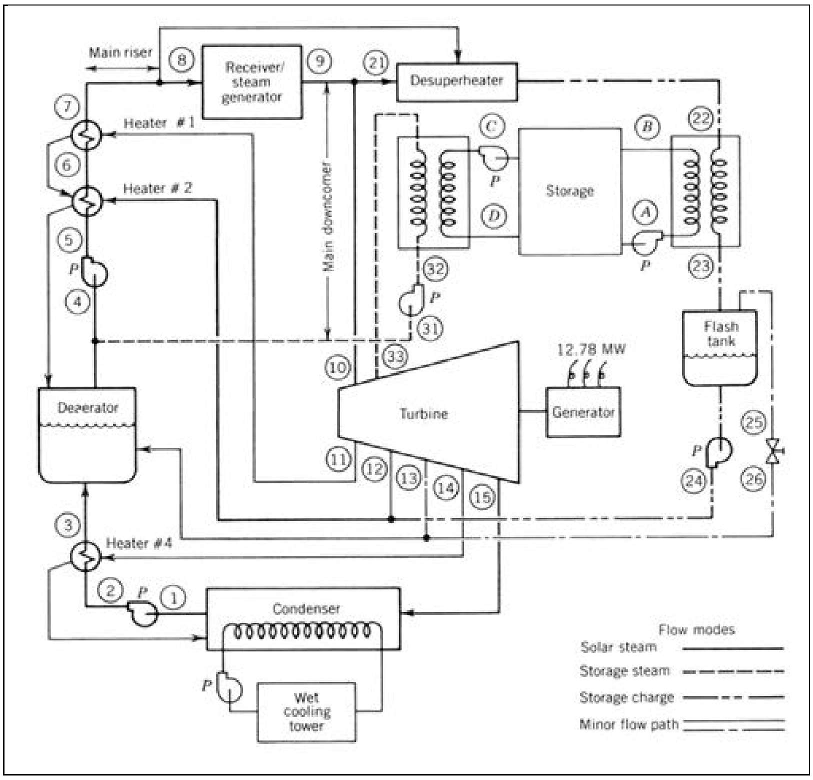

Figure 22: Schematic of Solar One CSP Plant

Source: (Geyer & Stine, 2001)

2.10.8 Cost Reductions in Concentrating Solar Power

Advances within the wider CSP industry have taken place mainly in parabolic trough technology, which currently has the most installed capacity worldwide. There are several components of the central receiver plant in which possible improvements have been identified. This would lead to economic reductions in system costs. The biggest improvements are being made in the, "solar collection and heat conduction [subsystems]," (Skumanich, 2010). Individual heliostat facet efficiencies are being improved, thereby bringing LCOE downwards, (Landman & Gauché, 2013). Such work has looked at optimising the surface profile of the heliostat through modelling solar flux density annually, amongst several other parameters. The purpose of defining an optimised heliostat surface profile for manufacturing was to ascribe financial value to this modification, (LCOE). The author suggests direct cost improvements can be attained by manufacturing an optimised heliostat aperture profile, (Landman & Gauché, 2013).

In discussing available cost reductions for CSP plants, Pitz-Paal, (2008), suggests that the majority of improvements will occur in the heliostat field and storage technologies. More advanced and cheaper HTFs will also decrease the overall costs. As stated, "collector/receivers and storage systems consist of conventional material, mainly glass, steel and concrete where technical optimization appears feasible," (Pitz-Paal, 2008). The power block of a CSP plant is very similar to that used in conventional thermal plants and will most likely not experience major cost reductions or improvements, (Pitz-Paal, 2008), as these technologies have undergone improvements and modifications since their invention.

The material properties of organic thermal oils used as HTF in PT plants mean that beyond 400°C, these oils denature and lose their usefulness (Skumanich, 2010). This is not true for the current generation of CSP plants that use molten salt which is atomically stable at 500°C. The upper temperature limits of CSP are still being explored.

2.10.9 Technology Learning Rates

When a technology is used for a prolonged period of time, it normally becomes progressively less expensive through the process of 'learning by doing'. In such a case the efficiency of the processes and materials used during manufacture improve. As a particular component is repeatedly built, the manufacturing process becomes more streamlined and efficient as the technology matures (Mcdonald & Schrattenholzer, 2001). Technology learning rates are applied to cost analyses to describe the decreasing trend in price observable within various types of manufacturing processes. It is noted by researchers that within industrial learning curve theory a reduction in cost of around 20% can be expected each time the number of units constructed doubles, (Richter et al., 2009). Such a 20% reduction case is described by a progress ratio of 0.80. Given the most recent developments within the CSP industry, a progress ratio of 0.90 has already been achieved. The learning rates that are used within the modelling process here are adapted from those used in the IRP update within the new base case scenario, (DOE, 2013a). The projected learning rates for different technologies up until 2030 are displayed in Figure 23 below. Within this analysis CSP is envisioned to experience roughly a 50% reduction in cost by 2030, with PV expecting greater reductions. Wind energy is expected to undergo less learning, as this technology is the most mature of the three renewables in the analysis. Within the sensitivity analysis in Section 3.4.6, advanced combined cycle gas turbines were assigned a learning rate of 0.76% over the period from 2012 to 2030, (Kost et al., 2013).

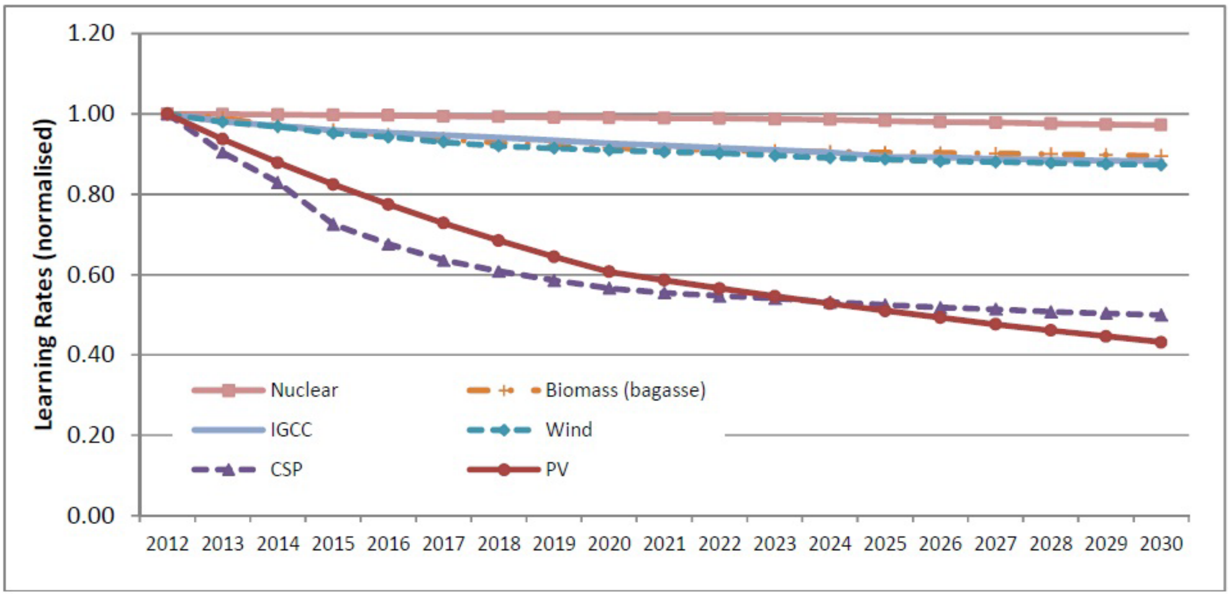

Figure 23: Technology learning rates used in the IRP update

Source: (DOE, 2013a)

2.10.10 Dry Cooling

Energy researchers propose that dry cooling facilities be used for CSP plants, (Pistocchini & Motta, 2011). In a dry cooled example, a phase-change material is used as storage, which absorbs heat during the hot day and cools itself while producing electricity at night. As stated earlier in Section 2.10.6.4 the larger temperature range between night and day of the desert environment mean a dry-cooled plant is able to save on its cooling costs at night. Dry cooling has been successfully demonstrated in current operation at the Matimba 4,000MW dry cooled coal power station near the town of Ellisras in the Limpopo province of South Africa, (Eskom, 2012). In the proposed dry-cooling CSP plant which uses a phase-change material, the 'parasitic power consumption' needs of the cooling plant are shifted to night-time periods when electricity prices are reduced, (Pistocchini & Motta, 2011). A reduction in investment costs provided by saving on cooling, indicates potential savings on overall plant costs (Pistocchini & Motta, 2011).

2.10.11 Energy Storage

The notion of 'energy storage' can be applied to every compound used as fuel within society. Biomass products are commonly used by society and are composed of naturally stored solar energy. Through the process of photosynthesis solar energy was originally stored as cellulose and was further concentrated by the formation of coal and oil. The storage and release of energy guides our electricity generation industries. Energy storage is vital to the viability of RE, bringing it within the range of performances attained by conventional thermal generators. Different technologies are being investigated for the storage of energy of which several are listed below in Figure 24.

Large scale energy storage technologies	Response Time	Discharge Time	Efficiency ηWh (%)
Pumped Hydro Storage (PHS)	Minutes	10h<	70-80
Compressed Air Energy Storage (CAES)	Minutes	Hours	41-75
Thermal Energy Storage	Minutes	Hours	95-98
Lower Quality Applications (transient stability and frequency regulation)			
Flywheels	<1s	<10m	80-90
Capacitors	<1s	<10m	
Superconducting Magnetic Energy Storage	<1s	<10m	75-80
Bridging Power (contingency reserves, load following, additional reserves)			
Lead-Acid	1s<1m	±1h	75-90
Nickel-Cadmium	1s<1m	±1h	60-80
Nickel Metal Hydride	1s<1m	±1h	65-75
Lithium-ion	1s<1m	±1h	85-98
Energy Management			
High-Energy Batteries:			
• Sodium Sulphur			70-85
• Sodium Nickel Chloride			80-90
• Vanadium Redox			60-75
• Zinc Bromine			70-75

Figure 24: MWh scale energy storage technologies

Sources: (Denholm, et al., 2010), (*Electrical Energy Storage White Paper*, 2011)

The 'round-trip' efficiency of a storage device is calculated by knowing the amount of energy initially stored and the energy subsequently returned. This is defined as the roundtrip efficiency, (ηWh), of the device. The following section provides a brief overview of three types of energy storage technologies that offer MWh capacities.

2.10.11.1 Compressed Air Energy Storage (CAES)

There are two instances of 100 MWh CAES facilities worldwide, one in Huntorf, Germany and the other in Alabama, America, (Garrison & Webber, 2011). These rely on natural underground caverns allowing for large volumes of highly compressed air to be stored at cool temperatures underground. An integrated wind and solar energy storage system has been proposed by energy researchers. In this instance wind power would be used to compress air, while CSP would replace the gas fuel stock normally needed to heat the cold, compressed air before being used in a high and low pressure turbine for energy generation (Garrison & Webber, 2011). This example is mentioned to show how wind and solar power can be integrated to increase reliability of electricity supply.

2.10.11.2 Pumped Hydro Storage

Pumped hydro is the most widely used method of energy storage. Energy is kept as gravitational potential energy within elevated water. This technology is dispatchable with response times primarily dependent on the length of the penstock. The penstock is the tube which carries water from the top reservoir down to the turbine. PHS has recently experienced tighter land use regulations as environmental legislation becomes more stringent.

There are three large-scale Pumped Hydro Storage (PHS) facilities currently in use in South Africa. The Drakensberg facility was designed to produce 1,000MW for ten hours, (10GWh storage) and began operation in 1981, (Eskom, 2014a). The Palmiet facility was completed in 1988 and can produce 400 MW for 25 hours, (10GWh storage), (Eskom, 2014b). The newest PHS facility was constructed on the boundary of the Free State and KwaZulu Natal (Eskom, 2014c). This facility, named Ingula, is scheduled to begin operation in 2014 and has a storage capacity of 21.31GWh. The new Ingula plant can produce 1332MW for 16 hours, (Eskom, 2014c). Although Eskom is currently using a limited number of PHS facilities, the nature of the topography of South Africa indicates that there is room to build future plants. Before the site for Ingula was selected, some 90 other potential locations were investigated, (Eskom, 2014c). Although many locations exist, more modern and thorough environmental regulations mean that the majority of these locations are unavailable. A main concern is the flooding of large reservoirs used in PHS, whereby the existing land use is converted to water storage. This removes plant and animal species in the area, which has direct implications for local biodiversity.

2.10.11.3 Thermal Storage

The storage of heat energy within CSP plants is primarily achieved through pressured steam, molten salts, liquid metals, hot rocks, solid state, (concrete, metal), and phase change materials. TES has significantly high round-trip efficiencies, (as high as 95%), when compared to lithium ion batteries and pumped hydro facilities which range near 80%, (Denholm & Mehos, 2011). The different chemicals and materials used within thermal storage media fall into one of two categories of heat characteristics, namely sensible or latent, (Ter-Gazarian, 1994). The former deals with heat energy that actually can be registered, (sensed), as a change in temperature of the chemical materials, whereas latent heat is “based on the energy associated with a change of phase for the storage medium, (melting, evaporation or structural change),” (Ter-Gazarian, 1994). Lithium hydride and lithium fluoride with working temperatures of 686°C and 850°C respectively both rely on phase change properties to store large amounts of energy (Ter-Gazarian, 1994).

2.10.12 Dispatchability

An energy utility needs to operate and maintain a large number of different types of power plants. Each plant is categorised according to its functionality to the utility. In most cases coal and nuclear plants are used to meet the largest share of continuously demanded electricity and are termed ‘base load’ plants. A second category of ‘load-following’ or ‘cycling’ plants is used to accommodate the predictable increase in daily demand. A third category of ‘peaking plants’ is used to meet peak demand periods. This category of peaking plants normally only needs to operate “less than a few hundred hours per year,”(Denholm et al., 2010). A fourth category of plants is maintained by an energy utility to meet unpredictable increases or sudden fluctuations in demand, such as the failure of a base load plant or transmission line, or any other event which might disrupt the integrity of the system, (Denholm et al., 2010). This category of plants is termed ‘operating reserves’ and is used to mitigate “frequency regulation, load-forecasting errors and contingencies,” (North American Electric Reliability Corporation, 2008), originally quoted by (Denholm et al., 2010). In other literature this fourth category of plants is classified by utilities within ‘ancillary services,’ (Garrison & Webber, 2011). The management of the problems associated with frequency regulation and contingency requirements means a utility must keep several plants on 'idling' or ‘spinning reserve’. This increases the overall expense to a utility and decreases the efficiency of these plants.

The most common method used to produce industrial scale electricity quickly in response to demand is via pumped hydro or OCGT/CCGT facilities. Both of these are able to match peak demands when necessary through the release of stored energy. Dispatchable power is also useful to a utility for, "load-balancing [and] the ancillary services market," (Garrison & Webber, 2011). The ability to dispatch energy when needed is of primary interest to this thesis. The TES capability of CSP places it in the same category of energy generation technologies as gas and pumped hydro storage. Utilities can release stored thermal energy when needed, such as during, "periods [of] peak power demand, cloudy weather or even at night," (Skumanich, 2010). One of the first examples of dispatchable power provided from a solar plant was Solar One. This plant had a CF of 65% through the use of thermal storage, an improvement of 260% over the 25% CF of previous generations, (Garrison & Webber, 2011).

In the discussion of dispatchability, an added benefit of CSP is the ability to complement the integration of Wind and PV into a grid, both of which are intermittent and currently lack storage options that can compete with thermal storage. As Wind and PV prices are steadily dropping, a greater penetration of these technologies can take place with the inclusion of CSP. CSP allows for increased overall flexibility within the grid (Denholm & Mehos, 2011). This flexibility relates to CSP altering its production depending on how climatic conditions affect other renewables. The incorporation of large amounts of Wind and PV into a grid can create difficulties for a utility because of their higher intermittency and lower operability (Dinter & Gonzalez, 2013). These authors suggest that CSP plants can "contribute to system flexibility supporting the continued reliability of the electric power system," (Dinter & Gonzalez, 2013). It is stated that CSP can "accommodate the forecast uncertainty and variability of non-dispatchable renewable generation," (Trabish, 2012), mainly due to thermal storage.

Current research shows that a greater use of PV is feasible with greater penetration of CSP into an energy grid, (Denholm & Mehos, 2011). The intermittency of PV is complemented by the thermal storage of CSP, making it more financially viable and attractive to investors by lowering the levelised operational costs of the plant. There are other benefits to utilities derived through incorporating energy storage facilities. The installation of additional transmission and distribution systems can be avoided by situating energy storage nearer to the load, (Denholm et al., 2010). Also mentioned is the role of energy storage in power quality and stability control on the customer side, where the regulation of, "voltage spikes, sags, momentary outages and harmonics," (Denholm et al., 2010), is achieved through the utilisation of energy storage devices. Included below are two figures taken from the Denholm and Mehos study, (2011). Both of these figures deal with PV penetration into the California energy mix and the effect of this on other technologies within the grid.

Figure 25 shows the difference between a 0% and 10% PV penetration, i.e. up to 10% of the electricity requirement of California is provided for by PV. Each of the four segments of the graph illustrates a typical day. With a higher penetration of PV, the overall reliance on combined cycle, hydro, pumped storage and gas turbine power plants diminishes substantially. Figure 25 represents the simulated dispatch occurring on a summer day when electricity requirement is high to accommodate air conditioning.

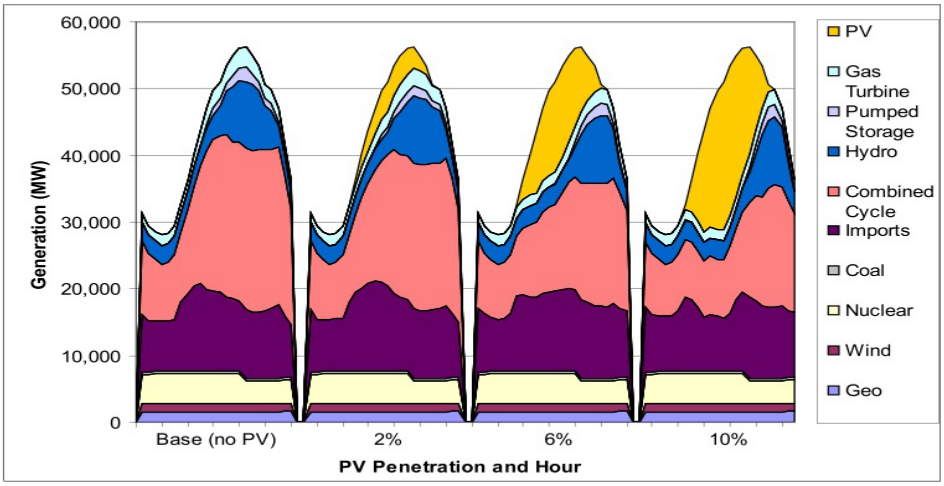

Figure 25: Simulated dispatch for California Summer day, 2011

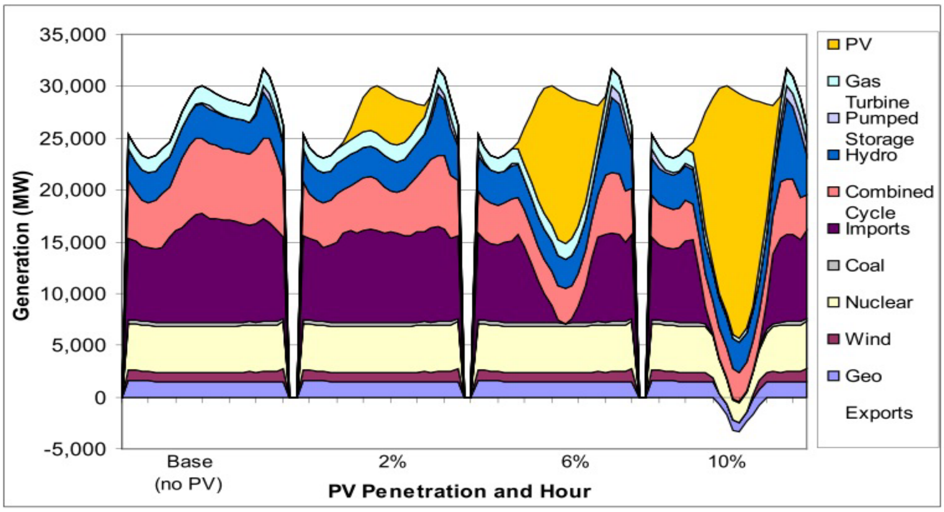

Figure 26: Simulated dispatch for California Spring Day, 2011

Source: (Denholm & Mehos, 2011)

The electricity requirements during Spring when PV penetration is set to 10%, are substantially lower than the comparative summer day. Here we observe that PV is able to play a more significant role in that it displaces several types of conventional generators. Imports of electricity into California are totally displaced, and the State begins to export surplus electricity. The model used to produce Figure 25 and Figure 26 demonstrates the ability of the system to incorporate variable renewable generators, by defining the flexibility of conventional generators to either increase or decrease production. The above figures were created using the REFlex program, which "is a reduced form dispatch model designed to examine the general relationship between grid flexibility, variable solar and wind generation, and curtailment," (Denholm & Hand, 2011). The models constructed in this thesis use a similar approach to that outlined above.

In terms of dispatchable power, coal plants and the Koeberg nuclear plant are not able to easily or effectively change their production output over short timescales of minutes to hours, (Denholm &

Mehos, 2011). This is for a number of reasons. The temperatures within the furnaces of a coal plant are maintained at constant levels. High thermal inertia means the production output cannot easily be throttled. These plants also aim to maintain set CFs over the course of a year which is intricately tied to the financing of the plant. The mechanical components of a coal plant, (steam turbines/boiler), are not adapted to being continually cycled as this significantly increases attrition of the mechanisms. Most wear and tear occurs during the critical start-up phase of a plant when cold components experience the most stressful conditions. As stated, "cycling operations, that include on/off start-up/shutdown operations, on-load cycling, and high frequency MW changes for automatic generation control can be very damaging to power generation equipment," (Lefton & Besuner, 2006). For reasons such as these coal plants are not suited for providing peaking power.

Recent research released by NREL compared a molten salt power tower, (CR), with a parabolic trough plant, (PT), using production cost modelling, (Jorgenson, Denholm, Mehos, & Turchi, 2013). This work focused on the operation of these CSP-TES plants across one year and specifically, on the dispatch of electrical energy both directly from the solar field during daylight hours, and from thermal storage when the solar resource drops. To optimise electrical energy output over the year, the authors evaluated the effect of changing the Solar Multiple, (SM), which is a function that coordinates the size of the heliostat field in relation to the associated power block, (Jorgenson, et al., 2013). Some observations made by this research point to the higher efficiency of the turbine in the CR plant, caused by higher temperatures attained at the receiver. The energy production profile of the CR plant also displays lower variability over the year, on account of the cosine effect being more noticeable during the winter months for PT plants, (Jorgenson, et al., 2013). The cosine effect is explained in Section 1 of the Appendices.

In this research the two types of solar plants analysed were required to produce the same volume of energy annually, (1.2 TWh). However, to achieve the same annual power production, the capacity of the power block for the PT plant needed to be higher. This is necessary because the system advisor model calculates the performance of an individual trough when the sun is directly above, (Jorgenson, et al., 2013). This model assumption represents an optimum power output point for the trough, and does not accurately represent the effect to system performance caused by seasonal variations, (Jorgenson, et al., 2013). The Solar Multiple, which aims to optimise the performance of each plant, then assumed a higher rated annual performance for a given size of solar field, (PT). The result, in summation, is that the turbine rating of the PT needs to be greater to account for the underperforming solar field.

The CR plant is less affected by seasonal variations, meaning the turbine rating and the solar field are more effectively matched, allowing for a smaller turbine to achieve the same annual production. Further optimising was conducted using the changing effect of different storage capacities on LCOE. One of the outputs from this research, showing energy output from both plants, is supplied below in Figure 27. This result shows the differences in the energy production profile between the two plants. One of the main conclusions obtained here is that "a parabolic trough CSP-TES plant may require a higher capacity, at a greater expense, than a similar molten salt power tower to achieve the same annual output, largely due to a larger seasonal variation in output, lower thermal efficiency, and greater storage losses," (Jorgenson, et al., 2013).

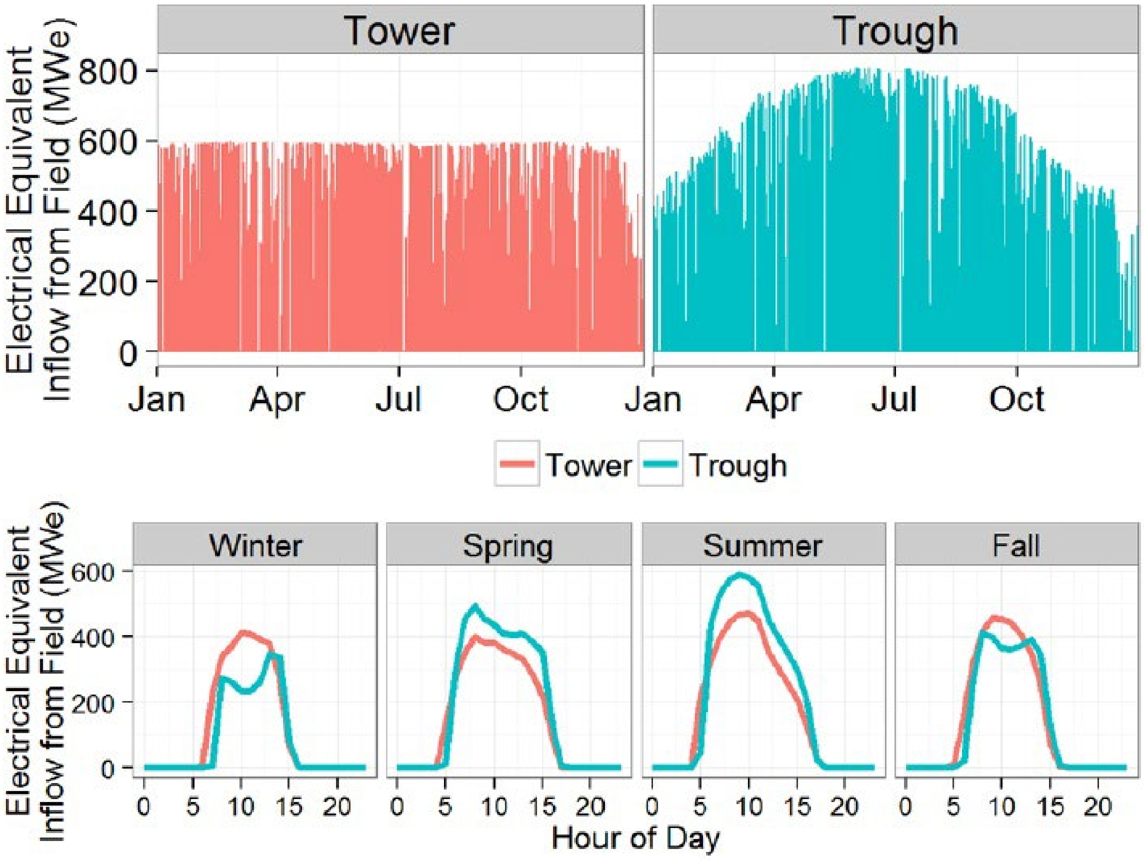

Figure 27: Modeled electrical energy output modeled for CR and PT plants

Source: (Jorgenson et al., 2013)

2.10.13 Energy Systems Modeling

The main investigative technique used in this thesis is a computer model to explore hypothetical scenarios of high rates of penetration of renewable generation technology over the long term using 2050 as the time horizon. The software platform chosen was Excel. A model, as it applies to this thesis, is a computer based representation of a real world situation, whereby mathematics is used to describe physical properties of the investigated situation. A model is formally described as, "a prototype of something that is real." (Bisschop, Roelofs, 2008), and can be concrete, (tangible) or abstract, (intangible). The language of mathematics is very powerful when applied to modelling. Mathematical concepts, variables, parameters, operators and data may be integrated in order to produce a required answer. A model can include unknowns and if the model is developed specifically to calculate these unknowns, then the model can be solved, (Bisschop, Roelofs, 2008). This is critically important because unknown variables may then be formally described through assigning a mathematical value to them.

A computer model can have any number of purposes, such as understanding a complex system that would otherwise be inaccessible due to the amount of data involved. This means that tools are necessary for a user to investigate real world situations. For instance, in the engineering discipline, models are used to analyse "the processes of a specific component or sub-components [within a larger system]," (Bhattacharyya & Timilsina, 2010). Within the energy research field, different aspects of the energy sector's of countries can be analysed according to the "energy-economy interactions at the national and international levels," (Bhattacharyya & Timilsina, 2010). Using a computer model allowed the calculation of energy production required from the three renewables to meet an exogenous demand profile in 2050. Wider implications regarding the scale of the scenarios were then drawn.

2.10.13.1 Optimisation modelling

Within the analysis of the energy sector, there are two general types of model platforms, namely, optimisation and simulation models, (Merven, Cohen, Hughes, Stone, 2013). Within the former model type, constraints on the energy system are used that aim to ensure a certain outcome or result. This optimisation result normally tends towards improving system efficiency, based on user-defined requirements or types of technologies under investigation. For instance, a model used in the petroleum industry controls certain parameters of a refinery. Here, a constrained optimisation model is used to maximise profit by minimising inefficiency, (Manne, 1956). Examples of the constraints within this model are that the amount of crude oil used in processing does not exceed the amount of crude oils purchased, and upper and lower boundaries on the quality of the final products. Any constraint may be used in energy modelling, dependent on the required outcomes of the energy system being researched, (Merven, et al., 2013). Optimisation models are normally deterministic in nature, which leads to a certain degree of simplification of real world complexity and randomness, through the use of linear programming. This has meant the development of more complicated, "multi-stage stochastic optimisation [models]," (Merven, et al., 2013), which use algorithms to partially depict the chaotic nature of complex systems through the use of probability calculations of potential ranges. Examples of widely used modelling programs that have stochastic features are the TIMES and MARKAL energy models.

A problem with optimisation models is that they introduce, "knife-edge/winner takes all effects," (Merven, et al., 2013), whereby an objective winner is selected to the exclusion of all other potential alternatives. Real world consumer behaviour means that alternatives are sometimes chosen based on subjective criteria. These subjective criteria are problematic to represent in optimisation models, because they are difficult to parametize mathematically, (Merven, et al., 2013).

2.10.13.2 Simulation modelling

The second general type of modelling used for medium and long term energy planning, is simulation modelling. The most basic form of a simulation model is a simple accounting spreadsheet, where the user specifies each and every input, (Merven, et al., 2013). The level of sophistication of a simulation model can increase, dependent on the purpose for which the model is being used. Simulation modelling can be used in circumstances where algorithms are not required to calculate one optimal solution. Rather, a range of possible solutions is found by the model user. Simulation models are useful because they avoid the 'winner-takes-all' effect identified above, as the user can set their own subjective constraints. Simulation models are also, "very helpful for representing and understanding complex interactions that exist within the energy system, that are generally poorly represented in optimisation models," (Merven, et al., 2013).

Simulation modelling was chosen for use in this thesis. The model studied the integration of the three RE technologies within a future hypothetical grid. This means that the study was not a technology choice investigation that might have led to a single ‘knife-edge’ technology being dominantly represented by the model. The purpose was to investigate how variable RE technologies might interact at different capacities, both with each other and a fluctuating demand for electricity. Using simulation modelling allowed flexibility in assessing these interactions, because a range of possible future scenarios are created with different technology capacities. The system constraints were defined to appropriately address the research objectives of the thesis. Examples of simulation models are those used within climate mitigation research for the IEA Energy Outlook as well as SEI’s LEAP model and the IAEA’s MAED spreadsheet model.

2.10.14 Environmental Impacts of Renewable Energy Plants

As capacity of installed RE facilities increases around the globe, the potential for environmental impacts increases. Even ‘Green’ technologies have impacts which are becoming more thoroughly understood. Causes of environmental impacts are complex, with only some discussed here.

Concern around bird fatalities is often raised with regard to wind farms. This relates to birds being unable to see rotating wind turbine blades. Also, bird populations could be negatively affected if a wind farm disturbs established migratory routes. However, a study by De Lucas et al, (2004), found that bird deaths associated with a wind farm studied in the Andalusia province of Spain did not seem to be greater than those caused by other manmade structures, such as “highways, power lines, radio/television towers [and] glass windows,” (De Lucas, et al., 2004). Similarly, a study conducted in 2009 calculated bird deaths attributed to different energy technologies, namely, wind, coal and nuclear, finding, “between 0.3 and 0.4 [bird deaths] per GWh for wind, and 5.2 per GWh for fossil fuel,” (Sovacool, 2009). One of the results of this study found that in the United States 7,000 birds were killed by wind farms in 2006, 327,000 by nuclear and 14,5 million by fossil fuel. The causes for these deaths within coal and gas generation were, “collision and electrocution with operating plant equipment, and from poisoning and death caused by acid rain, mercury pollution, and climate change,” (Sovacool, 2009). The assessment for nuclear power related avian deaths looked at the upstream and downstream fuel cycle processes. This comparison between energy related fatalities from different energy technologies provides useful perspective into the relative impacts of a renewable technology such as wind power.

Bird fatalities have been reported at CSP and PV plants. Recent incidences of this occurring took place at the Ivanpah plant in San Bernardino county, California. This plant consists of 173,500 heliostats covering an area of 2.6km^2. The plant has three towers, each 140 meters in height, (NREL, 2013). The height and large size of future central tower systems mean that collisions might occur when birds are unable to avoid them, (Tsoutsos, et al., 2005). These authors state that “central concentrator power systems could pose a danger to birds, but operational experience shows that birds avoid any danger areas,” (Tsoutsos, et al., 2005). The large amount of sunlight being reflected from the heliostat field onto each tower creates a zone adjacent to the receiver where concentrating sunlight generates a solar flux of an intensity that can kill flying insects and birds. The issue of high solar flux temperatures potentially impacting on airborne species was reported as early as 1984, when researchers studying the Solar One facility in Clark county, Nevada, found that insects were being more frequently killed than birds, (McCrary, et al., 1984).

2.10.15 Conclusion

Current literature on the role of renewable energies indicates that these technologies are likely to contribute greater proportions of electrical energy in the future. This statement is supported by literature indicating that the costs of RE are set to decline compared to conventional generation technologies as economies of scale improve and greater capacities are installed worldwide, (Landman & Gauché, 2013; Pitz-Paal, 2008; Skumanich, 2010). Further literature has discussed some of the direct benefits of thermal energy storage in terms of higher flexibility to support more intermittent renewables, (Denholm & Hand, 2011; Denholm & Mehos, 2011), and also those benefits of energy storage normally employed by utilities, that is, in terms of load following, power quality control and ancillary services, (Denholm et al., 2010), (Dinter & Gonzalez, 2013). Such benefits of CSP indicate that this technology can contribute favourably to the operation of a power market beginning to incorporate larger fractions of RE, especially in light of having higher reliability of electricity production.

Chapter Three - Method

3.1 Introduction

This chapter is structured to clearly and incrementally describe the methodological process. The main purpose of this thesis was to investigate a hypothetical large scale RE future for South Africa. Production from intermittent RE needed to be displayed in sufficient temporal and spatial resolution by developing a framework to represent the dispatch of electrical energy from a RE powerplant continuously for 8760 hours. The framework needed to simulate the combination of different technologies aiming to meet demand. When demand was not reached the imposed shortfall was measured and met by a completely dispatchable representative conventional technology. The intermittent nature of the RE resource meant that the conventional backup needed to respond on short timescales to the maximum possible demand shortfall during the year. The only generator that currently offers this level of dispatchability is gas turbine technology. For this reason an advanced combined cycle gas turbine was integrated into the modeled demand deficit from RE in each of the scenarios described in section 3.4.9 below. The cost implications of the representative dispatchable conventional are reflected in the sensitivity analysis described in Section 3.4.6.

3.2 Research Design

The Research Design process was built around fulfilling the Research Objectives outlined in Section 1.3.

- Given known solar and wind resources, (Section 3.3.2), the electrical energy outputs of selected capacities of the three RE technologies needed to be estimated. These 'selected capacities' were coordinated around the assumed 2050 demand, as described in Section 3.3.3. Calculating the RE outputs was done through the use of several models, which are described in Section 3.4.
- Once different penetrations of RE were set within the scenarios, certain criteria for selecting an optimal capacity had to be used. In this case, the performance criteria used are the fulfilment and curtailment coefficients. These are described in Section 3.3.1.
- Once the scenarios were developed, the effect on two key parameters, system fulfilment and curtailment (defined in Section 3.3.1) was analysed through the introduction of TES in a supporting role to Wind and PV, (Section 3.3.3).
- The economic performance of the RE scenarios investigated here was assessed relative to gas technology using a Levelised Cost of Electricity (LCOE) analysis. The conventional gas backup system was able to match the maximum demand shortfall imposed by the RE technologies during the year. Learning rates were incorporated into the LCOE in line with Section 3.4.5.
- To assess the potential implications and drawbacks of a large scale RE system in 2050, several indicators were used for system evaluation. These include land area, emissions (3.4.7) and water usage (3.4.8). All results from the indicators are listed in full in Appendices, Section 3.

The steps above allow a wider indication of grid reliability to be assessed, where planned and forced outages are ignored, along with other thesis limitations (Section 1.4).

The modelling technique used in this thesis has taken guidance from the research of Denholm and Mehos, (2011). These researchers analysed the potential role of dispatchable CSP within a large scale RE scenario. An output from this research is supplied below, in order to depict certain key concepts of the current thesis. Importantly, the quantity of Curtailed Solar is depicted and can be contrasted with Usable PV. In this model periods of production deficit from Wind and PV are fulfilled through dispatching thermal energy from CSP. This particular role of CSP is specifically investigated by the current thesis through Research Objective 2, (Section 1.3). Electrical energy production from conventional technology is also represented in Figure 28, showing expected lower variability compared to renewables. This model output from the Denholm and Mehos (2011) work therefore represents the key concepts of curtailment, fulfilment and dispatchability; all of which are used by this thesis. The Denholm and Mehos (2011) work concluded that the incorporation of dispatchable TES increased the cumulative amount of solar energy used from PV and CSP.

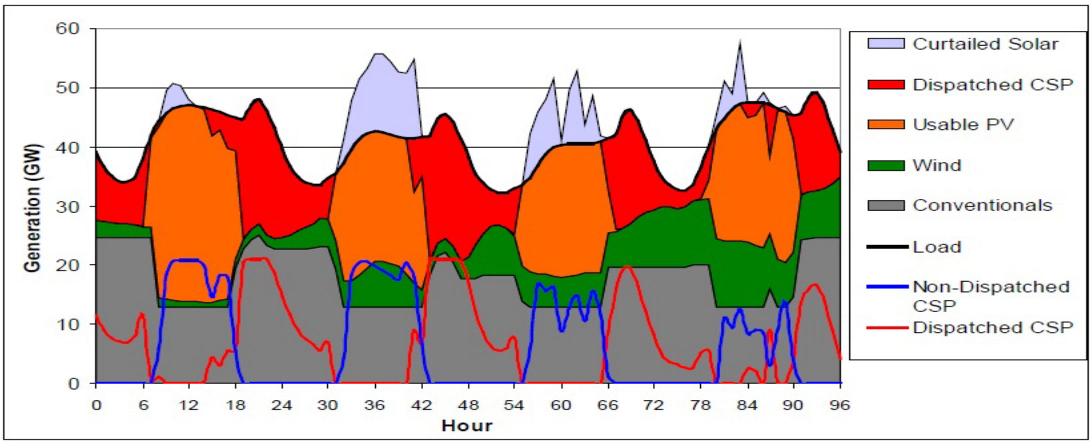

Figure 28: The interaction between conventionals, wind, PV and dispatchable CSP

Source: Denholm and Mehos, (2011)

3.3 Methodology

3.3.1 Definition of Fulfilment and Curtailment Coefficients

Curtailment of electrical energy and fulfilment of demand have been graphically represented below in Figure 29 to aid with clarity in discussing these concepts. Curtailment describes periods of over-production of electrical energy when there is a mismatch between variable production from renewables and the demand requirement. During these over-production events electrical energy must be curtailed, displayed by the orange proportions of Figure 29.

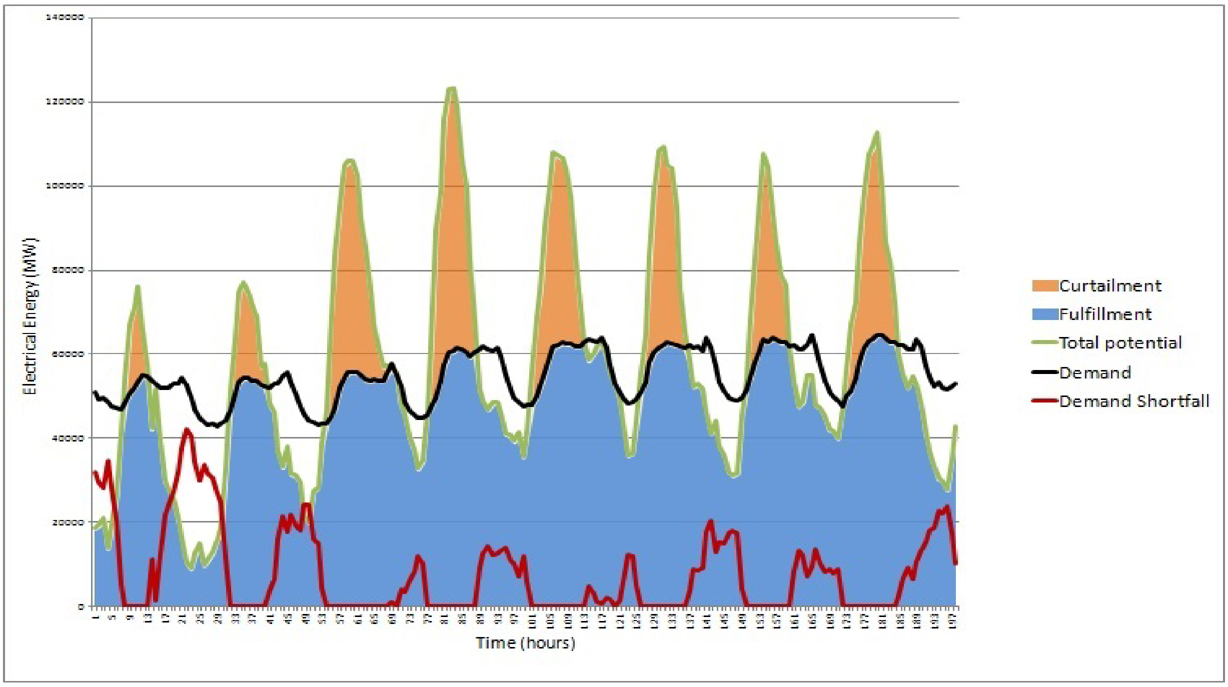

Figure 29: Representative 200 hours, showing concepts of curtailment and fulfilment

Periods of curtailment correspond to electrical energy that is not used immediately and cannot be stored. Curtailment is a problematic phenomenon prevalent in Wind and PV generation which lack financially viable and substantial electrical energy storage options. Curtailed energy translates into financial loss as it cannot be sold directly to consumers. This can detrimentally impact the LCOE of the technology. The amount of curtailment occurring within the modeled scenarios is defined as the Curtailment Coefficient (CC) and is mathematically described in Equation 1 below.

The Fulfilment Coefficient (FC) is the percentage of electrical energy sourced and used successfully from Wind, PV and CSP relative to the projected 2050 demand. Put differently, it is the amount of electrical energy demand that is successfully supplied by the group of RE generators. Fulfilment is designated by the blue sections of Figure 29. The concepts of curtailment and fulfilment are used as a method to help improve the simulation modelling process by providing indicators of the effectiveness of dispatch in meeting demand. The size of the RE system, (combined Wind, PV and CSP – constituting large scale RE scenarios), and the amount of electrical energy subsequently derived from each source is increased or decreased according to the goals of maximum fulfilment and a minimum curtailment. This forms a type of optimisation process, where the objective is to attain the maximum amount of production with the minimum amount of curtailment, (Gauché, 2012d).

The criteria used to assess the Fulfilment and Curtailment Coefficients in this thesis follow on from work previously performed on the integration of variable generation into existing networks. Some of the results from this work is summarised below in Figure 30.

Year	Country	Wind (GW)	Solar (GW)	Total System (GW)	RE penetration	Curtailment
2012	Canada	1.5			5%	0%
2011	Denmark	4.44		13.5	33%	
2012	Ireland	2.1				2.10%
2012	Italy	8.1	16.6		9.80%	1.24%
2011	Japan	2.4	4.9		0.90%	8%
2012	Portugal	4.5			20%	
2012	Spain	22.6			18.10%	3.10%
	United States:					
2011	BPA	4.5		11.5	39%	5-6%
2012	SPP	7		54	12.90%	40%
	MISO	12		98	12.20%	1-3%
	Modelling Studies:					
2011	Brinkman, et al.				20%	8%
2010	Denholm, et al.				35%	10%

Figure 30: Curtailment and Fulfilment Data

Notes: Bonneville Power Administration (BPA), Southwest Power Pool (SPP), Midcontinent Independent System Operator (MISO), Eastern Reliability Council of Texas (ERCOT).

Data sources: (Brinkman, G. Denholm, P. Drury, E. Margolis, R. Mowers, 2011), (Denholm, et al., 2010), (Lew, et al., 2013), (SONI, 2012).

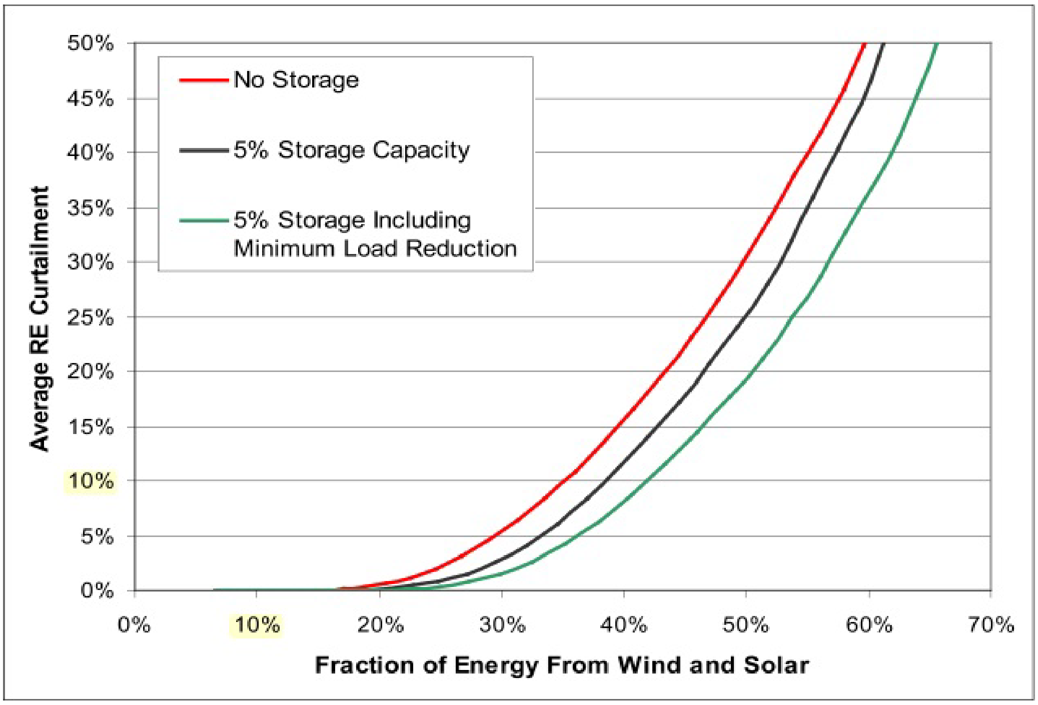

Figure 31: Energy production from wind and solar against average curtailment

Data source: (Denholm, et al., 2010).

The data represented above in Figure 28 to Figure 31 formed the guiding framework for assessing the Fulfilment and Curtailment Coefficients in this thesis. The latter figure shows the result of modelling variable generation (VG) and observing the correlated curtailment (Denholm, et al., 2010). Here, total system capacity was 60GW where the introduction of a 3GW storage device was tested. This storage device had 20 hours of capacity with an efficiency of 75%, and was modeled to “absorb otherwise unusable energy,” (Denholm et al., 2010). By introducing storage into this RE system, losses incurred due to curtailment were reduced. When RE accounts for 50% of system energy and storage is not used, curtailment is 30%. When storage is used at the same RE penetration, 50%, curtailment is reduced to 20%. It is observed by these authors that, “a maximum VG curtailment of 10% allows VG to provide about 35% of the total electricity demand, [while] adding energy storage increases the contribution of VG to about 42% of total demand,” (Denholm, et al., 2010). This maximum curtailment value was used in this thesis as a reference performance point and broad guideline. However, it should be noted that the thermal storage device used in this thesis has a higher round-trip efficiency of 98%, and does not only absorb unusable energy, but is designed to continuously charge the thermal storage units when the solar resource allows.

The issue of assessing curtailment from RE can become complex, as it is a function of integrating multiple factors. For instance, curtailment would be effected by the types of conventional technologies comprising the existing grid and their ability to respond to changes, the reserve margin, the demand profile and structure of the economy, and the availability of solar and wind resources. This list is not exhaustive, but serves to indicate that each electricity system is unique. The introduction of renewables into conventional systems and the effects on curtailment have to be studied individually and are specific to an energy system.

The RE penetrations stated above are comparatively low compared to those used in this thesis. This implies that the fulfilment criteria are more ambitious here, and have been set at a target of 90% of total system demand provided by different combinations of RE within the scenarios analysed. To calculate the curtailment events over the year, the demand requirement is subtracted from total RE production. Any periods when this value is positive equate to surplus, or curtailed electrical energy. Periods when this value is negative indicated production deficits from RE. The concept of the curtailment coefficient displays the percentage of electrical energy curtailed relative to total production from each technology

$$Curtailment\ Coefficient = \sum Curtailed\ Energy\ RE / \sum Production\ RE$$

(Equation 1)

The fulfilment coefficient indicates the total percentage of electrical energy produced by each technology and successfully used in relation to system demand, factoring in the reduction in usable electrical energy caused by curtailment

$$Fulfillment\ Coefficient = \sum (Production\ RE - Curtailed\ Energy\ RE) / \sum Demand$$

(Equation 2)

The FC and CC represent the amount of electrical energy either generated and used, or wasted by the system according to demand. These coefficients are used here as an indication of system performance. Importantly, the FC and CC are used as proxies to describe the behaviour of the technologies. By increasing the FC of one technology, specific behaviour might be amplified. The criteria above, maximum fulfilment and minimum curtailment, are used to control the installed capacities of each technology.

A full list of equations in Section 3.3.1 is provided in the Appendices, Section 6.

3.3.2 Selected Sites and Resource Data

This thesis uses site-specific historical times series data of the RE resource in South Africa. Wind data was obtained from the South African Wind Atlas, (WASA), website. The WASA project, as described earlier in Section 2.10.1, is intended to provide reliable wind data to strengthen and incentivise a local wind power market. As the most complete data series available was that for 2011, it is the wind data chosen for use in this thesis.

Solar data was acquired through an agreement between GeoModel Solar and the SU Solar Thermal Energy Research Group, (STERG). The satellite data was recorded at hourly intervals. The data consisted of three types, namely Direct Normal Irradiance (DNI), Global Horizontal Irradiance (GHI), and air temperature at ground level. The locations for this data were chosen across South Africa using a robust solar resource map from Geomodel Solar, with these shown below in Figure 32, (Meyer, 2012).

Eskom load profile data for 2011 was obtained through the Energy Research Centre at UCT. This data had originally been provided via Eskom and was recorded at five minute intervals across the year, (Eskom, 2011).

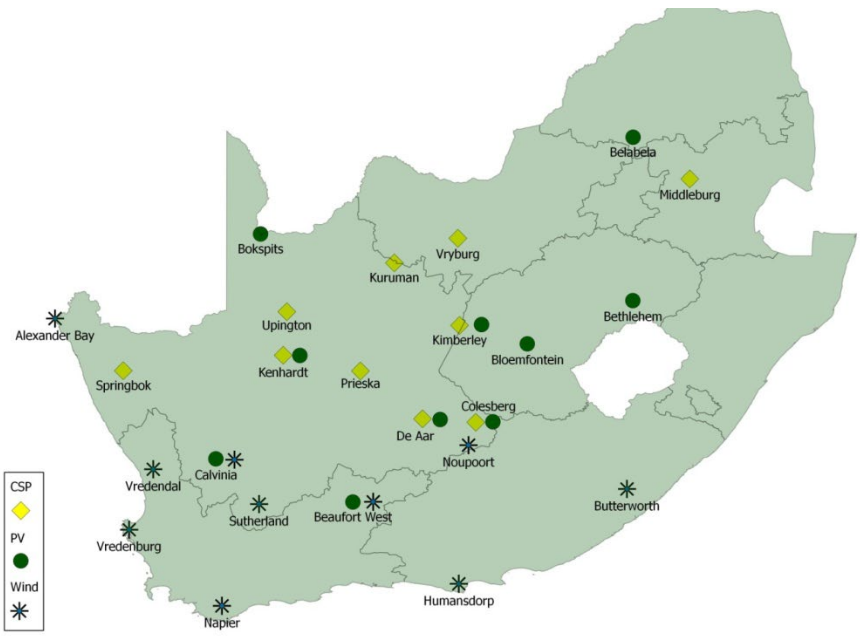

Figure 32: The 10 wind data locations, with the 20 PV and CSP locations

3.3.3 Model and Analysis Process

The steps below provide a summary of the modelling process:

1) Development of a wind generation model assuming units based on an existing 3MW commercial turbine and using real wind data from the ten locations indicated in Figure 32. This produces hourly wind power outputs. A description of the wind model is given in Section 3.4.1.
2) Using the PV and CSP models developed at Stellenbosch University, (Gauché, 2012a, 2012c), to produce hourly power outputs for the 16 locations indicated in Figure 32. Sections 3.4.2 and 3.4.3 describe these two models.
3) The electrical demand input to the model was derived from the IEP 2050 projection and Eskom load profile data for 2011. The observed 2011 demand profile was scaled upwards until total energy demand matched the IEP Base Case's 2050 demand projection of 1,900.6PJ, (DoE, 2013b).
4) This step involved scaling the electrical energy outputs found in Steps 1 and 2 to match or approximate, as closely as possible, the new 2050 demand derived in Step 3. Scaling here involved increasing the number of RE plants at each location to reach a targeted FC, outlined by the scenarios for each RE technology. These targeted FCs are displayed in the scenario design section, (3.4.9), and are calculated for individual technologies. The combined electrical energy output from Wind, PV and CSP accounts for total system fulfilment, and will not necessarily match the targeted FCs due to the manner in which the technologies are combined within the model. Wind is introduced first, then PV, then CSP in order to test the role of CSP being dispatched. Therefore, when combined in this manner, a greater proportion of energy is curtailed because the capacities of the RE technologies are added to each other. This means that although the targeted FCs for individual technologies might together equal 100%, this will not be achieved when combined by the model to give total system fulfilment.
5) The best possible match between yearly RE output and the 2050 demand is defined above as that which attains the highest level of fulfilment (90%) with the lowest level of curtailment, (target of 10%). This step additionally provided the production deficit imposed by Wind and PV technologies.
6) To carry out the assessment of TES supporting Wind and PV, (research objective 2), a further model was used that given the capacity of CSP calculated in Step 4 as an input, controlled the dispatch of TES to reduce the deficit in production from Wind and PV found in Step 5. This TES model is outlined in Section 3.4.4. Importantly, the scenarios are run with and without dispatchable TES, with the effects on the system fulfilment, curtailment and LCOE being analysed.
7) Once the above series of modelling exercises was completed, the number of RE plants at each location and the electrical energy outputs, (MWh), were used within the LCOE model to establish system cost for the large scale RE scenarios under investigation here. This process addresses research objective 3. The LCOE model is described in Section 3.4.5.
8) Various indicators used to address research objective 1 were additionally calculated by the model. The entire modelling process is summarised in the flow diagram below.

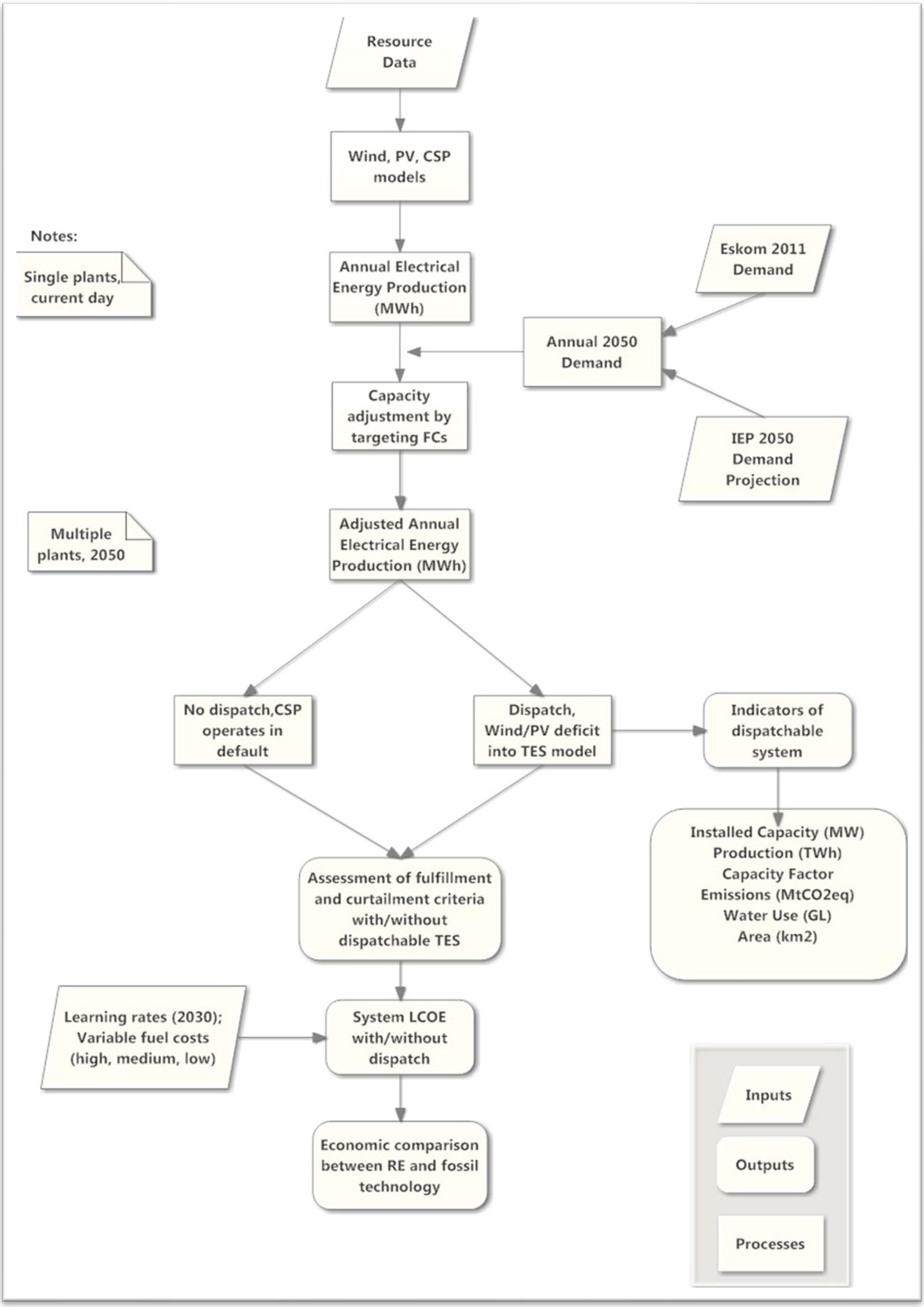

Figure 33: Method flow diagram

3.4 Model Descriptions

3.4.1 Wind Model Description

The wind model was designed using first principles. The velocity, density and area of a parcel of air need to be known to calculate the theoretical available power in the air current. This is termed the wind power factor (WPF) and is found using the following formula:

$$\text{power} = \frac{1}{2}\rho V^3 A$$

Source: (Grogg, 2005) (Equation 3)

This provides an indication of the maximum available power in a moving air current. However, no wind turbine is able to extract all available power from the wind. For this reason the wind power factor, obtained using equation 3 above, needs to be multiplied by the power coefficient of the specific turbine being used. In this case, the power coefficient for the Vestas 3.0MW wind turbine used in the model was found knowing the real world power outputs of the turbine at different wind velocities. The Vestas 3.0MW wind turbine has a swept area of $9852m^2$. The air density used in the model was taken as $1.225kg/m^3$. The WPF was calculated for each wind speed from 3.0m/s to 25.0m/s at 0.5m increments using equation 3 above. The power coefficients at different wind speeds were then found by dividing the known power outputs by the WPF at the same speeds. An example of the first set of values is provided below.

Wind Speed	WPF (W)	Known Outputs (W)	Power Coefficient
3	162928	26000	0.16
3.5	258723.7	73000	0.28
4	386199.8	133000	0.34
4.5	549882.1	207000	0.37
5	754296.4	302000	0.40
5.5	1003969	416000	0.41
6	1303424	554000	0.42
6.5	1657189	717000	0.43
7	2069789	907000	0.43
7.5	2545750	1126000	0.44
8	3089598	1375000	0.44
8.5	3705858	1652000	0.44
9	4399057	1958000	0.44
9.5	5173719	2282000	0.44
10	6034371	2585000	0.42

Figure 34: Example of wind model power coefficients calculation method

The next step involved multiplying the calculated WPF by the appropriate power coefficient, according to the known wind speed ranges. The results obtained here provided electrical energy output generated from a single wind turbine, given a known wind speed velocity at 10 minute intervals over one year. Every hourly wind energy output was then extracted from the series.

3.4.2 Photovoltaic Model Description

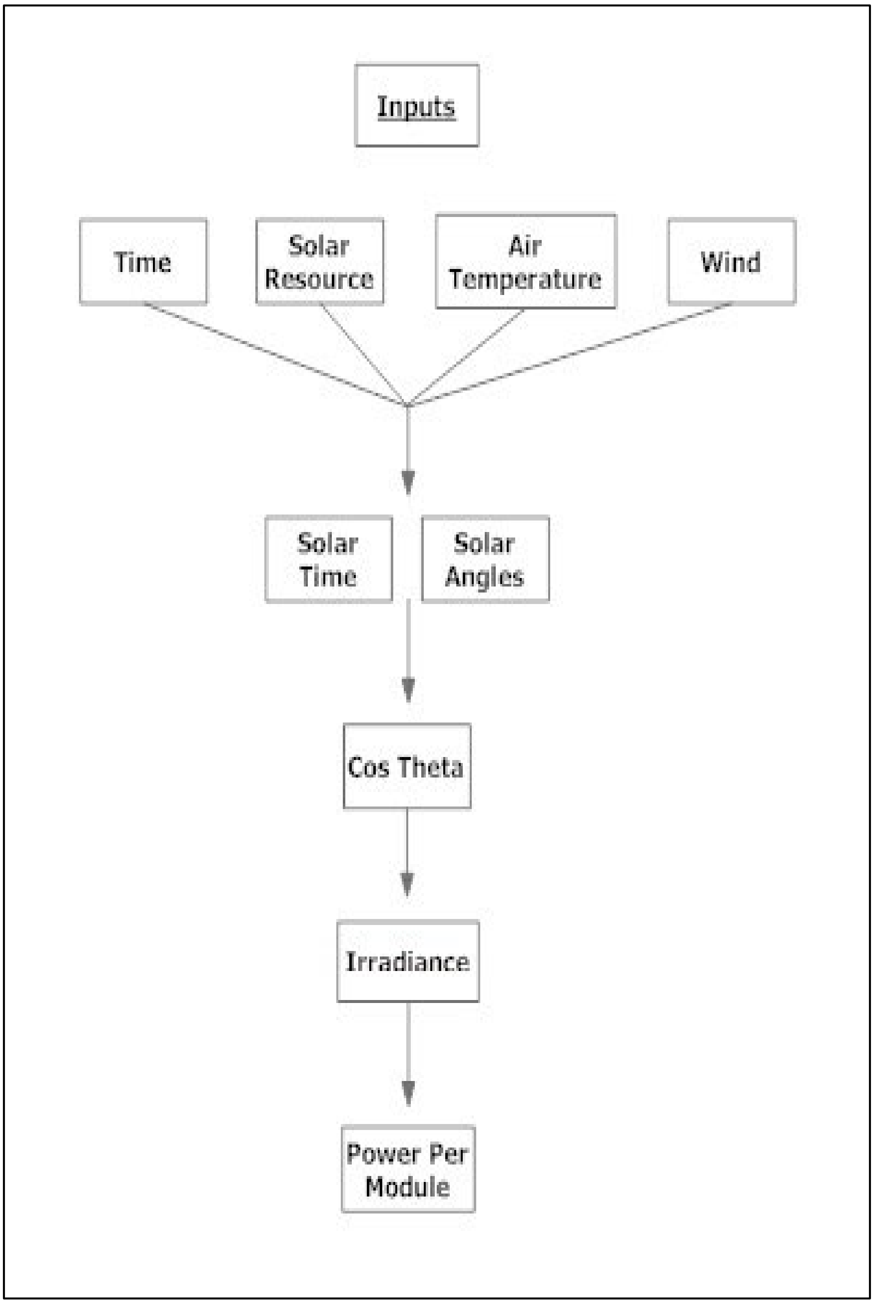

Figure 35: PV model flow diagram

Note:

Solar Time is described in Appendix Section 1.

Cos Theta represents the angle with which incoming beam radiation strikes a flat surface relative to the Sun's zenith for a specific location at a certain time of year. This angle is called the solar zenith angle and is formally described in Section 1 of the Appendices.

Source: (Geyer & Stine, 2001)

The PV model was supplied by Stellenbosch University and used with adaptations for this thesis. The PV, CSP and TES spreadsheets were supplied with a comprehensive database of solar irradiance measurements for a number of sites acquired by Stellenbosch University for their renewables research programme, (GeoModel, 2010). The principle data inputs, displayed in Figure 35 above, are added to the model, allowing for the subsequent calculations based on the solar resource, solar time and solar angles. The main output delivered by the process comprises power output (W) per modeled PV plant at hourly intervals over one year. Figure 36 below shows the abbreviated PV model characteristics. The MWh/year value here was calculated using an assumed CF for PV of 25%.

PV model characteristics	Amount
Number of modules	25
Total module aperture (m^2)	1,875
Total land (m2)	10,000
Land utility ratio	0.1875
Total plant power (MW_p)	0.2813
Cell efficiency	0.15
Storage (min)	5
Inverter efficiency	0.98
Generated electric energy (MWh/year)	616

Figure 36: Basic PV model parameters

3.4.3 Concentrating Solar Power Model Description

The CSP model was supplied from Stellenbosch University and is based on the Gemasolar plant design specifications described in Section 2.10.7, (Gauché, 2012b). The modelling process outlined in Section 3.3.3 describes how electrical energy output from CSP is being scaled up (Step 4), in such an event more Gemasolar plants are theoretically being built. The rated capacity of the plant model is 20MW_e, with a total thermal storage capacity of 15 hours. This means that when the sun sets the plant is able to generate at full capacity for 15 hours. The solar angles and time considerations necessary to derive the energy production from the available hourly solar resource input data are provided in the Appendices, Section 1. Several energy conversion steps are described by the model, with only the abbreviated description provided below in Figure 37. These conversion steps describe the transformation from thermal to electric energy, which approaches 40% efficiency. The conversions begin with a portion of the solar resource being transferred into the heat transfer fluid, molten salt in the case of Gemasolar, to generate steam. This steam powers a turbine allowing for mechanical energy to be used for the generation of electrical energy. The associated changes in efficiencies, described by each of these model steps, are incorporated into the energy transfer calculations of both the receiver component and the thermal storage unit, with the latter being described in Section 3.4.4.

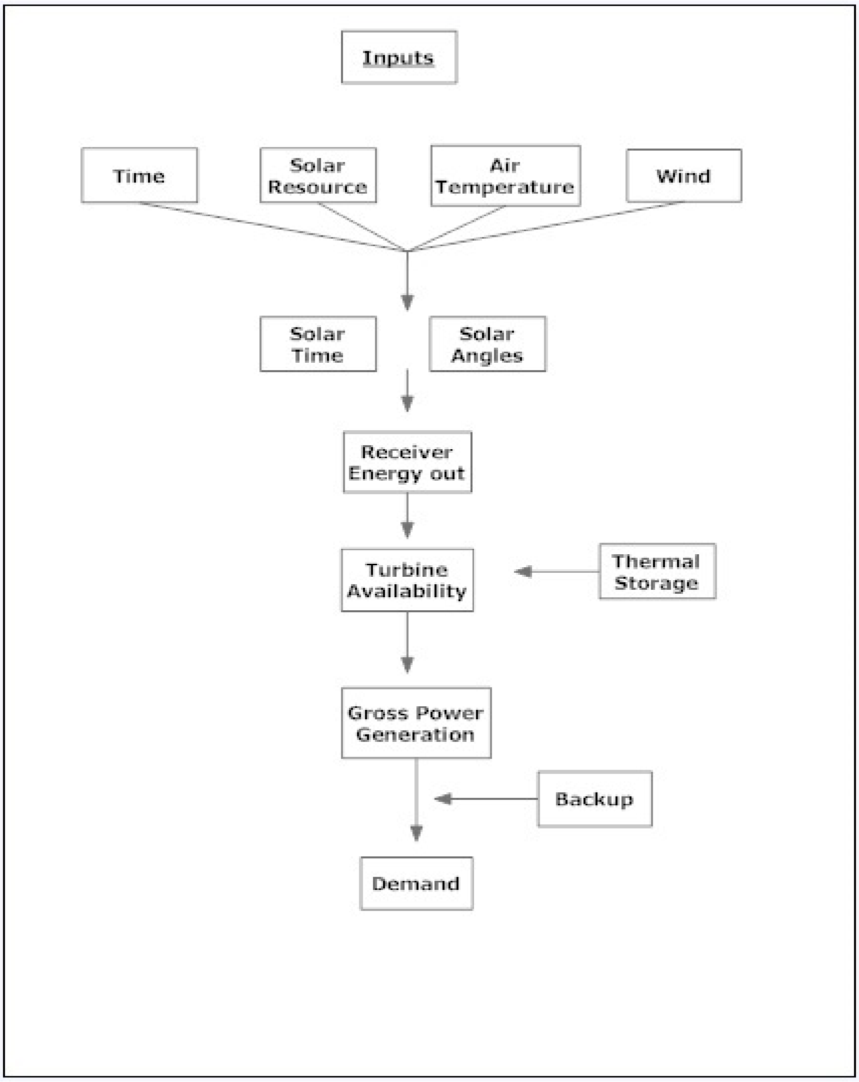

Figure 37: Central Receiver model flow diagram

Note:

In the figure above 'backup' indicates that CSP can potentially be backed-up by natural gas at a rate of 15% per annum. Gas backup facilities at each CSP plant were not used in the current work, but where rather incorporated to meet the total system demand shortfall, as described in section 3.1.

CR model characteristics	Amount
Number of heliostats	2,650
Total reflective area (m^2)	318,000
Tower height (m)	140
Receiver power (MW_{th})	120
Turbine power (MW_e)	20
Storage size (hours)	15
Storage tank dimensions (height x diameter(m))	10.5 x 23
Mass of salts (tonnes)	8,500
Generated electric energy (MWh/year)	110,000

Figure 38: Basic CR model parameters

Source: (Burgaleta et al., 2011; Gauché, 2012b)

3.4.4 Thermal Energy Storage Model Description

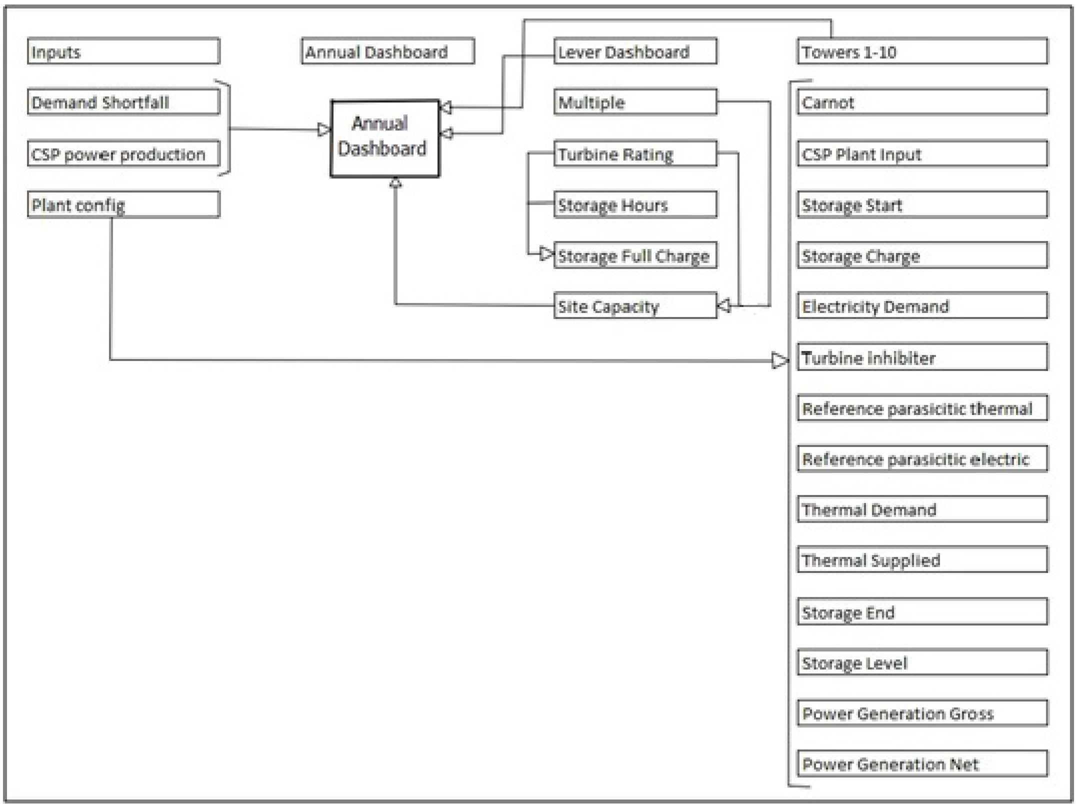

Figure 39: Thermal Energy Storage model flow diagram, (Dispatch model)

The thermal storage model is similar to the CR model and was supplied by Stellenbosch University, (Gauché, 2012a). The plant characteristics of the CR model (Figure 38) are therefore not replicated here. The TES model operates in a configuration to release stored electrical energy when a demand gap from Wind and PV is identified. During periods when demand can be matched by a combination of Wind and PV, the TES model begins to store as much solar energy as is available. The ten TES model locations are the same as the CSP locations, with different capacities of TES being used according to the scenario under investigation. TES locations are ranked according to the heat energy content of the storage tanks. Those tanks with the highest level of thermal energy are utilised first when needed to dispatch electrical energy in the support of Wind and PV within the system.

3.4.5 Levelised Cost of Electricity (LCOE) Model

The LCOE method of price analysis is very useful for cross comparison of energy costs between different technologies over the lifespan of the plant. The LCOE indicator is generated by knowing the upfront capital costs, the annual cost of running the system, (maintenance and operation), and the volume of electrical energy produced in one year. These inputs are integrated according to Equation 4. The LCOE indicator can be used to demonstrate the financial feasibility of a plant by assessing the cost of production over the operational lifetime of the plant so that it can be compared to actual current and projected tariffs. In this thesis the LCOE model was used to analyse the associated financial costs of the electrical energy outputs of the Wind, PV, CSP and TES model results from the 30 locations investigated around South Africa. The LCOE is calculated dynamically, as the size of the RE system is changed, with the LCOE component being linked to the electrical energy outputs from the models. The process of carrying out this LCOE analysis is adapted from previous work done at STERG, (Gauché, 2013b).

$$LEC = \frac{\sum_{t=1}^{n} \frac{I_t + M_t + F_t}{(1+r)^t}}{\sum_{t=1}^{n} \frac{E_t}{(1+r)^t}}$$

(Gauché, 2010) (Equation 4)

An example of the layout of the LCOE model is included in the Appendices, (Section 4). The layout shown is used for all the individual technologies. To find the cumulative LCOE for the 2050 scenarios that comprise the different percentages of each technology needed to match the electrical demand, the LCOE's are incorporated to produce a final system LCOE for each scenario. The cost assumptions used in the LCOE model are included below. A discount and interest rate of 10% and 10%, respectively, were used. As illustrated by equation 5 below, operation and maintenance costs were assumed to be 1% of 110% of investment costs, allowing for a 10% safety margin in assumed capital costs. This safety margin on capital cost was chosen to buffer against cost overruns during construction, (Gauché, 2013b). O&M was not inflated annually to account for degradation of the power plants. Increases in repayment costs incurred through interest during construction are not factored into the LCOE model.

Technology	Costs 2012 (R/W)	Cost 2030 (R/W)	Nominal Capacity (MW)	Plant Cost 2030 (R)
Wind	13.89	12.3	3	37,095,008
PV	15	6.3	0.28	1,771,875
CSP	57.01	28.5	20	570,198,188
CCGT	6.406	6.406		2,562,400,000

Figure 40: LCOE energy cost inputs for 2012

Sources: Wind (Fingersh, Hand, & Laxson, 2006), PV (Gauché, 2013a), CSP (Kolb et al., 2011), CCGT (*IRP*, 2014)

Symbol	Input	Value
OMP	O&M (First year) proportion of Capital Cost	1%
e	O&M annual escalation	0%
S	Safety Margin	10%
i	Interest Rate on Capital	10%
d	Discount Rate	10%
R	Exchange Rate	8 (R/$2012)

Figure 41: LCOE model assumptions used throughout

$$Annual\ O\&M\ in\ Year\ 1 = OMP\ \times (Capital\ Cost\ \times (1+S)) \times (1+e)\hat{}(i-1)$$

(Equation 5)

	R/MWh	$/MMBtu
Low	430.19	8
Med	645.29	12
High	860.38	16

Figure 42: Gas prices used in sensitivity analysis

Source: ERC SATIM

The capacity (MW) and cost of the individual power plants used in the LCOE model, for both 2012 and 2030, are included above in Figure 40. Learning rates have been applied to the cost assumptions of the LCOE calculation in 2030 and have been extracted from Figure 23. The assumed learning rates used for the 2030 sensitivity analysis are provided in Figure 43 below.

Technology	Expected price reduction (% of 2012)
Wind	0.84
PV	0.42
CSP	0.5
CCGT	0.00

Figure 43: Potential Technology Cost Reductions in 2030 relative to 2012 using assumed learning rates

Sources: Renewable Energy Technologies (Department of Energy, 2013a), CCGT (Kost et al., 2013)

An important consideration when dealing with the selling price of electricity from different technologies, is the time of day that the electricity is delivered to the grid. Currently in South Africa, the period from 17:00 in the afternoon to 21:00 in the evening is considered 'peak period' and electricity delivered during this time can be sold at a premium to users on a structured tariff. CSP operating with sufficient TES capabilities, such as the 15 hours of storage within the model, would likely aim to dispatch electricity specifically during this peak period, to capitalise on the available incentive. Inclusion of this effect into the current cost model would have reduced the LCOE of CSP, but was not formally investigated here.

3.4.6 System LCOE vs. Renewable Energy Fraction

The financial implications of the scenarios are analysed here using the LCOE. To understand how a changing penetration of renewable energy affects the LCOE of a whole system that includes gas fired generators, a sensitivity analysis was carried out for varying penetration rates of RE for different cases of variable operating costs, (fuel prices), for the gas fired generators, represented by one technology, advanced combined cycle gas turbines. In each scenario the maximum demand shortfall in the year from the three RE technologies was filled by a completely dispatchable combined cycle gas turbine

The four fulfilment coefficients for Wind, PV, CSP and CCGT were varied at 0.5% increments, with the LCOE being calculated each time. The fuel price sensitivity analysis was then carried out by changing the variable O&M (fuel) costs for CCGT technology. This incremental assessment of the costs for the whole system was conducted with three different fossil fuel prices. The results of this fuel sensitivity analysis are supplied in the Results and Analysis chapter, (Section 4.5).

3.4.7 Emissions from Energy Technologies

The IPCC has identified six direct GHGs which contribute towards radiative forcing in the atmosphere and its warming. These gases are released during many human processes, such as aluminum production and fossil fuel combustion, (ICBE, 2014). A table of these direct GHGs is shown in Figure 44. Direct GHGs are those compounds which contribute to global warming and exhibit a measurable Global Warming Potential (GWP), using the atmosphere heating value of CO_2 as the reference. This provides the CO_2 equivalent (CO_2eq) value for the different types of emissions that may be released by burning fossil fuels.

Indirect GHGs are those compounds that themselves do not add to warming, but in the presence of the correct catalyst and conditions might be chemically altered into a direct GHG, or may have an effect on the quantities of direct GHGs in the atmosphere. Examples of indirect GHGs are nitrous oxides (NO_x), sulphur dioxide (SO_2), black carbon and other particulate matter released through a range of human activities, (EPA, 2012).

CO_2	Carbon Dioxide
CH_4	Methane
N_20	Nitrous Oxide
HFC's	Hydrofluorocarbons
PFC's	Perfluorocarbons
SF_6	Sulfur Hexafluoride

Figure 44: IPCC Direct Greenhouse Gases

Source: (ICBE, 2014)

For every kWh of electricity generated by a RE technology, it is assumed here that an electrical energy utility would otherwise have needed to produce that energy conventionally and would have emitted associated GHGs during the process. The table below shows the GHGs and criteria pollutants that are avoided by every kWh of electricity generated from either, "solar thermal, solar electric, wind and hydro-electric systems," (ICBE, 2014). These values are 'approximate averages' because GHG emissions produced for every kWh of electricity generated differs substantially between utilities and countries.

Greenhouse Gases		Criteria Pollutants	
CO_2	1 kg	**CO**	0.00015 kg
CH_4	0.00001 kg	**NMVOC's**	0.00002 kg
N_2O	0.00001 kg	**SO_2**	0.005 kg
SF_6	0.00000055 kg	**NOx**	0.0025 kg

Figure 45: Avoided emissions for every kWh of electricity generated by a RE

Note: Avoided emissions above are assumed to be approximate averages.

Source: (ICBE, 2014)

In order to calculate the avoided emissions achieved by the RE technologies within the 2050 scenarios in this thesis, a CO_2 eq value is calculated. The GWP values for the GHGs listed in Figure 44 above are provided below in Figure 46.

GHG	GWP
CO2	1
CH4	21
N2O	310
HFC's	140 ~ 11,700
PFC's	6,500 ~ 9,200
SF6	23,900

Figure 46: Global Warming Potentials of different Greenhouse Gases

Source: (ICBE, 2014)

A representative CO_2eq value for avoided emissions potentially achieved through the scenarios was calculated for the direct GHGs shown in Figure 44, namely CO_2, CH_4, N_20 and SF_6. There is considerable uncertainty around the actual GWP value of the indirect GHGs listed as Criteria Pollutants in Figure 42 above, due to the complexity and scale of individual chemical reactions occurring in the atmosphere. For this reason only the CO_2eq of the direct GHGs avoided by RE electricity generation has been calculated.

The process used to calculate avoided emissions follows:

$$CO2eq\ (kg) = \sum_{i=1\ to\ n} RE\ generated\ (kWh) X\ Avoided\ Emissions_i (\frac{kg}{kWh})\ X\ GWP_i$$

(Equation 7)

3.4.8 Water Usage

The calculation of water usage per quantity of electrical energy generated by PV and CSP within the modeled scenarios uses the known water consumption rates of the technologies. The water usage for the wet-cooled Gemasolar CSP plant is 1950.27 liters/MWh, while that for a dry cooled plant is approximately 98.42l/MWh, (Macknick, Newmark, Heath, & Hallett, 2011). The CSP plant used within the scenarios is dry-cooled. Water consumption for PV plants is taken from the same reference and has the same median as that for dry-cooled CSP, equally assumed here as 98.42 litres/MWh. For PV water consumption is primarily for cleaning solar panels. Water usage for CCGT was assumed to be 749.51 litres/MWh for a closed-circuit system using tower cooling according to Macknick, et al, 2011.

3.4.9 Scenario Design

To address the research objectives of this thesis, simulation modelling of several large-scale RE scenarios was carried out, with different penetrations of the three RE technologies. As stated in Section 3.3.3 above, the penetrations were imposed by changing the fulfilment coefficients of individual technologies by increasing capacity. The effect of using different penetrations within these scenarios is assessed relative to the targets outlined earlier, of 90% fulfilment and 10% curtailment. It is important to note that the FCs of each technology were initially calculated individually against demand using the method outlined in Section 3.3.1. After this user input, the model then provided the final system fulfilments and curtailments for all three RE technologies combined within the system.

The FCs targeted in the different scenarios are listed in Figure 47 and Figure 48. Various parameters are calculated by the model using these FCs, with these results listed in Figure 49. The outputs for each scenario are used to address each of the Research Objectives in Section 1.3.

In Scenario 1 the system is tested at even FCs, where one third of energy requirement is obtained from each technology. This first scenario was designed to investigate the behaviour of the three technologies for an equitably distributed mix of electrical energy over time.

In Scenarios 2 – 4 Wind, PV and CSP are individually required to provide 50% of the FC, representing a weighted bias towards single technologies. Here, the behaviour of individual technologies can be amplified to assess broad characteristics of each technology.

Scenario 4 is also used as a testing platform for CSP, to investigate the effect on the system of using dispatchable TES. An analysis of the energy profile over time allows periods of demand deficit from Wind and PV to be found and used to coordinate dispatch within the TES model.

In Scenarios 5 – 7 80% of total FC is sourced from combinations of only two technologies. These three scenarios were designed to evaluate whether or not the two technologies operate in a complementary manner to each other.

Scenario 8 was designed with 19 different cases, each investigating different proportions of RE technology. By observing the effect of dispatchable TES on the fulfilment and curtailment coefficients of the 19 cases within Scenario 8, observations can be made regarding any potential benefits to system operation gained through using dispatchable TES.

To understand how changing fuel costs might affect LCOE values, different fuel cost inputs were used for CCGT, according to Scenarios 8-10 listed in Figure 48 below. Here, the low, medium and high fuel cost options are assessed. This fuel price sensitivity analysis was run using learning rates for 2030, comprising Scenarios 11-13.

Scenario 8 was employed to observe total water usage and avoided emissions. This analysis could be run using only Scenario 8, because the installed capacities of RE are identical in Scenarios 9-13.

	Targeted FCs*			
	Wind	PV	CSP	CCGT
Scenario 1: Base Case	0.33	0.33	0.33	0
Scenario 2: Large Wind Case	0.5	0.25	0.25	0
Scenario 3: Large PV Case	0.25	0.5	0.25	0
Scenario 4 Large CSP Case	0.25	0.25	0.5	0
Scenario 5: Large Wind/PV Case	0.4	0.4	0.2	0
Scenario 6: Large PV/CSP Case	0.2	0.4	0.4	0
Scenario 7: Large Wind/CSP Case	0.4	0.2	0.4	0

**These fulfilment coefficients are determined for a comparison of each resource individually against demand. When combined, the system fulfilment coefficient will be less than the sum of the individual coefficients due to instances where low resource availability coincides for each technology.*

Figure 47: Targeted Fulfilment Coefficients for RE technologies and gas

		Targeted FCs			
		Wind	PV	CSP	CCGT
Scenario 8: Low fuel cost	Case 1	0.02	0.02	0.02	0.95
	Case 2	0.03	0.03	0.03	0.90
	Case 3	0.05	0.05	0.05	0.85
	Case 4	0.07	0.07	0.07	0.80
	Case 5	0.08	0.08	0.08	0.75
	Case 6	0.10	0.10	0.10	0.70
	Case 7	0.12	0.12	0.12	0.65
	Case 8	0.13	0.13	0.13	0.60
	Case 9	0.15	0.15	0.15	0.55
	Case 10	0.17	0.17	0.17	0.50
	Case 11	0.18	0.18	0.18	0.45
	Case 12	0.20	0.20	0.20	0.40
	Case 13	0.22	0.22	0.22	0.35
	Case 14	0.23	0.23	0.23	0.30
	Case 15	0.25	0.25	0.25	0.25
	Case 16	0.27	0.27	0.27	0.20
	Case 17	0.28	0.28	0.28	0.15
	Case 18	0.30	0.30	0.30	0.10
	Case 19	0.32	0.32	0.32	0.05
Scenario 9: 2012 Medium fuel cost					
Scenario 10: 2012 High fuel cost					
Scenario 11: 2030 Low fuel cost					
Scenario 12: 2030 Medium fuel cost					
Scenario 13: 2030 High fuel cost					

**The 19 cases run for Scenario 8 were additionally run for Scenarios 9-13. This scenario layout was used for the LCOE assessment, where 2012 and 2030 cost inputs were adapted to account for potential learning rates. In addition, it was used to assess the effect on system fulfilment and curtailment through using dispatchable thermal storage.*

Figure 48: Scenario layout used to calculate LCOE with learning rates

Results Format	
Finding 1	Investigation of system parameters within Scenarios 1-7:
	Energy Production (TWh)
	Coefficients of Scenarios 1-7 (FC,CC)
	Effect of dispatchable TES on LCOE 2030 (R/kWh)
	Avoided Emissions (CO_2)
	Water Usage (GL)
	Area (km^2)
	Viable Area (%)
	Demand projections (GWh)
Finding 2	Validating thermal energy storage model within Scenario 4
Finding 3	Testing the impact of dispatchable thermal storage on coefficients
Finding 4	Fuel Price Sensitivity Analysis and Learning Rates (2012/2030) within Scenarios 8-13
Finding 5	Avoided emissions vs. Water Usage within Scenario 8

Figure 49: Layout of major finding types

Chapter Four – Results and Analysis

4.1 Introduction

The results of the current investigation into a large scale RE system for South Africa in the year 2050 are presented below. Scenarios were designed to allow examination of various implications of a hypothetical high RE penetration grid, in line with the research objectives outlined in Section 1.3. These are reproduced here in brief:

1) To use several indicators to evaluate the potential implications and drawbacks to RE at high penetrations within a future hypothetical grid; through investigating numerous scenarios comprising different penetrations of the three RE technologies, specifically looking at a high total RE proportion within the grid;
2) To assess the role of TES in supporting Wind and PV technologies;
3) To carry out a broad economic assessment of a supply system with increasing RE penetrations in the form of wind and solar technologies where the balance of supply is provided, for the sake of simplicity, by one representative fossil-fuel technology, natural gas fired combined cycle gas turbines, taking into account assumed learning rates for the capital cost of different technologies and a fuel-price sensitivity analysis.

The modelling techniques used to investigate the future scenarios have been outlined in detail in the previous method chapter. The scenario design process used to create a future hypothetical grid has been outlined in Section 3.4.9. The layout of the results and analysis chapter has been structured in accordance with the three research objectives of this thesis.

Finding 1 comprises the results obtained for Scenarios 1 – 7. Here energy production from the scenarios is displayed, along with the associated fulfilment and curtailment coefficients. The LCOE in 2030 is looked at both with and without dispatchable TES. The results from the avoided emissions, water usage, and area calculations are all presented. The viable area percentage involves an assessment of the electrical energy outputs from the scenarios in comparison to similar large scale scenario studies done in South Africa for Wind and CSP. Finding 1 addresses Research Objectives 1 and 3.

Finding 2 shows the energy outputs from the three modeled RE technologies within the high CSP scenario, namely, Scenario 4. This scenario was chosen because investigation of the supporting role of CSP for Wind and PV within a scenario with low CSP penetration would under-represent the dispatchable abilities of TES. The aim here is to validate the results of the TES model and show how this ability of CSP can increase total system fulfilment when actively supporting Wind and PV. Testing the successful operation of the TES model in this way is of the utmost importance because the CSP component of the economic comparison between RE and gas technologies uses the fully dispatchable TES option, which increases total system fulfilment from RE. Finding 2 addresses Research Objective 2.

Finding 3 looks at the effect on RE system fulfilment and curtailment coefficients when using either dispatchable or non-dispatchable TES. This is investigated within Scenario 8. The installed capacities of each technology are included in this analysis, which show that Wind and PV technologies require larger installed capacities to attain higher levels of fulfilment due to intrinsically lower capacity factors. Finding 3 also addresses Research Objective 2.

Finding 4 investigates fuel price volatility and the effect of learning rates on technology costs. Here the LCOE for different fuel costs for CCGTs are investigated for a range of incrementally sized RE systems. Assumptions for the LCOE analysis are provided in Section 3.4.5. Finding 4 addresses Research Objective 3.

Finding 5 examines total water usage and avoided emissions for the 19 different cases of Scenario 8. Finding 5 addresses Research Objective 1.

4.2 Finding 1: Investigation of system indicators within Scenarios 1-7

Energy Production (TWh) and System Coefficients

Energy (TWh)					Curtailment Coefficient		Fulfilment Coefficient	
Scenario	Wind	PV	CSP*	Total	Non-dispatch**	Dispatch**	Non-dispatch	Dispatch
1	173.29	182.3	125.5	481.13	0.2	0.08	0.81	0.85
2	265.14	132.01	132	529.14	0.15	0.05	0.85	0.88
3	131.99	944.78	132	1,208.76	0.67	0.63	0.76	0.81
4	131.99	132.02	264	527.98	0.17	0.01	0.82	0.88
5	211.18	273.69	105.6	590.46	0.28	0.21	0.8	0.83
6	105.59	273.69	211.2	590.46	0.31	0.16	0.78	0.84
7	211.18	105.59	211.2	527.95	0.15	0.01	0.85	0.89

Installed Capacity (MW)				Max Demand Shortfall (MW)/CCGT***	TES Requirement (MW)****
Scenario	Wind	PV	CSP		
1	52,765	95,672	27,431	59,007.15	58,981
2	80,301	69,577	20,781	58,207.19	58,369
3	39,893	496,655	20,781	59,584.08	59,569
4	39,893	69,386	41,562	60,233.82	60,210
5	63,957	143,841	16,624	57,930.00	57,910
6	31,978	143,841	33,249	60,990.29	60,967
7	63,957	55,499	33,249	60,150.04	60,137

Capacity Factors					
Scenario	Wind	PV	CSP	TES	CCGT
1	0.33	0.15	0.61	0.53	0.15
2	0.33	0.17	0.63	0.50	0.12
3	0.27	0.05	0.44	0.47	0.19
4	0.33	0.16	0.61	0.56	0.12
5	0.32	0.13	0.58	0.50	0.17
6	0.32	0.12	0.57	0.52	0.16
7	0.33	0.17	0.63	0.54	0.11

Figure 50: Electrical energy produced via installed capacity for Scenarios 1 - 7

*** This refers to energy produced in the case of non-dispatchable TES for CSP. When dispatchable TES is used, total energy from CSP is reduced.**

**** These refer to non-dispatchable and dispatchable Thermal Energy Storage (TES) for CSP.**

*****Maximum annual demand shortfall after dispatch of RE technologies for the scenario, (assumed to be met by CCGT).**

****** TES requirement refers to the maximum hourly demand shortfall incurred by Wind and PV during the year, for each scenario**

Figure 47 above shows the amount of electrical energy that each technology needed to produce to reach the targeted FCs for Scenarios 1-7. Energy production was modelled over one year. The 2050 demand projection by the IEP (DoE, 2013a) for SA was 527.94 TWh, or 1,900.6PJ. Midday peaks in production are wasted when PV penetration is high, (50%), as the majority of this energy is curtailed. This is indicated by the unrealistically high levels of curtailment in Scenario 3. Even with dispatchable TES the FC in Scenario 3 is the lowest, as the smaller penetration (25%) of CSP is inadequately sized to effectively meet the large demand gap imposed by PV and Wind during periods of low production. In most of the scenarios, excluding the high PV case, the cumulative energy produced approximates the IEP projection of 1,900.6PJ, (527.94 TWh). The remaining portion of electrical energy needed to match exactly the IEP 2050 projection, is supplied by CCGT technology, according to the deficit imposed by RE technologies within the specific scenario.

To contextualise the energy production results, an estimate for South Africa of the total production from wind energy of 80.5 TWh in a realistic scenario is provided by Hagemann, (2008). This realistic scenario from the Hagemann (2008) study was based on constraints that include whether the wind resource is economically viable, proximity to infrastructure and the exclusion of restricted and protected areas. Fluri (2009) estimated that 547.6GW of CSP capacity is available to SA given transmission and land criteria constraints. Assuming a CF of 38.8%, (from Parabolic Trough, 6 hours storage), a total of 1861 TWh of energy would be available given the scale of the assumed resource. The scale of the wind scenarios investigated here was substantially larger than those found in the Hagemann (2008) study. None of the constraints used in the Hagemann study were used here, which has meant the wind scenarios were unbounded.

Indicator Results for Scenarios 1-7

Observation of the CCs indicates that a large amount of energy is being curtailed from Wind, PV and non-dispatchable CSP. A FC of 89% is the best achieved, occurring in the high Wind and CSP scenario, (Scenario 7). The CC and FC are used as proxies to indicate system performance within the scenarios modeled here. As stated, a large PV build increases CC and associated cost, (Figure 50). In this analysis, the failure of RE technologies alone to reach FCs above 89% is due to the fact that CSP contributes a maximum of 50% of total system fulfilment in Scenario 4. A CSP scenario with greater than 50% of total system fulfilment was not investigated because of the high cost of this technology.

Effect of dispatchable TES on Future LCOE (R/kWh) Assuming Learning for RE

The high level of curtailment for Scenario 3 (Figure 50) is reflected in the disproportionately higher LCOE value for the same scenario in Figure 51 below. In each scenario, the introduction of dispatchable CSP reduces the associated LCOE noticeably, as the solar resource is more effectively utilised through storage and dispatch operation. Medium fuel costs (R643.03/MWh dispatched) were used for the CCGT system in the LCOE values below.

Cost with 2030 learning rates (R/kWh)		
Scenario	Non-dispatch	Dispatch
1	0.70	0.68
2	0.65	0.64
3	1.32	0.83
4	0.69	0.68
5	0.74	0.69
6	0.78	0.73
7	0.66	0.65

Figure 51: LCOE of Scenarios 1-7

Avoided Emissions (MtCO_2eq)

The avoided emission values have been calculated for used energy only, with curtailed energy being discounted. Scenario 2 achieves the greatest avoided emission value and also represents the large wind scenario, (Figure 50).

	Avoided Emissions (Mt.CO2eq)
Scenario	Total
1	386.19
2	414.97
3	362.22
4	381.90
5	396.36
6	355.90
7	404.95

Figure 52: Avoided emissions of Scenarios 1-7 for dispatchable TES

Water Usage (GL)

Water Usage (GL)			
Scenario	PV	CSP	CCGT
1	17.86	12.65	57.82
2	13.03	8.95	47.32
3	93.00	8.38	75.39
4	12.99	20.09	47.46
5	26.93	7.16	65.49
6	26.93	14.92	62.42
7	10.39	15.61	42.66

Figure 53: Water usage within the scenarios

Note: It was assumed that wind energy uses no water.

To reduce the volume of water used in the scenarios, the dry cooled CSP option was adopted. Water was consumed at a dry-cooled rate of approximately 98.42 litres/MWh for both the power tower CSP and utility scale PV systems, (Macknick et al., 2011). It should be noted that dry-cooling technology utilises, "90% less water than water-cooled plants at the cost of only about 5% less electric power and 2-9% higher electricity prices," (USDOE, 2008). Although the impacts to efficiency of dry cooled plants are recognized and represented in the modelling process here, it is suggested that these marginal losses are potentially justifiable based on water savings. Dry-cooled CSP plants are particularly suited to the drier regions of South Africa.

Total Land Area (km2)

Total Land Area (km2)				
Scenario	Wind	PV	CSP	CCGT
1	17588	3390	2318	31
2	26767	2474	1756	30
3	13298	17656	1756	31
4	13298	2467	3512	31
5	21319	5113	1405	30
6	10659	5113	2810	32
7	21319	1973	2810	31

Figure 54: Total area used by the scenarios

The total land area of South Africa is 1219090km^2, (StatsSA, 2012). The largest wind scenario (2) analysed here would use roughly 2.1% of the land area of SA. Apart from the large PV scenario (3) the solar power technology options utilise relatively small amounts of land area by comparison. The best solar resources in SA are found in the Northern Cape, which has an area of 361,830km^2, (StatsSA, 2012). The area used by the PV scenarios is between 0.005-0.048% of the area of the Northern Cape, while that for CSP is between 0.003-0.009%.

Viable area (%)

% use of viable area			
Scenario	Wind	PV	CSP
1	114		16
2	174		12
3	86		12
4	86		25
5	138		10
6	69		20
7	138		20

Figure 55: Percentage of viable area used by scenarios

The information represented in Figure 55 shows the percentage of viable area which is used by the scenarios, in relation to the land area defined as being viable by virtue of proximity to current infrastructure and being outside exclusion zones by the reference solar and wind studies (Fluri, 2009; Hagemann, 2008). The land use to energy requirement in the Fluri (2009) study was assumed at 28km^2/GW, translating to 15,332.8km^2 for the estimated viable CSP potential of 547.6GW for SA. The same calculation was carried out for the Hagemann (2008) study, which assumed a total land use to energy requirement for wind of 500,000m^2/MW, (1km^2/0.002GW) requiring 13,090km^2 of land to attain 80.5 TWh of energy per year, using a CF of 35.1%. All the CSP scenarios are underrepresented in terms of the potential resource identified by Fluri (2009), indicating that much more of the available solar resource could realistically be harvested, compared to the scenarios modeled here. Four of the seven wind energy scenarios generate larger quantities of energy compared to the 80.5 TWh reference case, while the remaining three underperform.

4.3 Finding 2: Validating TES dispatch within a Large CSP Scenario

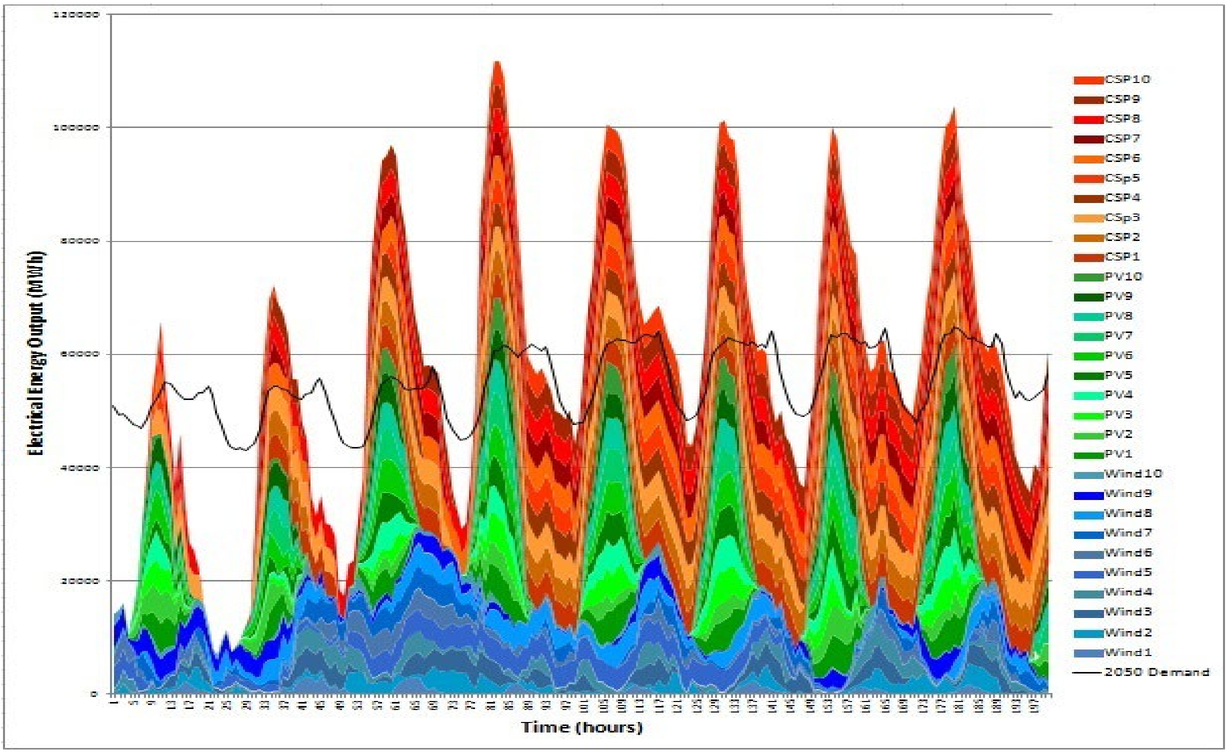

Figure 56: Scenario 4: January (200 hours) Wind, PV, CSP Electrical Energy Outputs in 2050 without dispatchable TES

The large CSP case in Scenario 4 has a target FC of 50% for CSP, as set out in Section 3.4.9, (Figure 47). This large CSP scenario is used primarily as a platform to test the operation of the TES model, within a system comprising a higher CSP penetration. The required capacity of each technology is calculated independently to fulfil their designated FCs according to the 527.94 TWh energy requirement. When the energy generation profiles of the three technologies are combined however, these will not necessarily combine to meet 100% of system fulfilment, which also depends on how the wind and solar resource correlates at each point in time as demonstrated in Figure 56 above. This interaction is depicted by the cumulative electrical energy production values (Figure 49). The values are represented by a final FC and CC and are analysed in Findings 3 below.

The electrical energy production profile for selected scenarios and months are presented in this section. Periods of time during the year when RE production does not match demand are indicated by the blank spaces beneath the 2050 demand profile. Thermal energy storage in Figure 56 and Figure 57 is not actively controlled to release stored energy in the most efficient manner to support production deficits from Wind and PV. Instead, CSP is operating in a default configuration, releasing stored energy when solar irradiance levels begin to diminish, typically during the late afternoon. This lower level of control within the system is problematic as the overall system production from the RE technologies is calculated additively. This causes a greater proportion of curtailed electrical energy, shown in Figure 56 and Figure 57, compared to a system with dynamic dispatchable thermal storage. In this thesis, dynamically controlled TES and default TES are designated as ‘dispatchable’ and ‘non-dispatchable’ TES. The high level of curtailment imposed on the system by non-dispatchable TES, is reflected in the figures above and below, where the CC for Wind, PV and CSP taken together is 17.5% within Scenario 4.

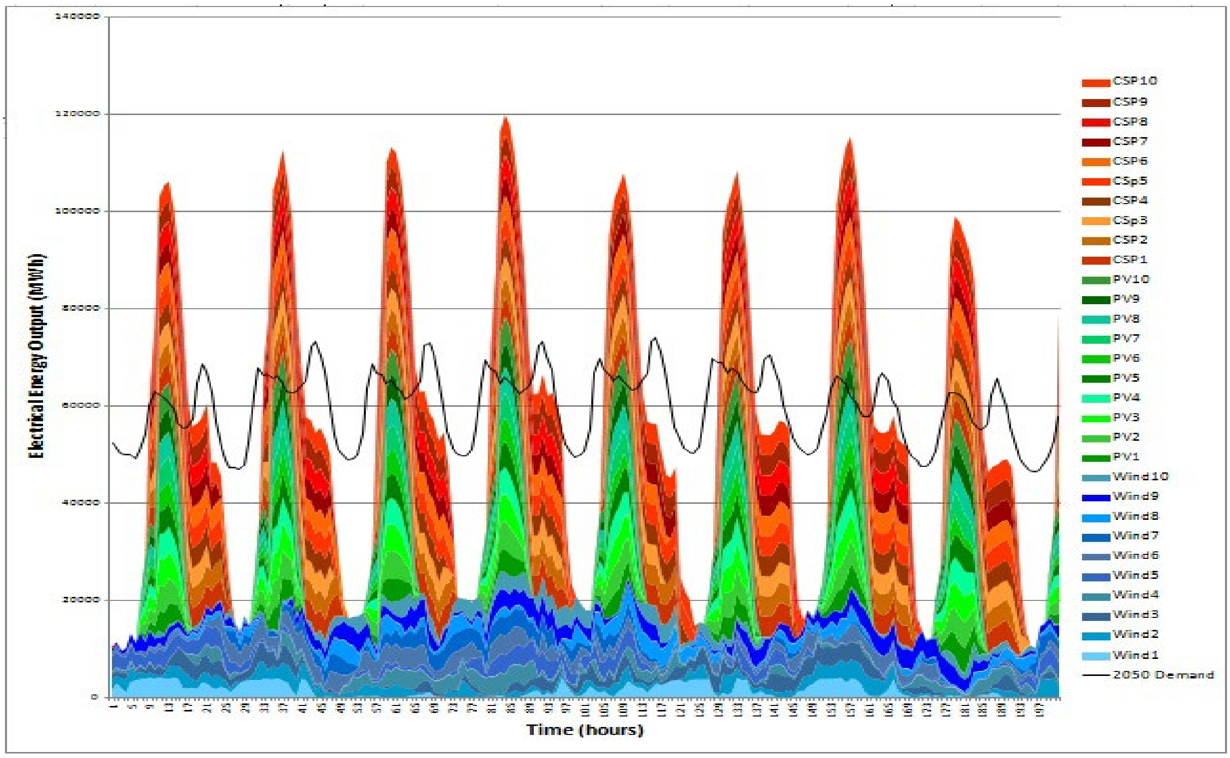

Figure 57: Scenario 4: July (200 hours) Wind, PV, CSP Electrical Energy Outputs in 2050 without dispatchable TES

Figure 58 presents the output of the CSP system for Scenario 4 as controlled by the dispatchable TES model. The demand shortfall calculated for PV and Wind alone is taken from the system displayed in Figure 56 and Figure 57. This demand shortfall controls the dispatchability of thermal storage. Electrical energy is being dispatched relative to the demand shortfall from Wind and PV when sufficient energy is available given storage levels and the solar resource at the time.

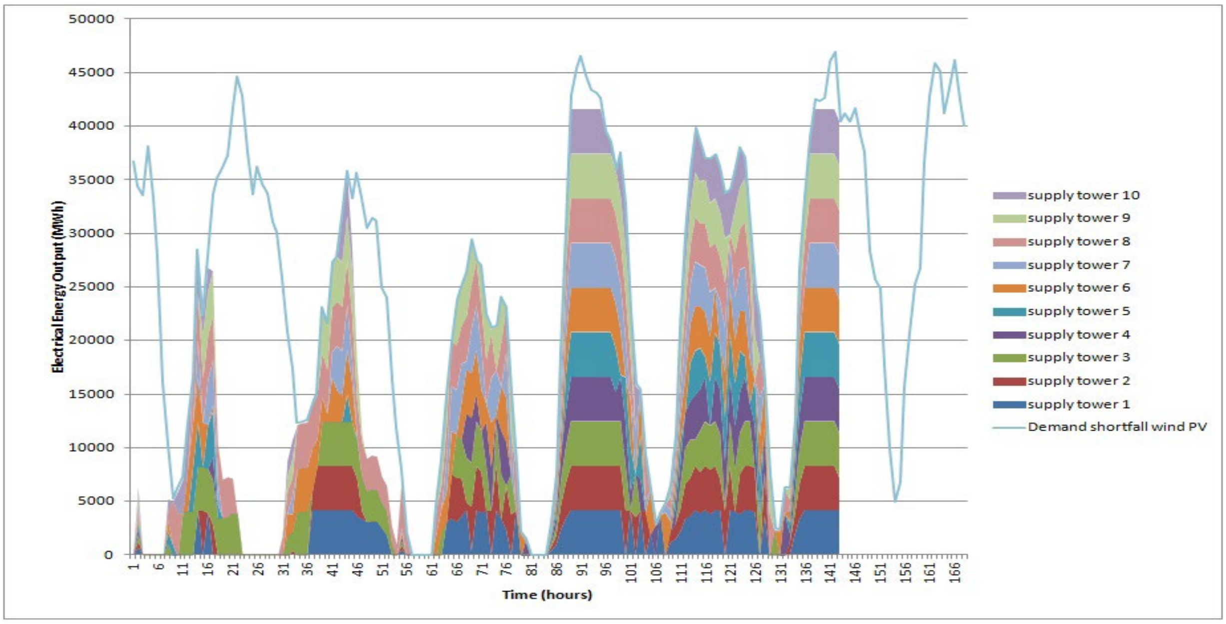

Figure 58: Validation of thermal energy storage model operation in Scenario 4

Figure 59 and Figure 60 show the thermal storage model being reintegrated back into the Wind, PV and CSP model results for Scenario 4. Several observations in the overall system become evident. The FCs for Wind, PV and CSP individually are the same (50% CSP, 25% Wind, 25% PV). The CC for Wind, PV and CSP together in the non-dispatchable example was 17.5%, while in the dispatchable example this value has dropped to 0.007%. The FC changes from 82.5% in the non dispatchable example, to 88% in the dispatchable example for the whole system. However, the increased FC is the direct result of the dispatchable CSP system more efficiently utilising the available solar resource by storing and releasing energy only when needed, ensuring that less curtailment occurs from this technology.

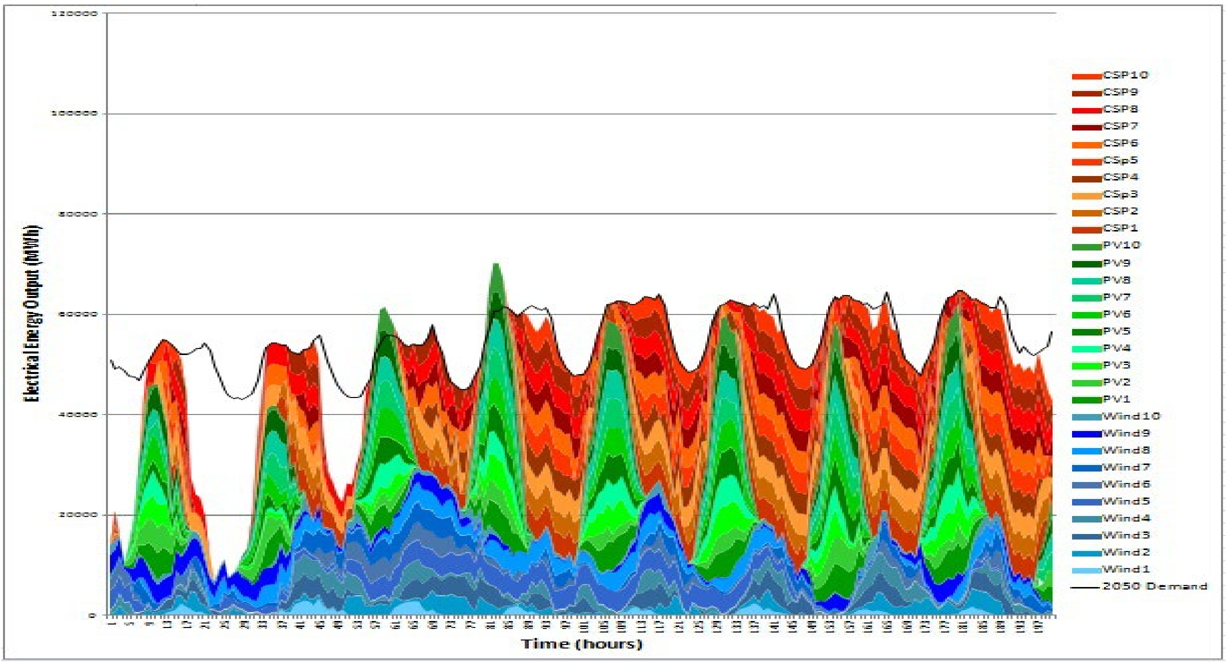

Figure 59: Scenario 4: January (200 hours) Wind, PV, CSP Electrical Energy Outputs in 2050 with dispatchable TES

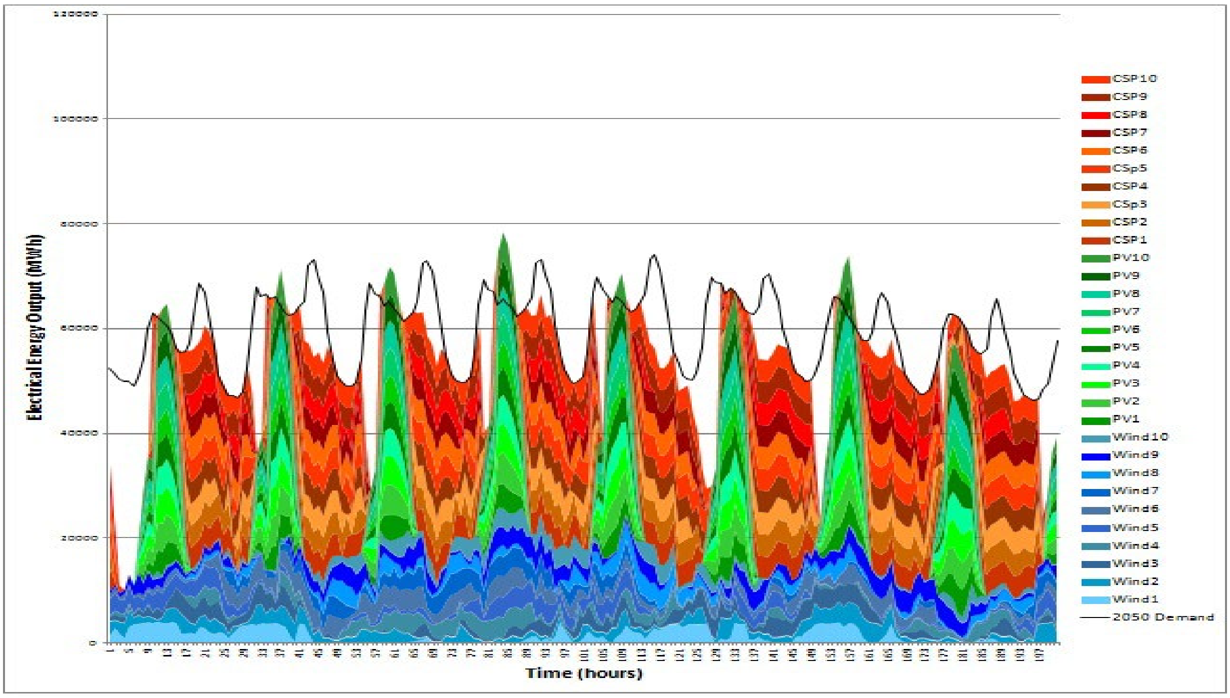

Figure 60: Scenario 4: July (200 hours) Wind, PV, CSP Electrical Energy Outputs in 2050 with dispatchable TES

4.4 Finding 3: Testing the impact of dispatchable thermal storage

The results in Figure 61 below are for scenario 8 with the 19 cases representing increasing penetrations of RE from 5% to 85% fulfilment coefficient.

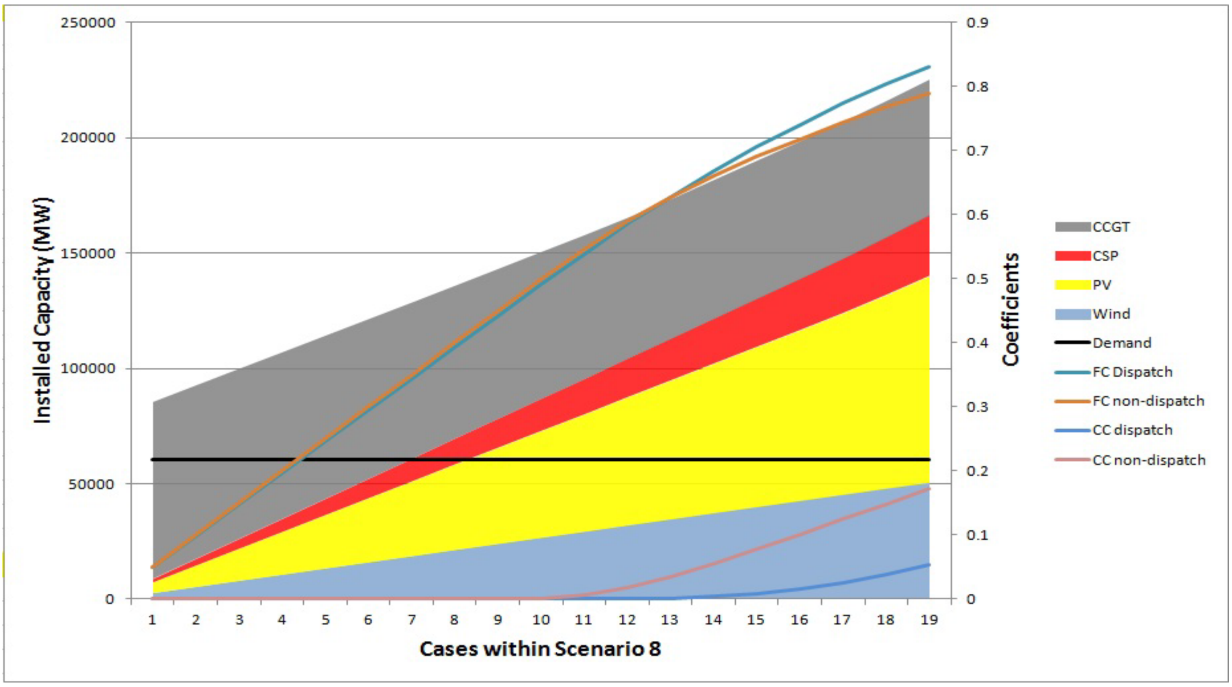

Figure 61: The effect of dispatchable TES on Fulfilment and Curtailment Coefficients

Note:

The demand line above of 60,249 MW is the average load for the projected 2050 energy requirement of 527 TWh and is included as an indication of average capacity factor in the system. For this reason it is lower than the peak of the scaled 2050 demand curve in Figure 60 of 78,299MW. In Case 1 the maximum demand shortfall during the year, after dispatch of RE generation, was therefore 76,824 MW when renewables together only contributed 1,475 MW to the system.

As shown in Finding 2, using dispatchable TES has an effect on both the total amount of system fulfilment and the level of curtailment taking place. In Figure 61 the varying RE MW penetrations of the three technologies are shown for each of the 19 cases. These examples cumulatively comprise Scenario 8. Note that these MW allocations have been automatically calculated by the model after assigning FCs as defined by the scenario design outlined in Figure 48.

The different capacity factors of these technologies mean that the MW allocations for Wind and PV are substantially overrepresented in the latter cases. When the FCs are each 31.6%, according to case 19 above, the combined MW capacity of the RE technologies needs to be 166,328MW, with 59,194 MW of CCGT to ensure that the backup system can match the maximum demand shortfall imposed by renewables. In this analysis the CF of the three RE technologies combined is 31.8%, calculated from actual electrical energy generated by the models as a proportion of energy potentially generated at full load. The instantaneous demand requirement is calculated as 60,249MW to match the yearly demand requirement of 527.94 TWh in 2050, as stated. The FC and CC for a dispatchable CSP system are shown. Curtailment of electrical energy from RE technologies starts in case 13 for the non-dispatchable system, when RE allocations reach 21.6% each. From this point onwards a marginally greater fraction of energy is progressively wasted by the system.

The inclusion of CCGT technology allows the system to meet the instantaneous demand at each hour across the year, with gas technology effectively backing up any demand deficit imposed by the RE technologies. Gas technology (usually OCGT) does normally function in a peaking role, so it is assumed to do so here to represent a completely dispatchable conventional system being integrated into a RE system for backup purposes. Figure 62 below contrasts RE technology installed capacity and energy production with the 2050 IEP demand of 527.94 TWh.

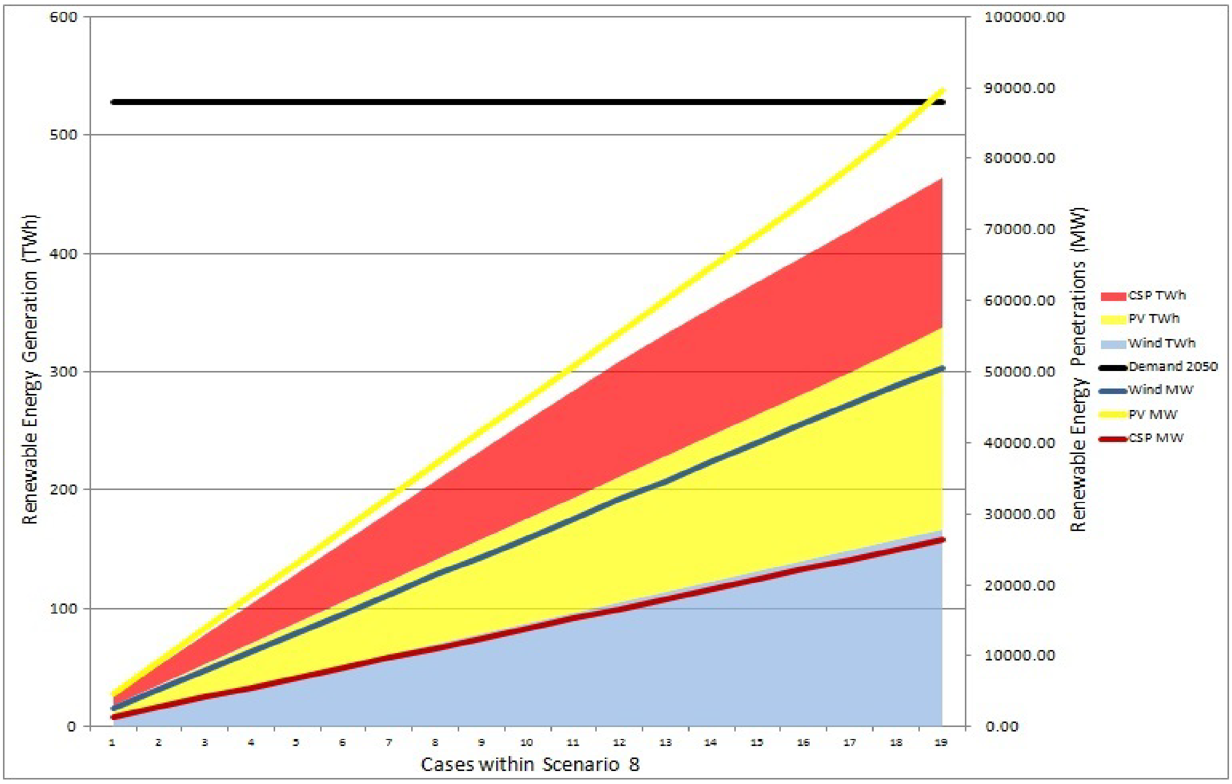

Figure 62: Total electrical energy production from renewable technologies

In the accompanying figure, total electrical energy generated by the technologies (TWh) was plotted against the MW penetrations calculated as being necessary to meet the forced FCs found by the model. The demand requirement in 2050 is also indicated, with the CCGT MW and TWh needed to match this demand excluded from the figure. Thermal storage is used in dispatchable operation within the CSP system, making more efficient use of the solar resource over time. This increases fulfilment of the whole system by pushing curtailment downwards, with this behaviour specifically indicated in Figure 63.

The penetration of RE technologies in the same proportions as for Scenario 8 were incrementally increased to find the capacity required to reach 100% fulfilment. Figure 62 above shows that 100% fulfilment is nearly being reached after 19 stages, at approximately 84% fulfilment. This graph was used as guidance for the testing of complete fulfilment. Therefore, the capacities in Figure 62, of 50,000MW Wind, 90,000MW PV and 20,000MW CSP were divided by 40 simply to find the capacity increments needed to reach approximately the same fulfilment values in Figure 62. This meant that the starting stages used were 1,250MW Wind, 2,250 MW PV and 500MW CSP. Each stage afterwards undergoes the addition of the same technology capacities. After 40 model runs the expected fulfilment was reached, being similar to that in Figure 62. After 138 model runs 100% fulfilment was reached in Figure 63. The penetrations of RE needed were unrealistically forced to high numbers to account for the CFs of the technologies.

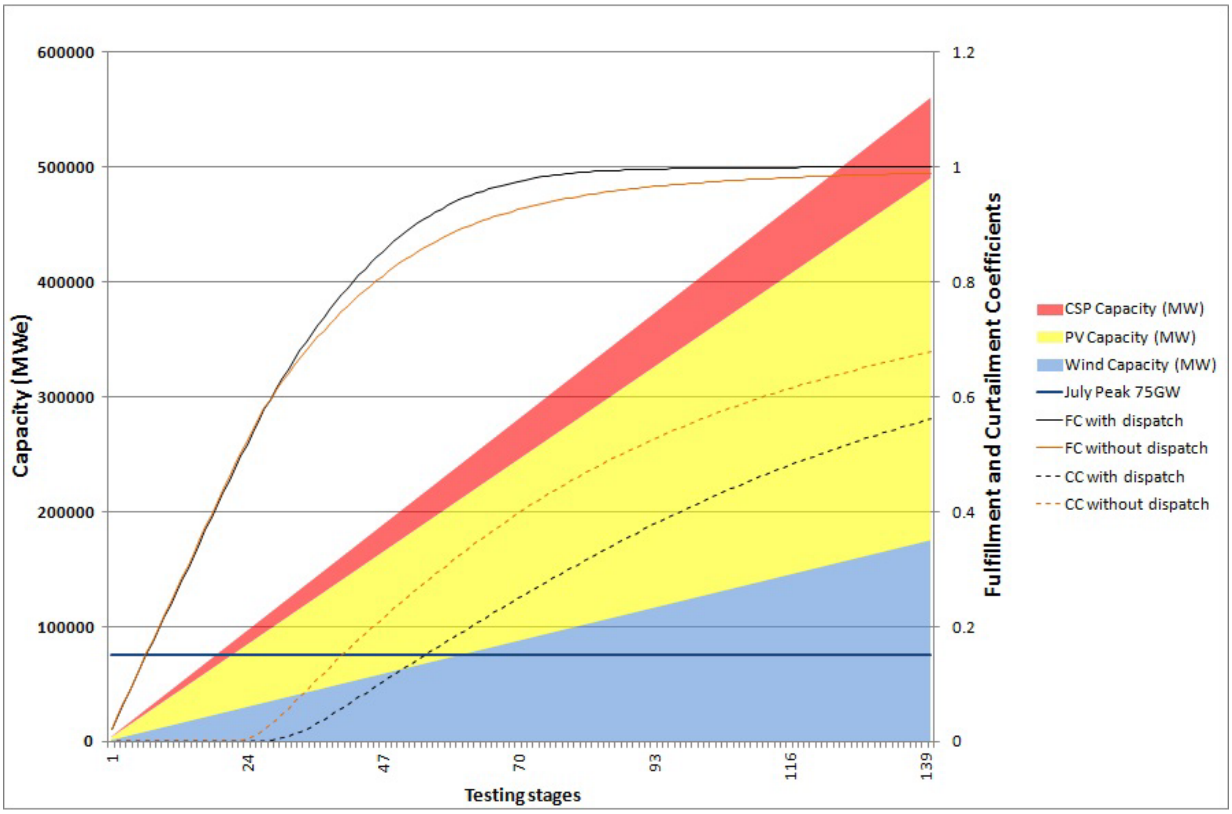

Figure 63: The attainment of 100% Fulfilment using only RE technologies

Note:

Many simulations could have been run using more CSP to lower the large size of the Wind and PV installed capacities, however, this example demonstrates the high capacity requirements necessary for only small improvements in FC particularly beyond an FC of around 85%. A more thorough type of optimisation here would coordinate the penetrations of each RE technology to push supply reliability upwards. A likely outcome of doing so would bring PV penetration down and include larger amounts of Wind. By using 15 hours of storage, CSP has the highest CF of all the RE technologies tested, and would complement more intermittent Wind and PV technologies. Due to these reasons it would make up the majority of supply in such a scenario.

4.5 Finding 4: Fuel price sensitivity analysis with learning rates, (Scenario 8-13)

The results of the sensitivity analysis presented in Figure 64 contrasts LCOE for increasing RE penetration for three cases of natural gas price for fuelling the CCGT technology, using 2012 input costs and assuming no learning rates. These 2012 cost inputs are shown in Figure 40 while the gas prices used in the sensitivity analysis are included in Figure 42. The result below was generated through the integration of the Wind, PV, CSP and LCOE models. Each of the fuel price examples represents a process of testing different penetrations of renewables and CCGT within the model, cumulatively matching 100% fulfilment of the expected demand. This process was carried out for the three gas price cases. The same process was run assuming learning on the capital cost of RE technologies and these results are presented in Figure 65 below.

In the low cost example below in Figure 64 variable O&M inputs are set at R430.19/MWh for CCGT (2012), causing the LCOE to gradually increase until Case 12, where it begins increasing more rapidly to R0.84/kWh in Case 19 as the share of renewable energy is raised. In the medium fuel cost example of R645.29/MWh the LCOE decreases slightly as RE penetrations increase to Case 12. At Case 12 the LCOE stops declining and begins to increase steadily to reach R0.85/kWh. The high fuel cost example of R860.38/MWh shows an interesting result where the decreasing LCOE is more pronounced from Cases 1 – 12 than in the medium fuel cost example. At Case 12 the LCOE increases noticeably to R0.88/kWh. When fuel costs are set to maximum, the LCOE of the large renewable system in Case 19 is fractionally less expensive than the large CCGT system in Case 1.

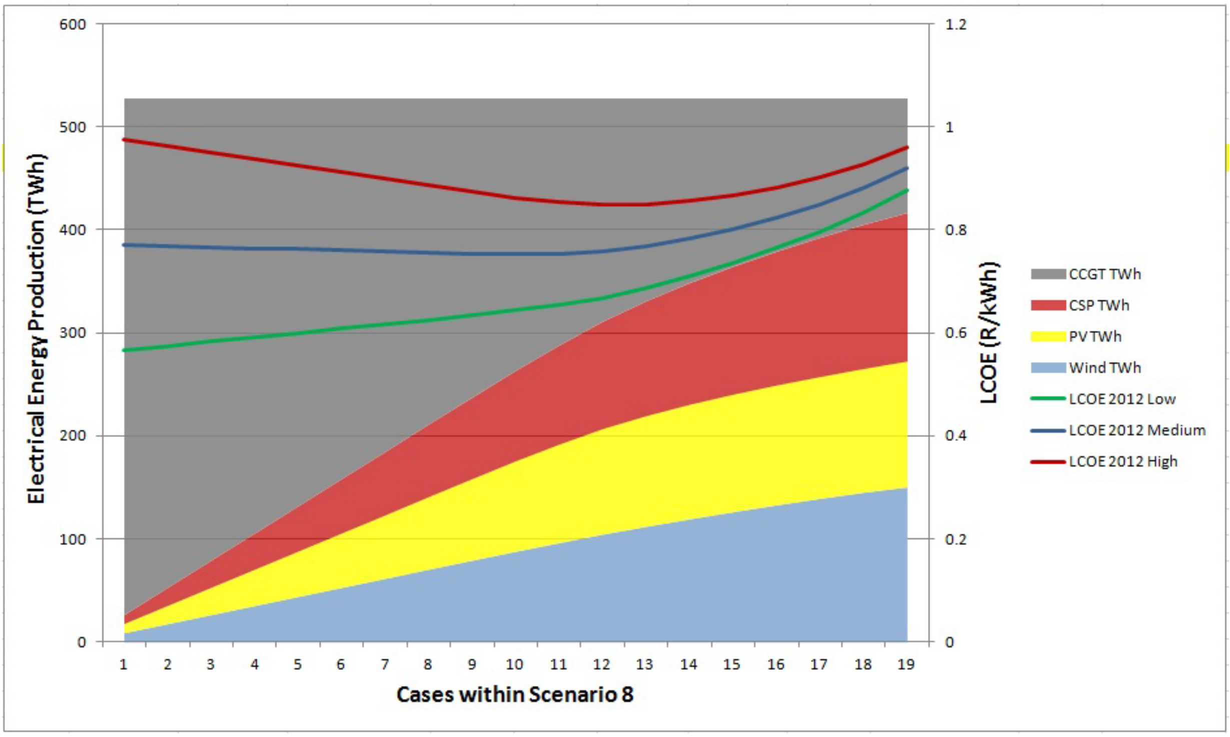

Figure 64: Total electrical energy production with 2012 LCOEs for high, medium and low gas prices

When learning rates are applied to the 2012 R/W cost inputs shown in Figure 64 above, the 2030 LCOE cost curves below in Figure 65 were generated. The assumed learning rates for the four technologies are shown in Figure 43. The 2030 LCOE results for the three different fuel cost input cases are more favourable for RE technologies. The effect of assumed learning is illustrated in Figure 66 where the dotted LCOE curves represent scenarios assuming learning. The impact of learning on 2012 LCOEs becomes more pronounced as the penetration of renewable energy increases.

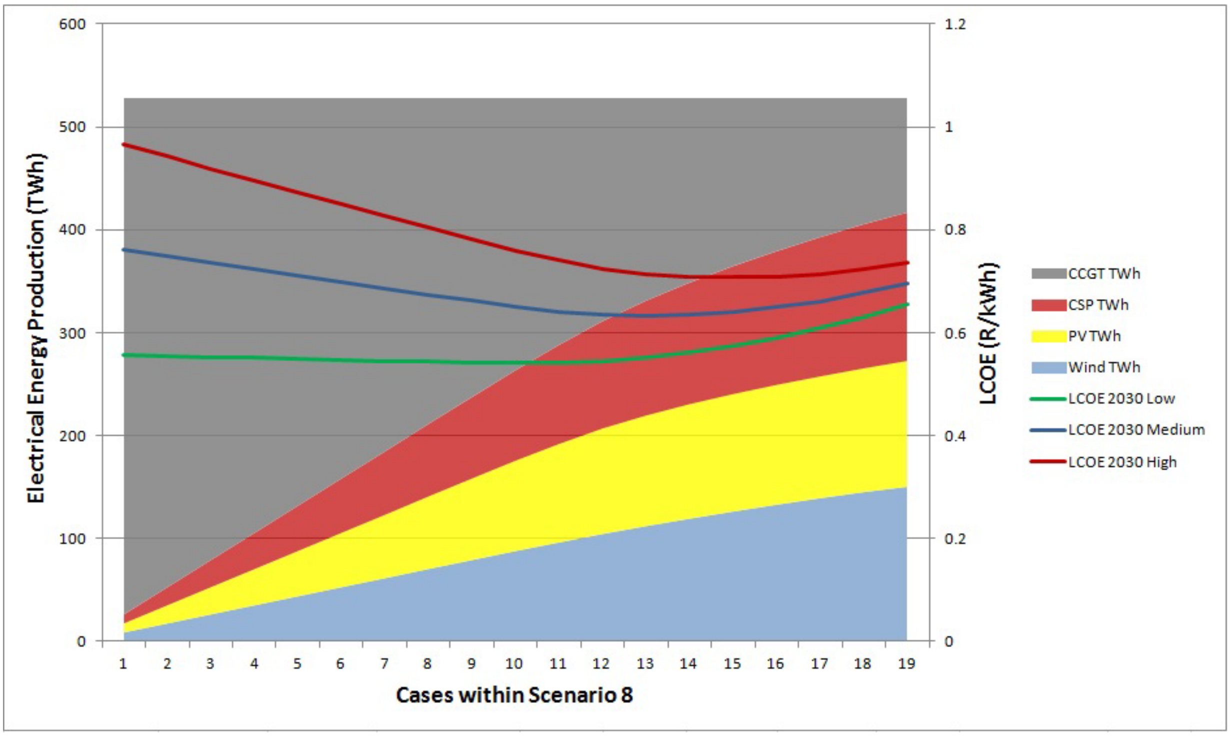

Figure 65: The effect of fuel price on system LCOE with learning rates (2030) for high, medium and low gas prices

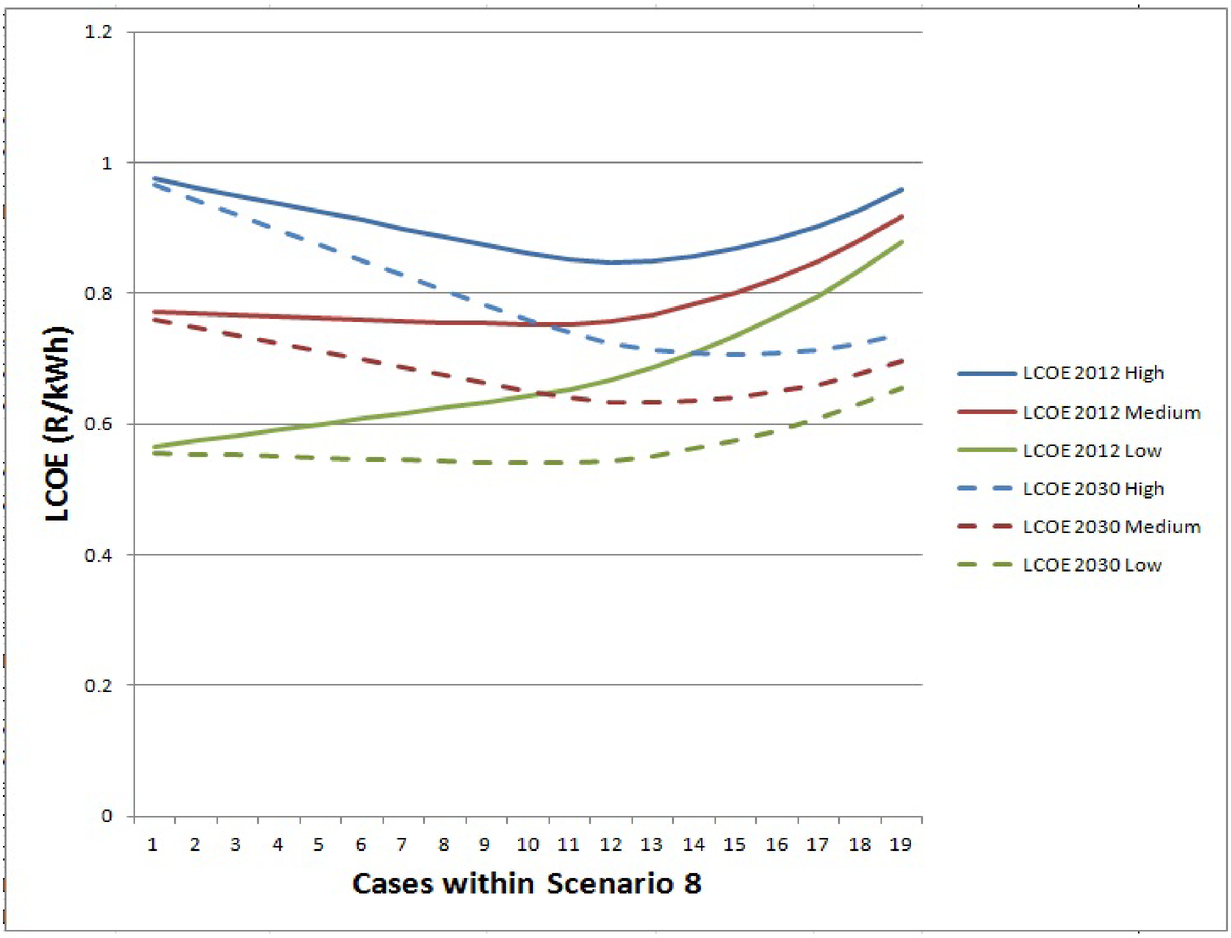

Figure 66: Impact of learning rates on 2012 LCOEs

The LCOE values for the analysis carried out in Finding 3 (Figure 63) above are included below.

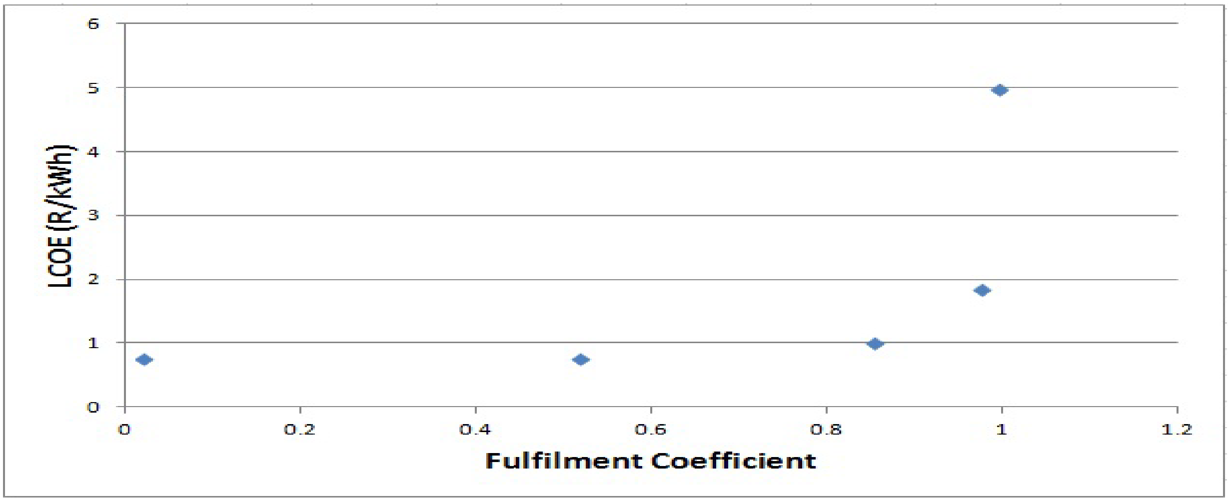

Figure 67: System LCOEs vs. Fulfilment Coefficients using 2012 costs

The corresponding LCOE values and FCs for the analysis carried out earlier in Finding 3 (Figure 63) are included above. This is for the 2012 medium fuel cost example and showed that as capacities of RE are forced towards total fulfilment, system costs are increased substantially.

The application of learning rates to 2012 technology costs caused the overall system to have a lower LCOE value, for a high RE penetration system, particularly if future gas prices are high (Figure 64 and Figure 65). The costs of the 2012 capacities shown in Figure 67 are unrealistic from about 85% fulfilment onwards. The assumed learning rates may be conservative given that they are the learning rates projected for 2030 by the IRP which suggests that actual learning rates achieved by 2050 may yield even greater reductions in LCOEs for a future large scale RE system.

4.6 Finding 5: Water Usage and Avoided Emissions versus RE Penetration

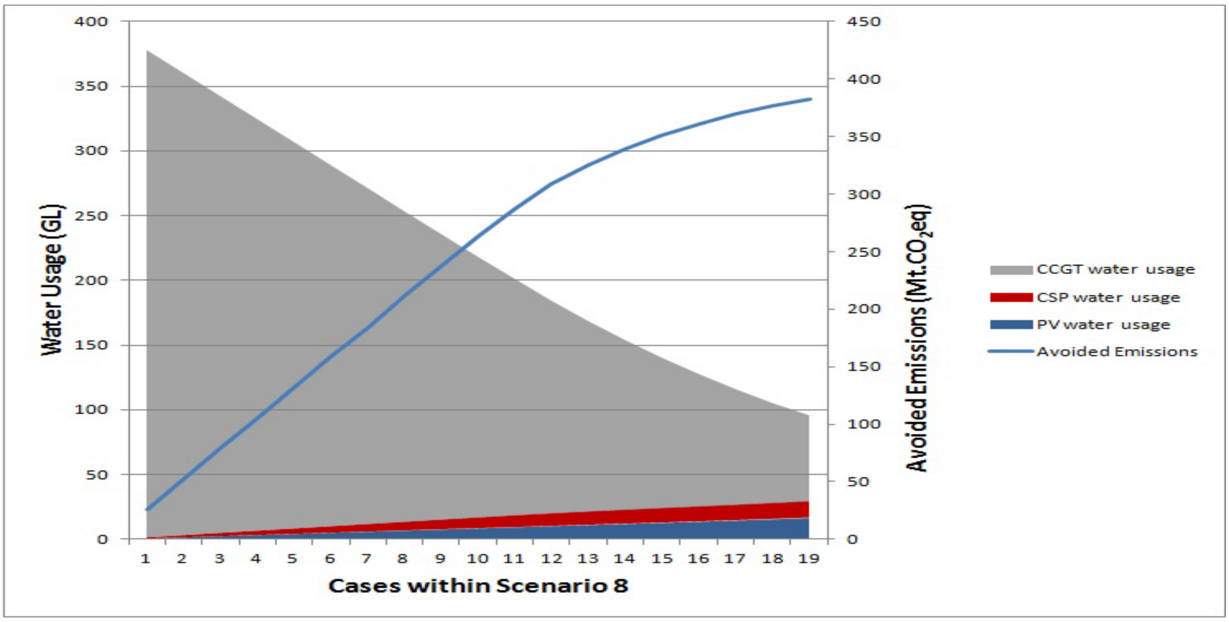

Figure 68: Water Usage vs. Avoided Emissions

The total volume of water used by the technologies is calculated for PV, CSP and gas according to Section 3.4.8. Wind technology is assumed here to have zero water requirements. Avoided emissions are calculated as CO2 equivalent using the GWP of the criteria emission pollutants as presented in Figure 46 applied to the emission factors (kg/kWh) presented in Figure 45. In Figure 68 above these two quantities are displayed together, showing that a system comprised mainly of gas technologies uses a substantial amount of water in comparison to a RE fleet producing the same amount of energy. This large gas fleet also achieves a much lower avoided emission value. In this analysis, PV technology used a larger volume of water than CSP, which is attributed to the larger MW capacities required by the technology to attain the targeted FCs within Scenario 8. When gas technology is required to provide only 26% of the system fulfilment in case 19, a disproportionately large amount of water is used by the gas system, compared to the CSP and PV systems that are each providing 31.6% of system energy at this point.

Chapter Five – Discussion

Finding 1: Investigation of system indicators Scenarios 1-7

Energy production

The CSP output (TWh) results indicate that the modeled CSP scenarios are greatly undersized in relation to potential, with significantly more energy available for use from this technology in SA according to the Fluri study, (2009). This underrepresentation of CSP technology in the scenarios indicates higher FCs could be achieved if greater proportions of this technology are used to support other intermittent RE sources.

Coefficients of Scenarios 1-7

Given the midday peaking behaviour of PV technology, the cumulative amount of energy produced in Scenario 3 greatly exceeds the 527.94 TWh energy requirement in 2050. PV needed to be forced to a very large scale to attain the 50% FC, with associated curtailment being unproductively increased, (Figure 50). The FC in the non-dispatchable example of Scenario 3 is the lowest in all scenarios, despite the oversized PV build. A FC approaching unity is not achieved in this modelling result due to the underrepresentation of high reliability technologies in the scenarios.

Effect of dispatchable TES on LCOE 2030

A change to the overall system cost is observed between the dispatch and non-dispatch results provided in Figure 51. This occurs due to changing levels of curtailment, as curtailed energy is not utilised when calculating the LCOE in the dispatch and non-dispatch example. It is presumed here that an energy utility would not accept high levels of curtailment. In such a case, Scenario 3 is undesirable based on loss of production and raised system costs.

Avoided emissions

The cumulative reduction in GHG emissions in CO2 equivalent terms achieved by the scenarios, is nearly double Eskom's emissions of 225 Mt for 2011 (Eberhard, 2011). The Mt.CO2eq value attained here incorporates a small percentage of SF6, which has a GWP of 23,900 compared to CO2. The policy adjusted scenario, adopted by the IRP 2011 and displayed in Figure 3 above, employs a carbon emission constraint of 275Mt per year beginning in 2025, (DOE, 2011). Although the carbon constraint for 2025 exceeds the reference year (2011), the scenarios still achieve an avoided emission total in excess of this 2025 constraint. However, the 2025 DOE value is calculated allowing for substantial portions of conventional technologies, which are entirely eliminated in the scenarios assessed here.

Water usage

South Africa is a water scarce country. Every year the annual rainfall for the country is 450mm, compared to the global average of 860mm. The combined water flow from all the rivers in SA per year is 49,000GL, (DWAF, 2004). Available water within storage reservoirs is 32,412GL, while the volume of ground water used yearly through agriculture and human consumption is 1,088GL, (DWAF, 2004). The total annual water consumption for South Africa was 13.28 billion m^3 (13280 GL) in 2000, (DWAF, 2000). The water requirement for Scenario 1 comprising of both PV and CSP was 30.55 GL, 0.002% of the annual water consumption in 2000. Eskom consumed 273 GL in 2004, used primarily for cooling purposes, (Pather, 2004). This implies that the water consumption for Scenario 1 was 11% of Eskom's total water consumption in 2004. In the event that the wet-cooled option is used for CSP, and taking the water consumption value to be the same as Gemasolar, (1,920.27 litres/MWh), then in Scenario 1 CSP would consume 246 GL of water, or 90% of Eskom consumption in 2004. These figures briefly contextualise total water use and availability in SA, in relation to the volume of water indicated for use by the RE technologies within the scenarios in one year.

Area

The scale of the RE build in the modeled scenarios indicates that large areas of ground surface will be impacted. The effects to both terrestrial and airborne creatures are not specifically analysed by this thesis. Research has raised concerns about particular species of insects that, "use the horizontal polarisation of light off bodies of water to find egg-laying sites," (Horváth et al., 2010). The displacement of eggs from regular spawning sites, (water), would disrupt reproductive cycles. However, an additional problem raised by this research was that PV plants start acting as environmental sinks for species, as birds are drawn towards the panels by the potential increase in insect abundance. Research covered in the literature review, (Chapter 2), contextualised animal deaths attributed to different energy technologies and found RE had significantly lower fatalities compared to conventional facilities.

A question posed when dealing with RE penetrations of this magnitude is the potential impact caused by the shading of large areas of ground surface by panels and heliostats. The increased reflectivity of the facet surface directs more solar radiation away from the ground, potentially causing a drop in temperatures and also affecting the temperature of the microclimate. The associated implication of this temperature reduction could involve impacts to species variety. A recognised concern within the global warming framework is the impact to species biodiversity. These potential impacts, caused by temperature variations around solar fields, are refuted by Delucchi and Jacobson, (2011). These researchers state that an overall reduction in radiative forcing is achieved by replacing fossil fuel generators with RE through lowering global CO2 emissions, (Delucchi & Jacobson, 2011).

Viable Area

The quantity of electrical energy production modeled for wind energy in this thesis is overstated, according to South Africa's onshore wind potential of 80.5 TWh found by other research. In the realistic scenario used in the Hagemann (2008) analysis, 2MW wind turbines were modeled with a system CF of 35.1%. This requires 26,180MW of installed wind capacity, in the form of 13,090 2MW wind turbines, utilising approximately 13,090km^2 of land surface area. The 80.5 TWh limit imposed here indicates that the energy output of the scenarios modeled in this thesis exceeds the 'realistic' scenario in the Hagemann study, (2008). The electrical energy generated by Scenarios 1 – 7 is more similar to the 'optimistic' scenario of the Hagemann (2008) study that provides 157.2 TWh of energy in one year. The small wind case option in Scenario 6 analysed here produces 105.59 TWh and is the closest match to the 80.5 TWh in the 'realistic' case of the Hagemann Study, (2008).

Finding 2: Validating TES dispatch within a Large CSP Scenario

The two graphs displayed in Figure 56 and Figure 57, (Scenario 4), represent the first 200 hours of midsummer and winter respectively, where the CSP outputs are not dispatched with the aim of responding to fluctuations in system demand and supply from intermittent generators. An intention of selecting these two time periods was to observe whether or not any noticeable differences were evident between the two peak seasons. Observation shows that the shape of the demand profile changes between summer and winter, with the daily winter evening peak becoming more pronounced. This is an expected change, as residential heating requirements would be higher during colder months. The afternoon energy demand also drops during winter, as air conditioning loads are reduced in the afternoons compared to the summer case.

Looking at the behaviour of the RE outputs separately, the PV energy output is greater during the summer and occurs over a longer period of each day. This is caused by longer daylight hours. Wind energy outputs during summer appear to display peaks in all the days displayed, except the fourth day. This behaviour appears in the summer graph, and does not occur in the winter graph, where the wind energy outputs are more evenly spread and do not display the same peaking behaviour during this period.

The behaviour of the CSP system also shows a noticeable difference between summer and winter months. Shorter daylight hours and less intense solar irradiance dominate during winter, causing a reduction in energy outputs from CSP, as with PV. The non-dynamic thermal storage, with no dispatch, is able to provide more energy over time in summer into the evening periods, while in winter the ability of thermal storage to provide electrical energy is reduced. This is particularly apparent in Figure 56, where electrical energy production from CSP with storage is continuous for the last five days shown. This is in stark contrast to the same period of days in Figure 57 where despite thermal storage CSP is not able to maintain continuous energy production during some colder winter days.

Due to the overall reduction in energy available for use by the RE technologies during winter, (Figure 57), the RE demand shortfall, represented as blank space underneath the demand profile, is noticeably greater during these colder months and required significant CCGT capacity to act as backup. As solar energy drives the climatological system, a greater RE demand shortfall is expected, as radiation levels drop relative to seasonal variations.

By showing CSP operating in a dispatchable configuration, actively controlled by the demand deficit from Wind and PV technologies, the results in Finding 2 seem to suggest that CSP can support more intermittent RE technologies. This is supported by the higher FC and the lower CC achieved in Scenario 4 when dispatchable CSP was employed, depicted in Figure 59 and Figure 60. The availability of sufficient solar resources is necessary for CSP to effectively carry out this supporting role for Wind and PV.

Finding 3: Testing the impact of dispatchable thermal storage

The FC and CC curves in Figure 61 account for the performance of the RE technologies only and do not include gas technology. No improved effect on system FC is caused by the use of dispatchable TES up until case 13, for which the target FC was 21.6% for each RE technology. The FC in the non-dispatchable system slightly outperforms the dispatchable system up until case 13 penetrations. These results suggest that no direct benefit is derived from using dispatchable thermal storage when CSP fulfills less than 21.6% of total system demand over the year. When CSP fulfilment increases as a percentage of the total, from case 13 onwards, a noticeable improvement to system fulfilment takes place.

This system behaviour reflects the higher CF of CSP relative to Wind and PV. When CSP accounts for more of the yearly demand requirement of 527.94 TWh, the effect of changing between dispatchable and non-dispatchable TES becomes more pronounced. At lower penetrations, the use of dispatchable TES has less effect on fulfilment. As the penetrations of RE technologies increase, the CC increases as expected. However, the use of dispatchable TES does cause a significant reduction in curtailment. In case 19, curtailment was 17.3% in the non-dispatchable system, becoming 0.007% in the dispatchable system.

The lower CFs of Wind and PV mean that these two technologies required high capacity penetrations, relative to CSP and gas technologies to meet target fulfilment. This overbuilding of capacity can be counterproductive in terms of financial and resource considerations. A system with a capacity closer to the maximum demand requirement, allowing for adequate reserve margins, makes more effective use of the electrical energy it generates. An overrepresented system with excessive MW allocations, accounting for the low CF of Wind and PV, will sometimes produce too much electricity. This is reflected by the curtailment curve (Figure 61) of the dispatchable system, which accounts mainly for Wind and PV curtailment.

Penetrations for PV technology exceed 90,000MW in the large RE system in Figure 62, where forced FCs are each 31.6%. The portion of energy generated by this capacity of PV is displayed in the TWh value. Wind technology similarly requires a large MW penetration to attain its energy production goals within this scenario, (TWh). The MW penetration of CSP would be more closely proportional to its TWh production value. The performance of each technology in Scenario 8 can be assessed based on CFs, knowing the quantity of energy generated by each technology in relation to its required MW penetration. In this analysis, CSP technology is indicated to have higher performance compared to Wind and PV, in terms of total energy generated against technology penetrations.

Finding 4: Fuel price sensitivity analysis with learning rates, (Scenarios 8-13).

The cost analysis investigated different total penetration rates of RE in 2050 with gas-fired (CCGT) generation supplying the balance of energy. The purpose of including conventionals into this RE system analysis was to assess the effect on system cost of changing penetrations of conventionals relative to renewables, as well as to specifically assess the effect of changing fuel costs. The modelling process can find any sized conventional system that allows 100% total fulfilment, with the remaining demand requirement being made up by RE. A more comprehensive description of the specific method used in this process is provided in the chapter on Method, Section 3.4.6.

In Figure 66 above LCOEs for three different gas fuel costs were presented with and without technology learning. Due to the expense of running CCGTs at the penetrations required to entirely backup the demand shortfall from the three RE technologies the large CCGT system in Case 1 (2012) is more expensive than the RE system, except in the low fuel cost example. The application of technology learning (Figure 66) through changing technology cost assumptions (R/W) showed a marked reduction in LCOE for the high fuel cost with increasing RE penetration, with a slight reduction for the medium fuel cost. For the low fuel cost assumption an increase in LCOE was observed with transition from a large CCGT system (Case 1) to a large RE system (Case 19), even with the assumption of technology learning.

Finding 5: Water Usage and Avoided Emissions versus RE Penetration

An assessment of the availability of adequate water resources is needed when siting CSP plants, (Fluri, 2009). This is particularly true in areas of SA that exhibit the highest solar resource, where access to water might become a concern if competing with local agricultural industries. The GL volumes of water consumed in the CSP and PV scenarios are hard to quantify without knowing the total future availability of water for the relevant regions of SA relative to future demand. Some statistics on water availability for SA were included in Section 3.4.8. These indicate that although sufficient quantities of water are available to meet the requirement of the scenarios, it is suggested here that dry-cooled CSP technology be considered in the more arid portions of the country. The logistics of transporting the required water are not addressed in the preliminary assessment of water resources done here. Water transportation issues, or concerns in siting CSP in proximity to water bodies, would likely be minimized by building dry-cooled CSP.

Although the scenarios analysed here have higher avoided emissions compared to the emission constraint used by the IRP RBS, a comparison between the two is not justified because the RBS uses large proportions of fossil generators, whereas the scenarios modeled here are attempting 100% RE penetrations. The global effect of SA achieving these levels of avoided emissions in 2050 is not studied here. However, it can be tentatively suggested that such reductions in emissions would be beneficial to the wider environment and would aid in maintaining stable atmospheric, ground and sea surface temperatures, among a range of benefits achieved through reducing atmospheric CO_2 concentrations.

LIMITATIONS OF THE MODEL AND FUTURE IMPROVEMENTS

The model developed in this thesis to analyse electrical energy output from the three renewable energy technologies did not account for planned or forced outages. For example, in the hypothetical scenarios investigated there is potential for a number of CCGT (or CSP) units to be offline simultaneously. This situation could either strain or seriously impact the reliability of an electricity network. The uncertainty around such unexpected events would need to have been calculated using a stochastic model, which was beyond the scope of this research exercise. For the current model, the option of using an expedient of 15% reserve margin could have accounted for the necessary increase to total capacity to strengthen reliability. However, this would have been the same for each scenario and would not have benefited comparison between them.

Wind and PV technology do not have commercial storage options at the current time, meaning there is additionally the possibility that renewable energy plant outages caused by intermittent resources could coincide with outages from either dispatchable or non-dispatchable conventionals. This typically means that as renewable energy penetrations increase, the reserve margin for the system must also be increased. Calculating the needed increase to the reserve margin as renewable energy penetrations increased relative to conventionals would have required a dispatch model targeting a specified system reliability, which was beyond the scope of this thesis. This could become a focus of extending this work.

When work began on integrating several spreadsheets into one master spreadsheet, the intention was to include both dispatchable and baseload conventionals into the analysis and to then assess the interaction with renewable energy, however, it proved challenging in the available time to implement several different types of thermal generator to supply the RE generation shortfall. Instead gas-fired CCGT only was included in the model given that this technology can operate with reasonable economy across a range of capacity factors and is relatively low carbon and is thus an appropriate technology to represent RE backup in a carbon constrained future. Future work on this topic could investigate the effect of including baseload conventionals, including coal and nuclear generators, on the curtailment from renewable energy. The conventional technology used in this thesis was assumed to be completely dispatchable and acted to produce the exact demand shortfall imposed by the renewable energy technologies relative to demand. This may have been unrealistic for some scenarios where OCGT would have been more appropriate for short term demand shortfalls. Due to the difficulties encountered in implementing different types of conventionals and the fact that the goal of the thesis was to investigate changes to technology costs and other indicators around the scenarios, it was decided that one representative dispatchable conventional would be used to meet the demand shortfall from high penetrations of RE technologies. Future work should address this shortcoming, with a more realistic representation of plant mix and its dispatch.

The production values (TWh) of the Wind and CSP capacities within the scenarios were compared against those estimated by Hagemann, (2008) and Fluri, (2009), respectively. The Wind scenarios were found to be overstated by this thesis relative to the 'realistic' 80.5 TWh estimation from Hagemann. The model used in this thesis was designed to explore a hypothetical year set in the long term future where it is likely that supporting infrastructure such as road networks and transmission lines would have been substantially expanded. This would open up more potentially suitable wind sites meaning that the 'optimistic' scenario from the Hagemann (2008) study would become more appropriate as a comparison to the wind potential found by this thesis.

Additionally, the 80.5 TWh estimation found by Hagemann (2008) is applicable to terrestrial wind energy potential for South Africa, and does not include offshore wind power. This suggests that the wind potential for South Africa, inclusive of offshore options, could well be larger than 80.5 TWh. The discrepancy between the size of the wind scenarios investigated here, and the 2008 study mentioned above is partially addressed in the results of Scenario 8, (Figure 62). This scenario evaluated varying penetrations of the three RE technologies. Reading off this figure, 80.5 TWh of wind power was reached at testing stage 10, where the installed wind capacity was approximately 27 GW. Future work could use the current model to investigate 80.5 TWh of wind energy, with a combination of PV, CCGT and dispatchable CSP making up the remainder of demand.

Chapter Six – Conclusions

In addressing Research Objectives 1 and 3, Finding 1 showed the results of various indicators used to assess potential future scenarios. The energy production values for Scenarios 1-7 showed that when PV capacity is set to match 50% of system fulfilment, significant quantities of electrical energy are wasted. This is reflected specifically in Scenario 3, where curtailment was 67% without dispatch and 63% with dispatchable thermal storage. This large amount of wasted energy equated to Scenario 3 attaining the lowest fulfilment of the group investigated and also the highest LCOE.

The quantity of electrical energy generated within the CSP scenarios was within the total available resource estimated by the Fluri study, (2009), which estimated that a total of 1861 TWh of electricity could be obtained within the viable high solar resource areas of SA. This under production of CSP in the current study occurs because CSP only matches 50% of demand fulfilment in the largest CSP scenario. In future work, the model could be used to analyse much larger capacities of CSP. In Figure 51, the effect of dispatchable TES on the LCOE of the first seven scenarios was displayed. In each case the introduction of the fully dispatchable CSP system caused a noticeable reduction in system costs, thereby strengthening the assertion that dispatchability through adoption of storage technology improves project finance.

The land areas used by the PV and CSP scenarios were calculated relative to the area of the Northern Cape, as this province experiences the best solar resources in South Africa. Given the large land area of the Northern Cape, the RE scenarios investigated here to meet a 2050 demand, would use approximately 0.005-0.048% of the Northern Cape land area for PV and 0.003-0.009% for CSP. Wind technology uses a larger proportion of land in this analysis, namely 2.1% of the land surface of South Africa in the largest wind scenario modeled here, (2). As more land is used in the scenarios the likelihood of environmental impacts increase. Avian deaths are an environmental consideration in the building and placement of large wind turbines. The expected rate of death for avian species from wind in this analysis was contextualised against fossil-fuel generators and nuclear technology. This showed avian deaths ascribed to wind energy as comparatively low.

In addressing Research Objective 2, the dispatchability of TES was investigated in the large CSP (50%) scenario. Figures 56-60 displayed the demand deficit imposed by intermittent Wind and PV production. Figure 58 showed the integration of this deficit into the TES model. A significant improvement in fulfilment was gained, through the reduction in total system curtailment. The dispatchable system, composed of 25% Wind, 25% PV and 50% CSP, reached a fulfilment of 88%. This is an improvement of 5.5% over the non-dispatchable system. The identified benefit of employing dispatchable TES corresponds with work done by other researchers, (Denholm & Mehos, 2011). The utilisation of dispatchable TES improves system performance within a large-scale RE system, when using energy production as an indicator of grid reliability over one year.

The system coefficients for the 19 test cases of Scenario 8, (Figure 61), confirmed the earlier findings, namely that a dispatchable system improved fulfilment and reduced curtailment. For this reason, the fully dispatchable system was used in Scenario 8. Figure 62 displays the relationship between technology penetration and production relative to projected demand in 2050. To reach the demand projection of 527.94 TWh, (DOE, 2013b), the penetrations of Wind and PV needed to be approximately 50,000 MW and 90,000 MW respectively. These large penetrations are caused by the low CFs of these technologies. In contrast, the penetration of CSP needed to be approximately 27,000 MW. CSP produces a more substantial quantity of total energy (TWh) relative to the installed capacity of this technology. The CF of the technologies were calculated here to be 37.6% for Wind, 21.7% for PV and 72.5% for CSP.

In addressing research objective 3, the economic comparison conducted within a hypothetical 2050 scenario found that when using today's (2012) capital costs for generation technologies, a system comprised mainly of renewables was more expensive in the case of medium and low natural gas cost for the CCGT meeting RE demand shortfall, while fractionally less expensive for the high fuel cost case (Figure 64). When learning rates were applied to the analysis, the costs of the RE weighted scenario (95%) dropped noticeably compared to the large CCGT scenario for the high and medium fuel cost examples in Figure 65. The low gas cost case including learning still shows an increase in system costs for the high RE scenario.

In the unlikely event that PV were to make up 50% of the fulfilment requirement, the quantities of curtailed energy would be excessive and prohibitive. The associated system cost would not be financially feasible, due to the amount of curtailment modeled to take place in such a scenario, (Figure 50). The cost of the system can be effectively lowered by using dispatchable TES, which reduces the total amount of curtailment taking place from solar technologies. The peaking behaviour of PV technology is not entirely suitable in large scale renewable penetrations, in terms of factoring in the midday increase in energy production. When PV penetrations are relatively low compared to the entire energy system, the lack of correlation of the peaking behaviour of PV with daily fluctuations in demand has less impact. In this analysis CSP technology is shown to actively complement such peaking behaviour within large scale penetrations where curtailment from PV might be problematic. CSP can achieve this by providing energy during troughs in RE production. The intermittency of wind technology is also complemented by CSP, in terms of increases to system FC when dispatchable TES is used.

When the LCOEs and fulfilment coefficients were plotted against each other in Figure 67 an exponential increase in system costs was observed for very high penetrations of RE above approximately 85% fulfilment where costs began to accelerate massively as fulfilment approached 100%. This indicates that a large scale RE scenario comprising of the technologies used here might be feasible below 85% fulfilment based solely on an LCOE analysis, however due to problems of intermittency and curtailment of specifically the PV component of the fleet, above 85% fulfilment from RE becomes prohibitive based on cost grounds.

In line with South Africa's current activities and plans towards renewable energy programmes, the current study has investigated the possibility of a large scale renewable energy future in 2050. The large capacities of RE needed to match 100% of demand were illustrated in Figure 63 and indicated that on cost grounds such scenarios are unlikely. More plausible future scenarios involve renewable energies being responsible for the greater portion of the yearly energy demand requirement, for example scenario 7, (Figure 50).

In this dissertation CCGT was modeled to backup the demand shortfall from renewables and showed that in large scale renewable energy scenarios a correlation event between low renewable resources and high demand requirement could cause a large demand shortfall and would necessitate a suitably sized CCGT system. However, running the CCGT plants at high CFs was shown to incur large fuel costs for gas prices at the upper end of projections as shown in Figure 64 and Figure 65. A more complex modeling exercise could be carried out to study the representation of non-renewables (OCGT, coal, nuclear) and how these different technologies might interact and compliment the three renewables studied here. It would also be interesting to investigate the potential of biomass/biofuel fired baseload to further increase renewable energy capacity.

The current cost of electricity has seen various price increases, meaning that given time, the cost of renewable energy could become more competitive with conventional generators, which were represented here by CCGTs. A professional energy specialist in South Africa, has stated that within two years the electricity cost of RE would be less expensive than Eskom, (Meiring, 2014). It could be expected that in 2050 these costs will be lower, mainly through technology learning for RE and fuel price increase for fossil fuels. Future work could look at cost optimal options for the modeled renewable and conventional fleet of generators.

An important consideration in the scale of the scenarios evaluated here are the environmental impacts which might arise through land use change and the operation of the Wind, PV and CSP plants. Each of these technologies has environmental impacts, for instance bird and insect fatalities were discussed. There is potential for mitigation, for example, using lightweight, light-permitting netting encompassing solar plants. There are numerous research avenues available with regards to renewable energy development and associated environmental impacts.

Another important consideration which this thesis investigated, was the intermittency of Wind and PV technologies. One potential option to address this problem was the use of TES equipped CSP plants, which were capable of dispatching electrical energy successfully during periods of reduced production from Wind and PV. This potential role for CSP was assessed within the large scale RE scenarios above. Future research could look at further optimising the relative capacity of renewable energy generators at different sites depending on resource availability to reduce the intermittency of supply. Such a study might investigate a greater number of sites compared to the 30 investigated here. This would provide a better understanding of the geographical distribution of renewable energy resources across South Africa.

Some additional recommendations towards future research are to carry out stochastic modeling to allow for more realistic plant reliability in the analysis. This would account for downtime due to unforeseen plant outages and scheduled maintenance. It would also be useful to investigate storage options for Wind and PV, with a range of emerging technologies showing potential. One option that has been discussed would be to store excess grid electricity at CSP storage plants. In this study molten salt was used as the storage medium for CSP, meaning the conversion efficiencies from electricity to thermal energy and then back to electricity would be low. However, this might still be viable if the excess electricity from Wind and PV would normally be curtailed and wasted.

Renewable energy technologies offer a feasible alternative method of electricity generation. The continued growth in the industry suggests the potential of these technologies is already recognised. South Africa has excellent wind and solar resources, identified in this and other research. Wind and PV without storage attain lower CFs at present compared to CSP with TES. The dispatchability of CSP allowed improvements in cost savings through reductions in curtailment. Renewable energy technologies with higher CFs and greater flexibility in dispatching electricity are of interest in supporting lower reliability zero-carbon technologies.

References

Bhattacharyya, S. C., & Timilsina, G. R. (2010). A review of energy system models. *International Journal of Energy Sector Management*, *4*(4), 494–518. doi:10.1108/17506221011092742

Bisschop, J. Roelofs, M. (2008). *AIMMS: Optimization Modeling* (p. 306). Amsterdam: Paragon Decision Technology. Retrieved from www.aimms.com

Brinkman, G. Denholm, P. Drury, E. Margolis, R. Mowers, M. (2011). Toward a Solar Powered Grid. *IEEE Power & Energy*, (june).

Burgaleta, J. I., Arias, S., & Ramirez, D. (2011). GEMASOLAR , THE FIRST TOWER THERMOSOLAR COMMERCIAL PLANT WITH MOLTEN SALT STORAGE. *SolarPACES*.

Calculating Greenhouse Gases. (2014).*International Carbon Bank & Exchange*. Retrieved from http://www.icbe.com/emissions/calculate.asp

CDIAC. (2013).*Carbon Dioxide Information Analysis Center*. Retrieved from http://cdiac.ornl.gov/

Cengel, Y., & Boles, M. (2011). *Thermodynamics: An Engineering Approach* (p. 981).

Concentrating Solar Power Commercial Application Study: Reducing Water Consumption of Concentrating Solar Power Electricity Generation, Report to Congress. (2008).*U.S Department of Energy*. Retrieved from http://www1.eere.energy.gov/solar/pdfs/csp_water_study.pdf

De Lucas, M., Janss, G. F. E., & Ferrer, M. (2004). The effects of a wind farm on birds in a migration point: the Strait of Gibraltar. *Biodiversity and Conservation*, *13*(2), 395–407. doi:10.1023/B:BIOC.0000006507.22024.93

Delucchi, M. A., & Jacobson, M. Z. (2011). Providing all global energy with wind, water, and solar power, Part II : Reliability, system and transmission costs, and policies. *Energy Policy*, *39*(3), 1170–1190. doi:10.1016/j.enpol.2010.11.045

Denholm, P., & Hand, M. (2011). Grid flexibility and storage required to achieve very high penetration of variable renewable energy. *Energy Policy*, *39*(3), 14.

Denholm, P., & Mehos, M. (2011). *Enabling Greater Penetration of Solar Power via the Use of CSP with Thermal Energy Storage* (p. 28).

Denholm, P., Milligan, M., Ela, E., & Kirby, B. (2010). *The Role of Energy Storage with Renewable Electricity Generation* (p. 62).

Department of Energy. (2011). *Electricity Regulation Act No.4 of 2006, Electricity Regulations on the Integrated Resource Plan 2010 – 2030, Department of Energy, Government Gazette No.34263, 6 May 2011*. *The Department of Energy* (p. 58).

Department of Energy. (2013a). *Integrated Resource Plan For Electricity (IRP) 2010-2030 Update Report 2013* (p. 114). Retrieved from http://www.doe-irp.co.za/content/IRP2010_updatea.pdf

Department of Energy. (2013b). *Integrated Energy Planning Report - Executive Summary* (p. 159). Retrieved from http://www.energy.gov.za/files/IEP/IEP_Publications/Draft-2012-Integrated-Energy-Plan.pdf

Department of Minerals and Energy. (2003). *White Paper on Renewable Energy* (p. 45). Retrieved from http://unfccc.int/files/meetings/seminar/application/pdf/sem_sup1_south_africa.pdf

Dinter, F., & Gonzalez, D. M. (2013). Operability , reliability and economic benefits of CSP with thermal energy storage : first year of operation of ANDASOL 3. *Proceedings of Solar Power and Chemical Energy Systems conference (SolarPACES 2013)*.

Duffie, J., & Beckman, W. (2006). *Solar Engineering of Thermal Processes* (p. 908).

Eberhard, A. (2011). The Future of South African Coal: Market, Investment and Policy Challenges. Retrieved from http://npconline.co.za/MediaLib/Downloads/Home/Tabs/Diagnostic/MaterialConditions2/The future of South African coal....pdf

Eberhard, A. (2013). Nuclear power is neither necessary nor cost-effective. *Business Day Live*. Retrieved from http://www.bdlive.co.za/opinion/2013/03/19/nuclear-power-is-neither-necessary-nor-cost-effective

EIA. (2013).*U.S Energy Information Administration*, 13. Retrieved from http://www.eia.gov/countries/analysisbriefs/South_africa/south_africa.pdf

Electrical Energy Storage White Paper. (2011).*International Electrotechnical Commission*. Geneva, Switzerland. Retrieved from http://www.iec.ch/whitepaper/pdf/iecWP-energystorage-LR-en.pdf

Energy Conversions. (2013).*ConvertUnits.com*. Retrieved from http://www.convertunits.com/from/tonne+of+coal+equivalent/to/tonne+of+oil+equivalent

EPRI. (2010). *Power Generation Technology Data for Integrated Resource Plan of South Africa*. Retrieved from http://www.energy.gov.za/IRP/irp files/Tech_Data_for_Integ_Plan_of_South_Africa_July_08_2010_Final.pdf

Eskom. (2011). *Eskom Load Profile Data*.

Eskom. (2014a). Drakensberg Pumped Storage Scheme. Retrieved January 29, 2014, from http://www.eskom.co.za/Whatweredoing/ElectricityGeneration/PowerStations/Pages/Drakensberg_Pumped_Storage_Scheme.aspx

Eskom. (2014b). Palmiet Pumped Storage Scheme. Retrieved January 29, 2014, from http://www.eskom.co.za/Whatweredoing/ElectricityGeneration/PowerStations/Pages/Palmiet_Pumped_Storage_Scheme.aspx

Eskom. (2014c). Ingula Pumped Storage Scheme. Retrieved January 29, 2014, from http://www.eskom.co.za/Whatweredoing/NewBuild/IngulaPumpedStorage/Pages/Ingula_Pumped_Storage_Scheme.aspx

Fingersh, L., Hand, M., & Laxson, A. (2006). Wind Turbine Design Cost and Scaling Model Wind Turbine Design Cost and Scaling Model. *National Renewable Energy Laboratory*, (December), 38.

Fluri, T. P. (2009). The potential of concentrating solar power in South Africa. *Energy Policy*, *37*(12), 5075–5080. doi:10.1016/j.enpol.2009.07.017

Gapminder.org. (2013).*Gapminder Database*. Retrieved from www.gapminder.org

Garrison, J. B., & Webber, M. E. (2011). An integrated energy storage scheme for a dispatchable solar and wind powered energy system. *Journal of Renewable and Sustainable Energy*, *3*.

Gauche, P. (2010). Solar Thermal Roadmap. *Stellenbosch University*.

Gauche, P. (2012a). Thermal Storage Model. Solar Thermal Energy Research Group.

Gauche, P. (2012b). Central Receiver Model. Solar Thermal Energy Research Group.

Gauche, P. (2012c). Thesis Meetings.

Gauche, P. (2013a). Thesis Meetings.

Gauche, P. (2013b). Levelised Cost Of Electricity Model. Solar Thermal Energy Research Group.

GDP Per Capita. (2013).*The World Bank*. Retrieved from http://data.worldbank.org/indicator/NY.GDP.PCAP.KD

Geyer, M., & Stine, W. B. (2001). *Power from the Sun*. Retrieved from http://www.powerfromthesun.net/book.html

Grogg, K. (2005). *Harvesting the Wind : The Physics of Wind Turbines*. *Physics and Astronomy Department*. Retrieved from https://dspace.lasrworks.org/bitstream/handle/10349/145/fulltext.pdf

Hagemann, K. (2008). *Mesoscale Wind Atlas of South Africa*. University of Cape Town. Retrieved from http://www.g7energies.com/Mesoscale_Wind_Atlas_of_South_Africa_-_KH_PhD.pdf

Hartnady, C. (2010). South Africa's Diminishing Coal Reserves. *South African Journal of Science*, *102*(9), 1–5.

Historic Exchange Rates. (2013).*GoCurrency*. Retrieved from http://www.gocurrency.com/v2/historic-exchange-rates.php?ccode2=ZAR&ccode=USD&frMonth=0&frDay=1&frYear=2000

Horváth, G., Blahó, M., Egri, A., Kriska, G., Seres, I., & Robertson, B. (2010). Reducing the maladaptive attractiveness of solar panels to polarotactic insects. *Conservation biology : the journal of the Society for Conservation Biology*, *24*(6), 1644–53. doi:10.1111/j.1523-1739.2010.01518.x

Hubbert, K. (1982). *"Techniques of Prediction as Applied to the Production of Oil and Gas," Presented to a symposium of the US Department of Commerce, Washington, D.C., June 18-20, 1980. In Saul I. Gass, ed., Oil and Gas Supply Modeling, pp. 57-58. National Bureau of Standar*.

Industry (% of GDP). (2012).*The World Bank*. Retrieved from http://api.worldbank.org/datafiles/NV.IND.TOTL.ZS_Indicator_MetaData_en_EXCEL.xls

INTEGRATED RESOURCE PLAN (2014). Department of Energy. Retrieved from http://www.doe-irp.co.za/content/IRP2010_updatea.pdf

International Energy Statistics. (2014).*IEA*. Retrieved from http://www.eia.gov/cfapps/ipdbproject/IEDIndex3.cfm?tid=44&pid=44&aid=2

Ivanpah Solar Electric Generating System. (n.d.).*National Renewable Energy Laboratory*. Retrieved January 15, 2014, from http://www.nrel.gov/csp/solarpaces/project_detail.cfm/projectID=62

Jorgenson, J., Denholm, P., Mehos, M., & Turchi, C. (2013). Estimating the Performance and Economic Value of Multiple Concentrating Solar Power Technologies in a Production Cost Model Estimating the Performance and Economic Value of Multiple Concentrating Solar Power Technologies in a Production Cost Model. *National Renewable Energy Laboratory*, (December), 37. Retrieved from http://www.nrel.gov/docs/fy14osti/58645.pdf

Kolb, G. J., Ho, C. K., Mancini, T. R., & Gary, J. A. (2011). *Power Tower Technology Roadmap and Cost Reduction Plan* (p. 38). Retrieved from http://prod.sandia.gov/techlib/access-control.cgi/2011/112419.pdf

Kost, C., Mayer, J., Thomsen, J., Hartmann, N., Senkpiel, C., Philipps, S., Nold, S., et al. (2013). *Levelized Cost of Electricity Renewable Energy Technologies* (p. 50). Retrieved from http://www.ise.fraunhofer.de/en/publications/veroeffentlichungen-pdf-dateien-en/studien-und-konzeptpapiere/study-levelized-cost-of-electricity-renewable-energies.pdf

Kröger, D. G. (2011). *The Stellenbosch University Solar Power Thermodynamic cycle*. *University of Stellenbosch* (p. 3).

Landman, W., & Gauche, P. (2013). *Influence of Canting Mechanism and Facet Profile on Heliostat Field Performance*. Stellenbosch University.

Lefton, S., & Besuner, P. (2006). The Cost of Cycling Coal Fired Power Plants. *Coal Power Magazine*.

Lenzen, M. (2008). Life cycle energy and greenhouse gas emissions of nuclear energy: A review. *Energy Conversion and Management*, *49*, 2178–2199. Retrieved from http://beta.eoearth.org/files/151301_151400/151359/lenzen-2008-nuclear-lca.pdf

Lew, D., Bird, L., Milligan, M., Speer, B., Wang, X., Carlini, E. M., Estanqueiro, A., et al. (2013). Wind and Solar Curtailment Preprint. *International Workshop on Large-Scale Integration of Wind Power Into Power Systems*. Retrieved from http://citeseerx.ist.psu.edu/viewdoc/download?doi=10.1.1.390.1983&rep=rep1&type=pdf

Macknick, J., Newmark, R., Heath, G., & Hallett, K. C. (2011). A Review of Operational Water Consumption and Withdrawal Factors for Electricity Generating Technologies A Review of Operational Water Consumption and Withdrawal Factors for Electricity Generating Technologies. *National Renewable Energy Laboratory*. Retrieved from http://www.cwatershedalliance.com/pdf/SolarDoc01.pdf

Majavu, A. (2007). South Africa: Behind the high cost of electricity. *The South African Civil Society Information Service*. Johannesburg. Retrieved from http://allafrica.com/stories/201207240171.html?viewall=1

Manne, A. S. (1956). Scheduling of petroleum refinery operations. *Harvard Economic Studies*, *48*.

Marquard, A. (2006). *The Origins and Development of South African Energy Policy*. The University of Cape Town.

McCrary, M.D., McKernan, R.L., Flanagan, P.A., Wagner, W. D. (n.d.). *Wildlife Interactions at Solar One*. Rosemead, California. Retrieved from http://docketpublic.energy.ca.gov/PublicDocuments/09-AFC-07C/TN200885_20131015T234810_Wildlife_Interactions_at_Solar_1_Facility.pdf

Mcdonald, A., & Schrattenholzer, L. (2001). Learning rates for energy technologies. *Energy Policy*, *29*, 255–261.

Meiring, K. (2014). Personal Conversation. Cape Town: Juwi.

Merven, B. Cohen, B. Hughes, A. Stone, A. (2013). *Guidelines for the selection of Long-Range Energy Systems Modelling Platforms to support MAPS processes Guidelines for the selection of Long-Range Energy Systems Modelling Platforms to support MAPS processes* (pp. 1–14).

Meyer, R. (2012). GeoSun. Cape Town: The University of Stellenbosch.

Müller-steinhagen, H. (2004). Concentrating solar power. *Energy*, *18*, 43–50.

Müller-steinhagen, H. (2010). *Solar Thermal Power Plants - On the Way to Commercial Market Introduction*.

North American Electric Reliability Corporation. (2008). Glossary of Terms Used in Reliability Standards.

NREL. (2013). Concentrating Solar Power Projects. *NREL*. Retrieved from http://www.nrel.gov/csp/solarpaces/project_detail.cfm/projectID=40

Odeh, S. D., Morrison, G. L., & Behnia, M. (1998). Modelling of parabolic trough direct steam generation solar collectors. *Solar Energy*, *62*(6), 395–406. doi:10.1016/S0038-092X(98)00031-0

Overview of the South African Water Sector. (2000).*Governing Board Induction Manual*. Retrieved from http://www.dwa.gov.za/io/Docs/CMA/CMA GB Training Manuals/gbtrainingmanualchapter1.pdf

Parabolic Trough Design. (2013).*Airlightenergy.com*. Retrieved from http://www.airlightenergy.com/Cms?path=prodotti/csp

Pather, V. (2004). Eskom and Water, (May), 659–664.

Photovoltaics. (2013). *Engineering.com*. Retrieved from http://www.engineering.com/SustainableEngineering/RenewableEnergyEngineering/SolarEnergyEngineering/Photovoltaics/tabid/3890/Default.aspx

Pistocchini, L., & Motta, M. (2011). Feasibility Study of an Innovative Dry-Cooling System With Phase-Change Material Storage for Concentrated Solar Power Multi-MW Size Power Plant. *Journal of Solar Energy Engineering*, *133*.

Pitz-Paal, R. (2008). Chapter 10: Concentrating Solar Power. *Futute Energy: Improved, Sustainable and Clean Options for Our Planet*.

Richter, C., Teske, S., & Short, R. (2009). Concentrating Solar Power Global Outlook 09. *Power*, *17*.

Rutledge, D. (2011). Estimating Long-Term World Coal Production with Logit and Probit Transforms. *International Journal of Coal Geology*, *85*, 23–33.

Sebitosi, A., & Meyer, A. (2010). *Renewable Energy Systems* (p. 192). Stellenbosch: Centre for Renewable and Sustainable Energy Studies.

Skumanich, A. (2010). CSP: Developments in heat transfer and storage materials. *Renewable Energy Focus*, *11*(5), 40–43.

Soltigua Concentrating Solutions. (2013).

SONI. (2012). *Curtailment Report*.

SOUTH AFRICA'S WATER SITUATION AND STRATEGIES TO BALANCE SUPPLY AND DEMAND. (2004).*Department of Water Affairs*. Retrieved from http://www.dwaf.gov.za/nwrs/LinkClick.aspx?fileticket=15NoZWfpDjY=&tabid=63&mid=412

Sovacool, B. K. (2009). Contextualizing avian mortality: A preliminary appraisal of bird and bat fatalities from wind, fossil-fuel, and nuclear electricity. *Energy Policy*, *37*(6), 2241–2248. doi:10.1016/j.enpol.2009.02.011

Tait, L, Wlokas, HL and Garside, B. (2013). Making communities count: Maximising local benefit potential in South Africa's Renewable Energy Independent Power Producer Procurement Programme (RE IPPPP). *International Institute for Environment and Development*.

Technology Roadmap: CSP. (2010).*International Energy Agency*, *5*, 1–52. doi:10.1787/9789264088139-en

Ter-Gazarian, A. (1994). *Energy Storage for Power Systems* (p. 232). London: Peter Peregrinus Ltd.

The land area of South Africa. (2012).*Statistics South Africa*. Retrieved March 10, 2014, from https://www.statssa.gov.za/census01/Census96/HTML/CIB/Land.htm

Trabish, H. K. (2012). Getting Renewables on the Grid, Part 4: Why PV and the Grid Need CSP. *GreenTechMedia*. Retrieved from http://www.greentechmedia.com/articles/read/Getting-Renewables-on-the-Grid-Part-4-Why-PV-and-the-Grid-Need-CSP/

Tsoutsos, T., Frantzeskaki, N., & Gekas, V. (2005). Environmental impacts from solar energy technologies. *Energy Policy*, *33*(3), 289–296. doi:10.1016/S0301-4215(03)00241-6

US GHG Inventory 2012. (2012).*United States Environmental Protection Agency*. Retrieved February 28, 2014, from http://www.epa.gov/climatechange/ghgemissions/usinventoryreport.html

World Development Indicators. (2013).*The World Bank*. Retrieved from http://data.worldbank.org/indicator/NY.GDP.MKTP.KD

World Energy. (2009).*BP Statistical Review*. Retrieved from https://spreadsheets.google.com/spreadsheet/pub?key=0Auk0ddvGIrGqcHlqNnRTY1pxbUVlaFJHLTltTUhZZGc&gid=0

World Energy. (2012).*BP Statistical Review*. Retrieved from http://www.bp.com/extendedsectiongenericarticle.do?categoryId=9041233&contentId=7075263

Appendices: Section 1

In order to describe the CR and PV models, certain concepts dealing with the assessment of solar radiation and heat need to be covered in detail. This will allow an outline of the creation of the models, as key solar irradiance and thermodynamic equations are adapted from research, (Duffie & Beckman, 2006) (Cengel & Boles, 2011). There are two factors which affect the rate at which solar irradiance reaches the surface of the earth. First is the fact that a degree of variability exists in the radiation emitted from the sun. However, this amount is negligible and "for engineering purposes, in view of the uncertainties and variability of atmospheric transmission, the energy emitted by the sun can be considered to be fixed," (Duffie, Beckman, 2006:9). Second, the distance between the earth and the sun changes due to the former's elliptical orbit. This creates a ±3.3% variation in the rate of solar radiation reaching the earth outside or above the atmosphere. The formula below is used to show "the dependence of extraterrestrial radiation on the time of year," (Duffie, Beckman, 2006:9) and is given by:

$$\mathrm{I_o} = \mathrm{G_{sc}}(1 + 0.033\mathrm{Cos}\frac{360\mathrm{n}}{365})$$

Where:

$\mathrm{I_o}$ = extraterrestrial radiation

$\mathrm{G_{sc}}$ = extraterrestrial radiation incident on the plane normal to the radiation on the n^{th} day of the year.

The notion of the solar constant must be included in a discussion of solar irradiance. A value of 1,367w/m2 is commonly accepted in the literature as the solar constant. This is the amount of solar radiation that reaches the top of the atmosphere of Earth after travelling one astronomical unit, (AU). One AU is equal to the distance from the surface of the sun to the outside of the atmosphere of the Earth = 1.496 x 1011m, (Geyer & Stine, 2001).

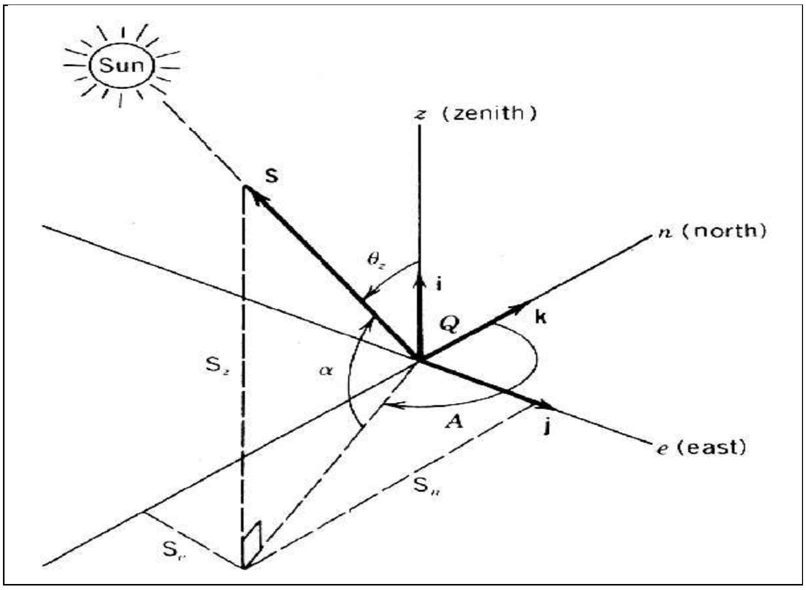

Figure 69: Solar angles used to calculate beam radiation properties.

Source: (Stine, Geyer, 2001).

In the figure above the angles are described as follows:

A = solar azimuth angle

ἀ = solar altitude angle

Θ_z = solar zenith angle

S = central sunray

Q = position of observer

i,j,k = unit direction vectors

The following angle descriptions are reproduced below from Duffie and Beckman, (2009):

Φ = latitude, the angular location north or south of the equator, north positive; -90°≤ϕ≤90°

δ = declination, the angular position of the sun at solar noon (i.e. when the sun is on the local meridian) with respect to the plane of the equator, north positive; -23.45°≤δ≤23.45°

β = slope, the angle between the plane of the surface in question and the horizontal; 0°≤β≤180°. (β>90° means that the surface has a downward-facing component).

y = surface azimuth angle, the deviation of the projection on a horizontal plane of the normal to the surface from the local meridian, with zero due south, east negative, and west positive; -180°≤y≤180°

ω = hour angle, the angular displacement of the sun east or west of the local meridian due to rotation of the earth on its axis at 15° per hour; morning negative, afternoon positive.

Θ = angle of incidence, the angle between the beam radiation relative to the Sun's zenith as reflected in the Figure 69.

(Duffie, Beckman, 2009:13).

The declination angle (δ) is found using the following formula:

$$\delta = \left(\frac{180}{\pi}\right)(0.006918 - 0.399912\cos B + 0.070257\sin B - 0.006758\cos 2B + 0.000907\sin 2B - 0.002697\cos 3B + 0.00148\sin 3B$$

The angle of incidence (Θ) of incoming beam radiation is calculated using the following equation:

$$Cos\Theta = \mathrm{Cos}\Theta\cos B + \sin\Theta z\sin B(ys - y)$$

The hour angle (ω) is found using the following equation:

$$\omega = 15(ts - 12)$$

Where:

ts = solar time

The zenith angle (Θ_z) is found by:

$$Cos\Theta_z = \text{Cos}\varphi\text{cos}\delta\text{cos}\omega + \text{sin}\varphi\text{sin}\delta$$

The solar azimuth (Ys) is found by:

$$Ys = sign(\omega)|(cos - 1\frac{\cos\Theta\sin\varphi - \text{sin}\delta}{\text{sin}\Theta\text{zcos}\varphi}$$

An important concept to consider when designing a solar power plant is the rate of reduction of solar irradiance with the angle of the collecting surface. This phenomenon is known as the cosine effect, and is shown in the figure below. A collecting surface parallel to incoming sunrays would collect all radiation by a factor of its surface area. If the same collecting surface is inclined at an angle, the same amount of irradiance is 'spread' over a larger surface area. As defined "solar irradiance falling on [a surface] will be reduced by the cosine of the angle between the surface normal and a central ray from the sun," (Stine, Geyer, 2001, Chapter 2).

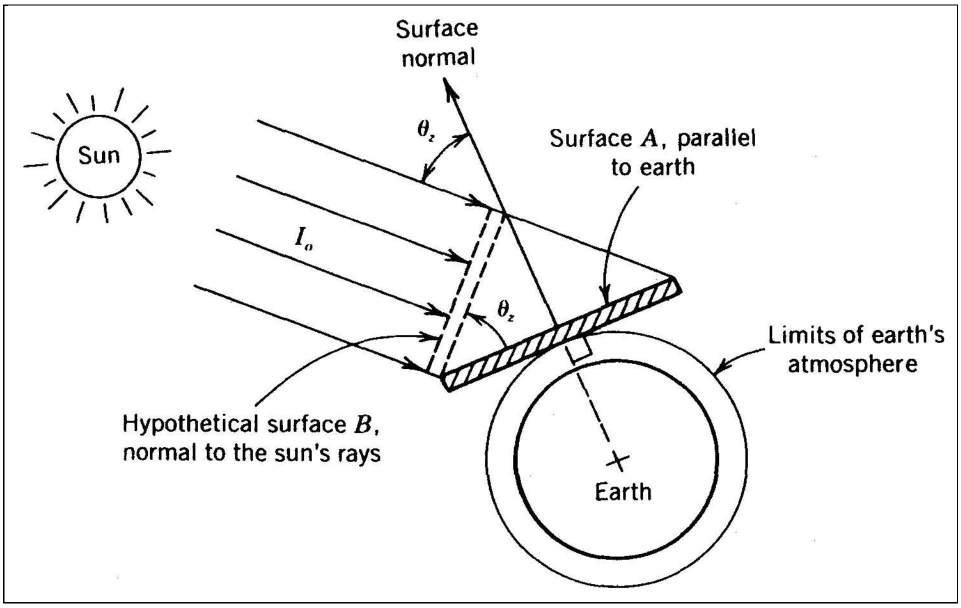

Figure 70: Diagram explaining the Cosine Effect.

Source: (Geyer & Stine, 2001)

The cosine effect is described by the following equation:

$$I_{o,h} = I_o Cos\Theta_z$$

Where:

$I_{o,h}$ = extraterrestrial solar irradiance falling on a surface parallel to the ground

I_o = maximum extraterrestrial solar irradiance

Θ_z = solar zenith angle (angle between the two surfaces)

In order to solve the solar zenith angle we use:

$$\Theta_z = 90° - \alpha$$

Where:

α = solar altitude angle

And

$$\alpha = sin - 1(sin\delta \sin\varphi + \cos\delta\cos\omega\cos\varphi)$$

Where:

δ = declination angle

ω = hour angle

φ =latitude angle

Descriptions of the angles above are provided for with explanations below for the solar time calculations.

Solar time is a fundamental consideration when dealing with solar energy systems as it is used to describe the angular position of the sun relative to an observer (or power plant) on the surface of the earth. As described by Stine and Geyer (2001) "the concept of solar time is used in predicting the direction of sunrays relative to a point on the earth," (Stine, Geyer, 2001). Solar time is extensively used when aiming to calculate the amount of incident solar radiation on a flat surface – a crucial consideration when designing a solar plant. Solar time is found using the following equation:

$$Solar\ time = standard\ time + 4(L_{st} - L_{loc}) + E$$

Where:

L_{st} = standard meridian for the local time zone

L_{loc} = longitude of location in question (0°<L<360°)

E = equation of time

The equation of time is described by:

$$E = 229.2(0.000075 + 0.001868cosB - 0.032077sinB - 0.014615cos2B - 0.04089sin2B)$$

Where B is found using:

$$B = (n - 1)\frac{360}{365}$$

Where:

n = day of the year

Once the solar time is known, there are a grouping of 'geometric relationships' which describe the position of the sun and the angle of incoming beam radiation, (direct normal irradiance). Using a vector approach the observer can calculate the intensity of incoming radiation by knowing the angles and meridian planes (described by latitude and longitude/solar time/time zones) shown in Figure 69 above.

Appendices: Section 2

Detailed Technology Description of the Photoelectric Effect

When incoming solar radiation impacts certain minerals, it has sufficient energy to create changes in the number of electrons orbiting the nucleus of the atoms within that illuminated material. This conversion of solar irradiance directly into electrical energy is termed the photoelectric effect, (Duffie & Beckman, 2006). When an electron is removed from its orbital by the addition of energy via a photon an "hole-electron pair," is formed, (Duffie & Beckman, 2006). This term describes an instantaneous moment when additive energy provided from incoming solar radiation displaces positively charged electrons from the orbitals of their atoms. These ions then move to other positions within the mineral, ("Photovoltaics," 2013), and the movement thereof can be harnessed to produce electrical current. When solar radiation is able to excite a material via the photoelectric effect in this way, it becomes a semiconductor. In the case of photovoltaic cell construction, the most commonly used semiconductor is silicon, (Si) and will be used here for an overview of the photovoltaic concept.

Silicon displays useful photoelectric properties, which can be altered by the addition of different minerals during the manufacturing process. To create a silicon-based matrix that produces greater numbers of positively charged ions, phosphorus is added, producing the N-type compound, ("Photovoltaics," 2013). This N-type term refers to the propensity of the material to generate free positively charged electrons when bombarded by photons from the sun. The P-type compound has different electrical properties to the N-type and is created via the addition of boron (B) to the silicon matrix. This P-type compound generates negatively charged ions more readily when exposed to light. A fundamental component of the photovoltaic cell is the use of a gateway that is placed between the two semiconductors. This transition layer is permeable to positively charged ions in one direction only, (from the N-type to P-type compounds), ("Photovoltaics," 2013). This effect results in the N-type compound becoming heavily negatively charged as positively charged ions are removed across the gateway into the P-type compound. The accumulation of positive charge in the P-type semiconductor generates a potential difference. This can be utilized by connecting a circuit to the electrodes of both semiconductors. The circuit allows the free flow of positively charged electrons to the load, where energy is used producing negatively (depleted) charged ions. These negatively charged ions move from the load after use back into the positively charged N-type semiconductor.

Incoming photons carry different amounts of energy depending on which wavelength they inhabit within the electromagnetic spectrum. When investigating the properties of incoming solar radiation it is interesting to note that within the electromagnetic spectrum "the wavelength limits associated with the various names and the mechanism producing the radiation are not sharply defined," (Duffie &

Beckman, 2006). Other parameters of the light spectrum can be calculated within acceptable tolerances for the modelling of photovoltaic generators.

Technology Penetrations (MW)					Cumulative Energy Generation (MWh)					Coefficients		
Wind	PV	CSP	CCGT	Total	Wind	PV	CSP	CCGT	Total	FC	CC	FC with CCGT
52757	95683	27431	0	175871	174197229	182038880	128462899	0	484699008	0.85	0.07	
80301	69578	20781	0	170660	265143534	132373334	90960397	0	488477265	0.88	0.05	
39894	496655	20781	0	557330	131722672	944896631	85120535	0	1161739837	0.81	0.63	
39894	69386	41562	0	150842	131722672	132008624	204169020	0	467900315	0.88	0.01	
63958	143842	16625	0	224425	211179467	273662126	72700997	0	557542590	0.83	0.21	
31978	143842	33250	0	209070	105587296	273662126	151621709	0	530871131	0.84	0.16	
63958	55500	33250	0	152708	211179467	105589734	158609013	0	475378214	0.89	0.01	
50514	89538	26267	59195	225515	166790655	170348145	126655366	88928977	552723143	0.83	0.05	1
47968	83853	24937	59439	216198	158384600	159532825	123717478	103373893	545008796	0.80	0.04	1
45298	78666	23549	59694	207208	149567858	149664023	120147377	119484309	538863567	0.77	0.03	1
42628	73927	22161	59949	198665	140751115	140646667	116182404	136772790	534352975	0.74	0.02	1
39974	69336	20781	60203	190294	131987167	131912853	112140198	155181540	531221759	0.71	0.01	1
37303	64735	19393	60458	181890	123170424	123159802	107874115	175093925	529298266	0.67	0.00	1
34633	60106	18005	60714	173458	114353681	114353681	103215093	196447739	528370195	0.63	0.00	1
31979	55500	16625	61324	165428	105589734	105589734	97649404	219193183	528022054	0.58	0.00	1
29261	50782	15212	62633	157888	96614606	96614606	90807061	243915954	527952227	0.54	0.00	1
26638	46231	13849	63896	150614	87956248	87956248	83238613	268797559	527948668	0.49	0	1
23984	41625	12469	65174	143252	79192300	79192300	75080548	294483519	527948668	0.44	0	1
21346	37046	11097	66444	135934	70481147	70481147	66822395	320163979	527948668	0.39	0	1
18644	32356	9692	67945	128637	61558815	61558815	58363230	346467808	527948668	0.34	0	1
15989	27750	8312	69419	121471	52794867	52794867	50054228	372304706	527948668	0.29	0	1
13319	23116	6924	70902	114261	43978124	43978124	41695172	398297248	527948668	0.25	0	1
10649	18481	5536	72385	107051	35161381	35161381	33336116	424289789	527948668	0.20	0	1
7995	13875	4156	73859	99885	26397433	26397433	25027114	450126687	527948668	0.15	0	1
5324	9241	2768	75342	92675	17580691	17580691	16668058	476119229	527948668	0.10	0	1
2654	4606	1380	76825	85466	8763948	8763948	8309002	502111770	527948668	0.05	0	1

LCOE (R/kWh)							Water Usage (GL)			Area (km2)			
2012 high	2012 med	2012 low	2030 high	2030 med	2030 low	MtCO2eq	PV	CSP	CCGT	Wind	PV	CSP	CCGT
1.08	0.90	0.81	0.86	0.68	0.59	386.67	17.91	12.64	57.73	17588.39	3401.14	2317.93	30.86
0.97	0.82	0.75	0.79	0.65	0.57	414.97	13.03	8.95	47.32	26767.11	2473.44	1756.01	30.38
1.68	1.52	1.44	1.00	0.84	0.76	362.36	93.00	8.38	75.28	13324.54	17655.72	1756.01	31.16
1.01	0.86	0.78	0.84	0.69	0.61	381.95	12.99	20.09	47.34	13324.54	2466.63	3512.01	31.50
1.17	0.99	0.89	0.88	0.69	0.60	396.36	26.93	7.16	65.49	21319.26	5113.47	1404.81	30.30
1.24	1.05	0.95	0.93	0.74	0.64	355.91	26.93	14.92	62.42	10659.38	5113.47	2809.61	31.90
0.94	0.81	0.74	0.79	0.66	0.59	404.95	10.39	15.61	42.66	21319.26	1972.98	2809.61	31.46
1.10	0.89	0.79	0.89	0.69	0.58	382.86	16.77	12.47	66.65	16838.06	3183.01	2219.59	30.97
1.13	0.89	0.77	0.93	0.69	0.58	376.96	15.70	12.18	77.48	15989.44	2980.93	2107.21	31.10
1.16	0.89	0.75	0.98	0.70	0.57	369.42	14.73	11.82	89.55	15099.36	2796.52	1989.91	31.23
1.20	0.89	0.73	1.03	0.72	0.56	360.58	13.84	11.43	102.51	14209.28	2628.03	1872.61	31.36
1.24	0.89	0.72	1.08	0.73	0.56	350.60	12.98	11.04	116.31	13324.54	2464.84	1756.01	31.50
1.29	0.90	0.70	1.14	0.75	0.55	339.00	12.12	10.62	131.23	12434.46	2301.28	1638.71	31.63
1.34	0.91	0.69	1.20	0.77	0.55	325.30	11.25	10.16	147.24	11544.38	2136.74	1521.40	31.76
1.40	0.92	0.68	1.27	0.79	0.56	308.44	10.39	9.61	164.29	10659.63	1972.98	1404.81	32.08
1.47	0.94	0.68	1.36	0.83	0.56	287.07	9.51	8.94	182.82	9753.56	1805.28	1285.40	32.77
1.55	0.97	0.68	1.44	0.86	0.57	263.13	8.66	8.19	201.47	8879.47	1643.49	1170.20	33.43
1.64	1.00	0.68	1.54	0.90	0.58	237.29	7.79	7.39	220.72	7994.72	1479.74	1053.60	34.10
1.72	1.03	0.68	1.63	0.94	0.59	211.20	6.94	6.58	239.97	7115.30	1316.96	937.71	34.76
1.81	1.06	0.68	1.73	0.97	0.60	184.47	6.06	5.74	259.68	6214.56	1150.25	819.00	35.55
1.89	1.08	0.68	1.82	1.01	0.61	158.21	5.20	4.93	279.05	5329.81	986.49	702.40	36.32
1.98	1.11	0.68	1.91	1.05	0.62	131.78	4.33	4.10	298.53	4439.74	821.75	585.10	37.09
2.06	1.14	0.68	2.01	1.09	0.63	105.36	3.46	3.28	318.01	3549.66	657.00	467.80	37.87
2.15	1.17	0.69	2.10	1.13	0.64	79.10	2.60	2.46	337.37	2664.91	493.25	351.20	38.64
2.23	1.20	0.69	2.20	1.17	0.65	52.68	1.73	1.64	356.86	1774.83	328.50	233.90	39.42
2.32	1.23	0.69	2.29	1.20	0.66	26.26	0.86	0.82	376.34	884.75	163.76	116.60	40.19

WIND	Q [MWh]	Cost	Safety	Total	O&M
		R 38 875 152 368.02	R 3 887 515 236.80	R 42 762 667 604.82	R 427 626 676.05
		R 38 875 152 368.02	R 3 887 515 236.80	R 42 762 667 604.82	R 427 626 676.05
		R 38 875 152 368.02	R 3 887 515 236.80	R 42 762 667 604.82	R 427 626 676.05
		R 38 875 152 368.02	R 3 887 515 236.80	R 42 762 667 604.82	R 427 626 676.05
		R 38 875 152 368.02	R 3 887 515 236.80	R 42 762 667 604.82	R 427 626 676.05
		R 38 875 152 368.02	R 3 887 515 236.80	R 42 762 667 604.82	R 427 626 676.05
		R 38 875 152 368.02	R 3 887 515 236.80	R 42 762 667 604.82	R 427 626 676.05
		R 38 875 152 368.02	R 3 887 515 236.80	R 42 762 667 604.82	R 427 626 676.05
		R 38 875 152 368.02	R 3 887 515 236.80	R 42 762 667 604.82	R 427 626 676.05
		R 38 875 152 368.02	R 3 887 515 236.80	R 42 762 667 604.82	R 427 626 676.05
SUM	92390277778	R 388 751 523 680.17	R 38 875 152 368.02	R 427 626 676 048.19	R 4 276 266 760.48

Year	Cost	Interest	Repayment	Principle	O&M	Total	Discount	Enum	Energy	Discount	Denom	R/kWh
1	R 427 626 676 048.19	R 34 210 134 083.85	-R 37 984 980 081.29	R 3 774 845 997.44	R 4 276 266 760.48	R 42 261 246 841.77	R 38 419 315 310.70	R 405 425 836 749.58	R 92 390 277 777.85	R 83 991 161 616.23	R 870 955 246 193.11	0.4655
2	R 423 851 830 050.75	R 33 908 146 404.06	-R 37 649 670 199.91	R 3 741 523 795.85	R 4 532 842 766.11	R 42 182 512 966.02	R 34 861 580 963.65		R 92 390 277 777.85	R 76 355 601 469.30		
3	R 420 110 306 254.90	R 33 608 824 500.39	-R 37 317 320 244.16	R 3 708 495 743.77	R 4 804 813 332.08	R 42 122 133 576.24	R 31 646 982 401.38		R 92 390 277 777.85	R 69 414 183 153.91		
4	R 416 401 810 511.13	R 33 312 144 840.89	-R 36 987 904 085.52	R 3 675 759 244.63	R 5 093 102 132.00	R 42 081 006 217.52	R 28 741 893 461.87		R 92 390 277 777.85	R 63 103 802 867.19		
5	R 412 726 051 266.50	R 33 018 084 101.32	-R 36 661 395 826.07	R 3 643 311 724.75	R 5 398 688 259.92	R 42 060 084 085.99	R 26 116 003 058.65		R 92 390 277 777.85	R 57 367 093 515.63		
6	R 409 082 739 541.76	R 32 726 619 163.34	-R 36 337 769 796.53	R 3 611 150 633.19	R 5 722 609 555.52	R 42 060 379 352.05	R 23 741 987 632.40		R 92 390 277 777.85	R 52 151 903 196.02		
7	R 405 471 588 908.57	R 32 437 727 112.69	-R 36 017 000 554.21	R 3 579 273 441.52	R 6 065 966 128.85	R 42 082 966 683.06	R 21 595 215 992.64		R 92 390 277 777.85	R 47 410 821 087.30		
8	R 401 892 315 467.05	R 32 151 385 237.36	-R 35 699 062 881.01	R 3 547 677 643.64	R 6 429 924 096.58	R 42 128 986 977.59	R 19 653 483 345.80		R 92 390 277 777.85	R 43 100 746 443.00		
9	R 398 344 637 823.41	R 31 867 571 025.87	-R 35 383 931 781.44	R 3 516 360 755.56	R 6 815 719 542.37	R 42 199 651 323.81	R 17 896 771 622.58		R 92 390 277 777.85	R 39 182 496 766.36		
10	R 394 828 277 067.84	R 31 586 262 165.43	-R 35 071 582 480.66	R 3 485 320 315.23	R 7 224 662 714.92	R 42 296 245 195.57	R 16 307 033 503.22		R 92 390 277 777.85	R 35 620 451 605.78		
11	R 391 342 956 752.61	R 31 307 436 540.21	-R 34 761 990 422.52	R 3 454 553 882.31	R 7 658 142 477.81	R 42 420 132 900.33	R 14 867 997 796.76		R 92 390 277 777.85	R 32 382 228 732.53		
12	R 387 888 402 870.30	R 31 031 072 229.62	-R 34 455 131 267.66	R 3 424 059 038.03	R 8 117 631 026.48	R 42 572 762 294.14	R 13 564 994 061.97		R 92 390 277 777.85	R 29 438 389 756.84		
13	R 384 464 343 832.27	R 30 757 147 506.58	-R 34 150 980 891.54	R 3 393 833 384.96	R 8 604 688 888.07	R 42 755 669 779.61	R 12 384 794 566.94		R 92 390 277 777.85	R 26 762 172 506.22		
14	R 381 070 510 447.31	R 30 485 640 835.78	-R 33 849 515 382.61	R 3 363 874 546.83	R 9 120 970 221.35	R 42 970 485 603.97	R 11 315 471 872.23		R 92 390 277 777.85	R 24 329 247 732.93		
15	R 377 706 635 900.48	R 30 216 530 872.04	-R 33 550 711 040.38	R 3 334 180 168.34	R 9 668 228 434.63	R 43 218 939 475.02	R 10 346 270 492.49		R 92 390 277 777.85	R 22 117 497 939.03		
16	R 374 372 455 732.14	R 29 949 796 458.57	-R 33 254 544 373.58	R 3 304 747 915.01	R 10 248 322 140.71	R 43 502 866 514.29	R 9 467 491 243.90		R 92 390 277 777.85	R 20 106 816 308.21		
17	R 371 067 707 817.13	R 29 685 416 625.37	-R 32 960 992 098.29	R 3 275 575 472.92	R 10 863 221 469.16	R 43 824 213 567.45	R 8 670 387 023.06		R 92 390 277 777.85	R 18 278 923 916.55		
18	R 367 792 132 344.21	R 29 423 370 587.54	-R 32 670 031 136.17	R 3 246 660 548.63	R 11 515 014 757.30	R 44 185 045 893.47	R 7 947 068 886.48		R 92 390 277 777.85	R 16 617 203 560.50		
19	R 364 545 471 795.58	R 29 163 637 743.65	-R 32 381 638 612.55	R 3 218 000 868.91	R 12 205 915 642.74	R 44 587 554 255.30	R 7 290 421 412.15		R 92 390 277 777.85	R 15 106 548 691.36		
20	R 361 327 470 926.67	R 28 906 197 674.13	-R 32 095 791 854.73	R 3 189 594 180.60	R 12 938 270 581.31	R 45 034 062 436.04	R 6 694 026 425.16		R 92 390 277 777.85	R 13 733 226 083.06		
21	R 358 137 876 746.08	R 28 651 030 139.69	-R 31 812 468 390.12	R 3 161 438 250.44	R 13 714 566 816.19	R 45 527 035 206.31	R 6 152 094 260.23		R 92 390 277 777.85	R 12 484 750 984.60		
22	R 354 976 438 495.64	R 28 398 115 079.65	-R 31 531 645 944.52	R 3 133 530 864.87	R 14 537 440 825.16	R 46 069 086 769.68	R 5 659 401 815.87		R 92 390 277 777.85	R 11 349 773 622.36		
23	R 351 842 907 630.77	R 28 147 432 610.46	-R 31 253 302 440.36	R 3 105 869 829.89	R 15 409 687 274.67	R 46 662 989 715.02	R 5 211 236 728.55		R 92 390 277 777.85	R 10 317 976 020.33		
24	R 348 737 037 800.87	R 27 898 963 024.07	-R 30 977 415 994.93	R 3 078 452 970.86	R 16 334 268 511.15	R 47 311 684 506.08	R 4 803 347 061.62		R 92 390 277 777.85	R 9 379 978 200.30		
25	R 345 658 584 830.01	R 27 652 686 786.40	-R 30 703 964 918.73	R 3 051 278 132.33	R 17 314 324 621.82	R 48 018 289 540.54	R 4 431 895 963.90		R 92 390 277 777.85	R 8 527 252 909.36		
26	R 342 607 306 697.69	R 27 408 584 535.81	-R 30 432 927 713.68	R 3 024 343 177.87	R 18 353 184 099.12	R 48 786 111 812.81	R 4 093 420 806.31		R 92 390 277 777.85	R 7 752 048 099.42		
27	R 339 582 963 519.82	R 27 166 637 081.59	-R 30 164 283 071.51	R 2 997 645 989.92	R 19 454 375 145.07	R 49 618 658 216.58	R 3 784 796 353.97		R 92 390 277 777.85	R 7 047 316 454.02		
28	R 336 585 317 529.90	R 26 926 825 402.39	-R 29 898 009 872.02	R 2 971 184 469.63	R 20 621 637 653.78	R 50 519 647 525.80	R 3 503 201 574.72		R 92 390 277 777.85	R 6 406 651 321.84		
29	R 333 614 133 060.27	R 26 689 130 644.82	-R 29 634 087 181.46	R 2 944 956 536.64	R 21 858 935 913.00	R 51 493 023 094.47	R 3 246 089 724.51		R 92 390 277 777.85	R 5 824 228 474.40		
30	R 330 669 176 523.63	R 26 453 534 121.89	-R 29 372 494 250.88	R 2 918 960 128.99	R 23 170 472 067.78	R 52 542 966 318.66	R 3 011 161 385.87		R 92 390 277 777.85	R 5 294 753 158.54		

Figure 71: Levelised Cost of Electricity layout

Wind Atlas mast information											
Site	Closest town	Dominant wind directions derived from SAWS	General boom directions	General anemometer direction	Latitude (Degrees, Minutes, Seconds)	Longitude (Degrees, Minutes, Seconds)	Latitude (Decimal degrees)	Longitude (Decimal degrees)	A.m.s.l.	Magnetic Declination (degrees)	Data Start date (15m mast)
WM01	Alexander Bay	South (Alexander Bay)	E-W	W	-28°36'06"S	16°39'51"E	-28.601882	16.664410	152	-19.5	2010/06/23
WM02	Calvinia	E/W (Calvinia);	NW-SE	SE	-31°31'29"S	19°21'38"E	-31.524939	19.360747	824	-24.5	2010/06/30
WM03	Vredendal	NW and SSE (Namaqua Sands)	WNW-ESE	ESE	-31°43'49"S	18°25'11"E	-31.730507	18.419916	241	-24.2	2010/06/24
WM04	Vredenburg	S and SSW (Langebaanweg)	E-W	W	-32°50'46"S	18°06'33"E	-32.846328	18.109217	22	-23.4	2010/05/18
WM05	Napier	W and E (Struisbaai and Hermanus)	N-S	S	-34°36'42"S	19°41'32"E	-34.611915	19.692446	288	-26.0	(2010/02/11) 2010/05/20
WM06	Sutherland	W to E, no dominant in reanalysis p gradient	N-S	N	-32°33'24"S	20°41'28"E	-32.556798	20.691243	1581	-24.9	2010/09/17
WM07	Beaufort West	E, ENE (Beaufort west), SW, SSW	NW-SE	SE	-32°58'00"S	22°33'24"E	-32.966723	22.556670	1047	-26.1	2010/05/28
WM08	Humansdorp	WSW (Tsitsikamma)	NW-SE	SE	-34°06'35"S	24°30'51"E	-34.109965	24.514360	110	-29.6	2010/08/04
WM09	Noupoort	SSE, NNW (Noupoort)	WSW-ENE	WSW	-31°15'09"S	25°01'42"E	-31.252540	25.028380	1806	-24.9	2010/09/01
WM10	Butterworth	SSW-W (Umtata)	NNE-SSW	SSW	-32°05'26"S	28°08'09"E	-32.090650	28.135950	925	-28.9	2010/08/05

Figure 72: Wind mast information for the WASA sites

Instruments used in Wind Atlas South Africa project

Cup Anemometers
Model: P2546A
Manufacturer: WindSensor, Denmark
Heights: 10m, 20 m, 40m, 60 m, 62 m
Calibrated by: Svend Ole Hansen ApS, Denmark

Potentiometer wind vanes
Model: W200P
Manufacturer: Vector Instruments, United Kingdom
Heights: 20 m, 60 m

Temperature and Relative Humidity Probes
Model: HMP45C
Manufacturer: Campbell Scientific Ltd, United Kingdom
Height: 60 m
Calibrated by: Vaisala Oyj, Finland

Temperature difference sensors
Model: P2642A Pt 500
Manufacturer: Risø, Denmark
Heights: 60m, 10m
Calibrated by: Risø, Denmark

Barometers
Model: PTB110
Manufacturer: Vaisala, Finland
Height: 6 m
Calibrated by: Vaisala Oyj, Finland

Data loggers/ CompactFlash Module
Model: CR1000 / CFM100
Manufacturer: Campbell Scientific, Inc, United Kingdom
Height: 6 m
Calibrated by: Campbell Scientific Ltd, United Kingdom

Data Capturing
Data are sampled with 0.5 Hz. Every 10 minute statistics of the measurements average/minimum/maximum/standard deviation are calculated and recorded together with time information.

Figure 73: Detailed wind Instrument information

Appendices: Section 6

1) $Demand\ Shortfall\ (Wind) = Wind - Eskom$
2) $Demand\ Shortfall\ (PV) = PV - Eskom$
3) $Demand\ Shortfall\ (CSP) = CSP - Eskom$
4) $Curtailment\ (Wind) = IF(demand\ shortfall > -1, return\ value, 0)$
5) $Curtailment\ (PV) = IF(demand\ shortfall > -1, return\ value, 0)$
6) $Curtailment\ (CSP) = IF(demand\ shortfall > -1, return\ value, 0)$
7) $Curtailment\ Coefficient\ (Wind) = \sum(curtailed\ energy)/\sum(Wind)$
8) $Curtailment\ Coefficient\ (Wind, PV) = \sum(curtailed\ energy)/\sum(Wind + PV)$
9) $Curtailment\ Coefficient\ (Wind, PV, CSP) = \sum(curtailed\ energy)/\sum(Wind + PV + CSP)$
10) $Fulfilment\ Coefficient\ (Wind) = \sum(Wind - curtailed\ energy)/\sum Eskom$
11) $Fulfilment\ Coefficient\ (Wind, PV) = (\sum(Wind + PV) - \sum(curtailed\ energy))/\sum Eskom$
12) $Fulfilment\ Coefficient\ (Wind, PV, CSP) = (\sum(Wind + PV + CSP) - \sum(curtailed\ energy))/\sum Eskom$